Investigating the cytotoxic effects of AZD5363 on lung cancer cells

A dissertation submitted

to the Faculty of Medicine and Surgery

University of Malta

in partial fulfilment of the requirements

for the degree of Master of Science in Pharmacotoxicology

Christianne Mizzi

2023

Project *Lung Cancer enhanced Novel therapy (LCeNT)* financed by the Malta Council for Science & Technology, for and on behalf of the Foundation for Science and Technology, through the FUSION: R&I Technology Development Programme

Acknowledgements

First, I would like to thank the Malta Council of Science and Technology (MCST) for funding this research study, as part of the LCeNT project, as well as the Department of Clinical Pharmacology and Therapeutics within the University of Malta, for giving me the opportunity to undertake this research as part of my MSc. degree.

Gratitude and appreciation go towards my supervisor, Dr Vanessa Petroni Magri, and co-supervisor, Prof. Anthony Fenech who, with utmost dedication and patience, have mentored, assisted, and encouraged me through the entirety of this project; I would not have been able to complete this research without their valuable knowledge and experience.

I would also like to thank all the staff of the Department of Clinical Pharmacology and Therapeutics for their assistance, particularly Mr Anthony F. Buttigieg and Ms Mirka Pereira, for their technical support, and for providing all the necessary laboratory equipment and materials to conduct my experiments.

I would not have completed this project without the unwavering support of my devoted parents, Joseph and Melina, my partner Mark, and my brothers Roderick and Mark, together with their respective families. I am also indebted to my friends and work colleagues for their encouragement throughout the past two years. A final thanks goes to Mr Stephen Falzon, Director of Pharmacy within the Pharmacy Department, Mater Dei Hospital, for granting me study leave to pursue this MSc. degree.

Abstract

Background: Lung cancer is reported to be the most commonly occurring cancer in the world, being the leading cause of cancer death among men, and the second most common cause of death among women after breast cancer (Sung, Ferlay *et al.* 2021). The PI3K/Akt/mTOR pathway has been strongly linked to the development and progression of NSCLC, which constitutes 85% of all lung cancers (Cheng, Shcherba *et al.* 2014, Papadimitrakopoulou 2012). This pathway is therefore a compelling target for anticancer therapy in NSCLC due to the extensive downstream signalling effects it has on the onset and progression of malignancy, as well as its potential impact on response and resistance to conventional therapies (Tan 2020). Among the PI3K/Akt/mTOR inhibitors is AZD5363 – a very potent and orally bioavailable pyrrolopyrimidine-derived pan-Akt kinase inhibitor which competes with ATP for Akt kinase association at the ATP binding site (Andrikopoulou, Chatzinikolaou *et al.* 2022). Besides the ongoing National Lung Matrix Trial (Middleton, Fletcher *et al.* 2020), few other investigations have, to date, tested the efficacy of this drug in different types of lung tumours. **Aim:** This study therefore aimed to investigate AZD5363 by sensitising two forms of aggressive NSCLC cells. **Methodology:** PrestoBlue™ cell viability assays were carried out to test the cytotoxicity of varying concentrations of AZD5363 on H520 (derived from squamous cell carcinoma) and A549 (originating from adenocarcinoma) cell lines. With the identified concentration that resulted in a 30% loss in cell viability, an ELISA assay was performed on A549 cells, to quantify how much of the protein eIF4E was being decreased. The same drug concentration was also utilised for wound healing assays, to investigate cell migratory behaviour of A549 cells in response to drug treatment. **Results:** The treatment of 10 – 100 µM AZD5363 on H520 cells failed to achieve a 30% loss in cell viability, and therefore no further investigations were conducted

on this cell line. With respect to A549 cells, the same treatment decreased cell viability in a concentration-dependent fashion, such that 55 µM AZD5363 was selected as the 30% inhibitory concentration (IC_{30}) for the subsequent investigations carried out on this cell line. In the ELISA assay, treatment of A549 cells with 55 µM AZD5363 achieved a reduction of 29% in mean eIF4E concentration. Following wound healing assays, percentage wound closure of A549 cells treated with 55 µM AZD5363 reached 33% after 72 hours of treatment, compared to 11% reached by cells treated with vehicle control solution. **Conclusion:** The reduction in mean eIF4E concentration achieved with 55 µM AZD5363 (IC_{30}), as well as the migratory inhibition observed, indicate that this drug may be further investigated in combination with chemotherapy or other investigational treatment regimens, to potentially improve survival and quality of life.

Table of Contents

List of Tables

List of Figures

List of abbreviations

Abbreviation	Expanded name
4DCT	4-dimensional CT
4E-BP1	Eukaryotic initiation factor 4E-binding protein 1
ABC	ATP-binding cassette
AC	Adenocarcinoma
AE	Adverse event
AI	Aromatase inhibitor
Akt	Protein kinase B (PKB)
ALK	Anaplastic lymphoma kinase
AMP	5’ adenosine monophosphate
AMPK	5’ adenosine monophosphate-activated protein kinase
ANOVA	Analysis of Variance
ASCO	American Society of Clinical Oncology
ASO	Antisense oligonucleotide
ATCC®	American Type Culture Collection®
ATG13	Autophagy-related protein 13
ATP	Adenosine triphosphatase
BAD	BCL2-antagonist of cell death
bFGF	Basic fibroblast growth factor
CLM	Colorectal liver metastasis
CO_2	Carbon dioxide
CRC	Colorectal cancer
CT	Computed tomography
Deptor	DEP domain-containing mTOR-interacting protein
DMEM	Dulbecco’s Modified Eagle’s medium
DMSO	Dimethyl sulfoxide
EDTA	Ethylenediaminetetraacetic acid

EGFR	Epidermal growth factor receptor
eIF4E	Eukaryotic initiation factor 4E
ELISA	Enzyme-linked immunosorbent assay
EML4-ALK	Echinoderm microtubule-associated protein-like 4 and anaplastic lymphoma kinase
ER+	Oestrogen receptor-positive
ERK	Extracellular signal-regulated kinase
ESMO	European Society for Medical Oncology
FBS	Foetal bovine serum
FDA	Food and Drug Administration
FKBP12	FK506 Binding Protein 12
FOXO	Forkhead box O
GAP	GTPase-activating protein
GEMMs	Genetically engineered mice models
GSK3	Glycogen synthase kinase 3
GTP	Guanosine 5’ triphosphate
HER	Human epidermal growth factor receptor
HER2	Human epidermal growth factor receptor 2
HIF-1α	Hypoxia inducible factor-1α
IARC	International Agency for Research on Cancer
IC_{30}	30% inhibitory concentration
IC_{50}	50% inhibitory concentration
IGF-1	Insulin-like growth factor
IGFR-1	Insulin-like growth factor receptor
INPP4B	Inositol polyphosphate-4-phosphatase type II B
IRS1	Insulin receptor substrate 1
iSH2	Inter-SRC homology 2
LCeNT	Lung Cancer enhanced Novel Therapy
KRAS	Kirsten rat sarcoma
LA	Locally advanced

LCC	Large cell carcinoma
LCINS	Lung cancer in never-smokers
LKB1	Liver kinase B1
LR	Lifetime risk
LTED	Long-term oestrogen deprivation
MAPK	Mitogen-activated protein kinase
MCST	Malta Council of Science and Technology
MDM2	Minute double minute 2
MDR	Multidrug resistance
mLST8	Mammalian lethal with SEC13 protein 8
MRI	Magnetic resonance imaging
mSIN1	Mammalian stress-activated protein kinase-interacting protein 1
mTOR	Mammalian target of rapamycin
mTORC1	Mammalian target of rapamycin complex 1
mTORC2	Mammalian target of rapamycin complex 2
NET	Neuroendocrine tumour
NFκB	Nuclear Factor kappa-light-chain-enhancer of activated B cells
NS	Not significant
NSCLC	Non-small cell lung carcinoma
ORR	Overall response rate
OS	Overall survival
PBS	Phosphate buffered solution
PDGF	Platelet-derived growth factor
PDGFR	Platelet-derived growth factor receptor
PDK1	3-phosphoinositide-dependent kinase 1
pen-strep	Antibiotic solution containing penicillin, streptomycin and amphotericin B
PET	Positron emission tomography
PFS	Progression-free survival
PH	Pleckstrin homolog

PHTS	PTEN hamartoma syndrome
PI3K	Phosphatidylinositol 3-kinase
PIKK	PI3K-related kinase
PIP2	Phosphatidylinositol 4,5-bisphosphate
PIP3	Phosphatidylinositol 3,4,5-trisphosphate
PKC-α	Protein kinase C-α
PORT	Postoperative radiotherapy
PRAS40	Proline-rich Akt substrate of 40kDa
Protor-1	Protein observed with Rictor-1
PS	Performance status
PTEN	Phosphatase and tensin homolog
Raptor	Regulatory-associated protein of mTOR
Ras	Rapidly accelerated fibrosarcoma
RCC	Renal cell carcinoma
RCF	Relative centrifugal force
RECIST	Response Evaluation Criteria in Solid Tumours
REDP	Research Ethics Review Procedures
Rheb	Ras homologue enriched in brain
Rictor	Rapamycin-insensitive companion of mTOR
Rpm	Revolutions per minute
RPMI-1640	Roswell Park Memorial Institute medium
rpS6	Ribosomal protein S6
RT	Radiotherapy
RTK	Receptor tyrosine kinase
S6K1, p70S6K1	Phosphorylated 70 ribosomal S6 kinase 1
SBRT	Stereotactic body radiotherapy
SCC	Squamous cell carcinoma
SCLC	Small cell lung carcinoma
SEM	Standard Error of the Mean

SGK1	Serum and glucocorticoid-induced protein kinase 1
SRE-BP1	Sterol regulatory element-binding protein 1
STK11	Serine threonine kinase 11
TCA cycle	Tricarboxylic acid/Krebs cycle
TDP	Technology Development Programme
TFEB	Transcription factor EB
TSC	Tuberous sclerosis complex
TKI	Tyrosine kinase inhibitor
TTF-1	Transcription termination factor
ULK1	UNC-51-like kinase 1
US	United States
VEGFR	Vascular endothelial growth factor receptor
WHO	World Health Organisation

Chapter 1
Introduction

1 Lung cancer

Lung cancer is reported to be the most commonly occurring cancer in the world, being the leading cause of cancer death among men, and the second most common cause of death among women after breast cancer (Sung, Ferlay *et al.* 2021). In the most recent Global Cancer Statistics, Sung, Ferlay *et al.* (2021) report that around 11.4% of cancer diagnoses and 18% of cancer deaths are attributed to lung cancer. Furthermore, the World Health Organisation (WHO), in its classification of thoracic tumours, estimates that in 2018 there were two million new cases and 1.7 million deaths linked with lung cancer (IARC WHO 2021b). The highest rates of incidence and mortality were observed in high-income economies, such as most parts of Europe and the United States (US); since the early 1990s however, incidence in males has generally been decreasing, whereas in contrast, rates of lung cancer among women have been on the incline (Baum, Winter *et al.* 2022, Lortet-Tieulent, Renteria *et al.* 2013). Such trend among the female population only started to stabilise after 2005, and this was observed in Northern Europe, Central and Eastern Europe, Switzerland, and Malta. As of 2020, according to the Global Cancer Observatory (2021a), lung cancer was the third most prevalent cancer diagnosis in Malta (10.3% of new cases), and the primary cause of cancer death (20.1%) among both sexes.

The majority of lung cancer deaths are attributed to tobacco consumption, accounting for 80-85% of cases globally. Besides more than 7000 chemicals, tobacco smoke also contains at least 69 carcinogens that include polycyclic aromatic hydrocarbons, tobacco-specific nitrosamines, as well as benzene (IARC WHO 2020, Planchard, Popat *et al.* 2018). A systematic analysis by Abdulkader, Abera *et al.* (2018) reported that worldwide in 2017 there were 1.19 million lung cancer deaths related to smoking, translating to an increase

of 23.3% of such deaths when compared with 2007. This means that the global cigarette smoking trends that have occurred over the past years are now essentially mirrored by the current patterns of lung cancer incidence both geographically and temporally (IARC WHO 2021b, Lemjabbar-Alaoui, Hassan *et al.* 2015). The hazards for smokers rise with the daily quantity of cigarettes smoked, and the number of years spent smoking; such risks gradually decrease after quitting, though never to the same degree as in individuals who never smoked. Lifelong non-smokers experience a much lower risk of being diagnosed or dying with lung cancer (Thun, Hannan *et al.* 2008); it is estimated that there is an annual rate of 5 – 10 cases of lung cancer diagnoses per 100,000 population, compared with 20 – 30 times higher rates among smokers.

Apart from tobacco smoking, around 29 substances have been identified as potential causes of lung cancer, with varied degrees of risk and incidence of exposure (IARC WHO 2020). These include asbestos, silica, numerous heavy metals, radon, as well as indoor air pollution resulting from solid fuel combustion and cooking emissions in poorly ventilated households. Moreover, the International Agency for Research on Cancer (IARC) has more recently categorised outdoor air pollution, particulate matter in outdoor air pollution, and diesel engine exhaust as carcinogenic to humans (Cogliano, Baan *et al.* 2011, IARC WHO 2022). These chemicals may become more important as causes of lung cancer, particularly in never-smokers. In a prospective observational study on lung cancer in never-smokers (LCINS), Couraud, Souquet *et al.* (2015) observe that this disease appears to have a strong geographical connection. For instance, LCINS is significantly more prevalent in Asia than in the US or Europe. This may be due to variable inherent susceptibility characteristics, as well as varying occupational and environmental carcinogen exposures in different geographic regions.

Lung cancer is very diverse and can develop in a variety of sites along the bronchial tree, resulting in a wide range of signs and symptoms, depending on the anatomic location (Lemjabbar-Alaoui, Hassan *et al.* 2015); in fact, up to 70% of lung cancers are diagnosed when the disease is already at an advanced stage. Eapen, Hansbro *et al.* (2018) report that although there may be regional disparities linking differences in treatment and diagnostic practices, lung cancer patients currently have a poorer 5-year average survival rate (18.6%) when compared to other prevailing cancers.

1.1 Classification of lung cancer

Almost all lung malignancies are carcinomas. Histologically lung cancer is categorised into two main types, namely small cell lung carcinoma (SCLC) and non-small cell lung carcinoma (NSCLC). NSCLC constitutes 85% of all lung cancers, and is further subdivided into adenocarcinoma (AC), squamous cell carcinoma (SCC), and large cell carcinoma (LCC) (Inamura 2017). The diagnostic workup is crucial for determining the precise type and stage of lung cancer, and the patient's ability to tolerate treatment, since the course of treatment differs significantly depending on the type and stage of lung carcinoma (Yoder 2006).

1.1.1 Small cell lung carcinoma

Globally small cell lung carcinoma accounts for 15% of lung cancer cases. It is a malignant epithelial tumour that very often expresses neuroendocrine markers, and is made up of cells with sparse cytoplasm, ill-defined cellular borders, finely granular nuclear chromatin, absent or inconspicuous nucleoli, a high mitotic count, and frequent and extensive necrosis and apoptosis (IARC WHO 2021b, Ryan, Burke 2017). The tumour cells typically develop in a sheet-like manner and are tightly packed. SCLC mainly involves the major airways and mediastinal lymph nodes; however, it can arise peripherally in 5% of patients. At

presentation, metastasis to the liver, bone, brain, ipsilateral and contralateral lung, and adrenal glands is prevalent, as are pleural and pericardial effusions. Patients usually present with rapid-onset symptoms due to intrathoracic tumour growth, extrapulmonary metastasis, paraneoplastic syndromes, or a combination of these. The complete spectrum of lung cancer imaging abnormalities is usually observed, but due to its rapid growth, at the point of diagnosis the tumour tends to be larger and more advanced than NSCLC, generally appearing as a massive hilar mass and bulky mediastinal lymph nodes. MRIs (magnetic resonance imaging) reveal metastases in about 15% of neurologically asymptomatic patients. The majority of SCLCs occur in individuals who have a history of heavy smoking however, though in rare cases, *de novo* SCLC can occur in never-smokers. Small cell carcinoma patients are usually too advanced in their disease to be candidates for surgery, hence chemotherapy is their first-line treatment (Ryan, Burke 2017); however despite the fact that it is more receptive to chemotherapy and radiation therapy than any other lung cancer type, the aggressive growth of SCLC and its widespread distribution at the time of diagnosis make it extremely difficult to treat (Lemjabbar-Alaoui, Hassan *et al.* 2015).

1.1.2 Non-small cell lung carcinoma

The distribution of NSCLC histological types has shifted over the last 25 years; in the US, incidence of AC has increased in both sexes, while SCC, which was historically the leading histotype, has decreased. In Europe, comparable trends can be observed among males, however both SCC and AC continue to rise among women (Planchard, Popat *et al.* 2018).

1.1.2.1 Adenocarcinoma

Adenocarcinoma is a malignant epithelial tumour that is usually located in peripheral bronchi, with central fibrosis and pleural puckering, and accounts for around 40% of all

cases of lung cancer; histologically making it the most common type of lung carcinoma (Lemjabbar-Alaoui, Hassan *et al.* 2015, Ryan, Burke 2017, Zheng 2016). Despite the fact that the majority of cases are related to smoking, AC occurs more commonly than any other histologic form of lung carcinoma among patients who have never smoked (IARC WHO 2021b). When solid, tumours typically have a sliced surface that is grey-white and might have lobulated, spiculated, or stellate borders (Ryan, Burke 2017). Lung AC produces mucin or has glandular differentiation; even in small biopsy specimens, the tumour can be classified as an adenocarcinoma when these morphologic characteristics are apparent. The pneumocytic markers, transcription termination factor (TTF-1) and Napsin-A, which are typically expressed by lung AC cells in more than 85% of cases, can be used as indicators of such neoplasm or adenocarcinoma differentiation in poorly differentiated tumours, as well as in limited biopsy sampling material (Zheng 2016).

1.1.2.2 Squamous cell carcinoma

Squamous cell carcinoma is the second most common type of lung cancer, making up about 20% of cases. Like AC, SCC is an epithelial tumour, however it is distinguished by the presence of keratinisation, intercellular bridges, or immunohistochemical markers of squamous cell differentiation. It usually originates from a main or lobar bronchus and, in at least two thirds of cases, is located in the central compartment of the lung (IARC WHO 2021b). SCC signs and symptoms are comparable to those of other non-small cell lung carcinomas; however, they are typically correlated with the site of the tumour. SCC has a propensity to be locally aggressive, with gradual involvement of peribronchial structures through direct invasion, but distant metastases develop similarly to other NSCLCs. Endobronchial obstruction causes symptoms such as haemoptysis, coughing, and recurrent

pneumonitis. SCC, like all lung cancers, but more so than adenocarcinoma, is strongly linked to smoking, and global trends in SCC incidence closely reflect changes in smoking habits. More than 90% of SCC patients are current or previous heavy smokers, and a male predisposition has been noted (IARC WHO 2021b). Smoking has a rather predictable mutagenesis signature (signature 4), acting predominantly on guanine base pairs and causing C>A mutations.

1.1.2.3 Large cell carcinoma

Large cell carcinoma is an undifferentiated NSCLC which does not have the cytological, architectural, immunohistochemical, or histochemical characteristics of SCLC, AC, or SCC (IARC WHO 2021b). It is a relatively uncommon form of lung cancer and is characterised by a poor prognosis and restricted therapeutic options (Chen, Cui *et al.* 2022). The tumour typically manifests as a sizeable peripheral mass composed of sheets or nests of big polygonal cells with conspicuous nucleoli, vesicular nuclei, modest amounts of cytoplasm, and significant necrosis (Ryan, Burke 2017). LCC shares several characteristics with other NSCLCs, including pathogenesis, aetiology, symptoms, imaging, and tumour dissemination. Most patients diagnosed with LCC are either current or former smokers. The diagnosis cannot be made with non-surgical biopsy or cytology but requires a well sampled resected tumour.

1.2 Staging of cancer

Cancer staging is a crucial step when diagnosing a tumour, and it serves to assist the clinician in formulating a treatment plan, provide insight into the prognosis, and assist in the assessment of treatment outcomes (Lemjabbar-Alaoui, Hassan *et al.* 2015). The anatomical extent of the disease is described using the worldwide TNM-based staging

system. The primary tumour's size and extent are described by the T category. The N category represents the degree of regional lymph node involvement. The M category defines whether distant metastasis is present or not. The severity of the cancer is indicated by the addition of numbers to these three categories. TNM subsets are constructed using every combination of the T, N, and M categories; those subsets with comparable prognoses are then grouped into stage groupings. Stages of NSCLC range from one to four (I through IV); the less the cancer has spread, the lower the stage.

There are two stages that define SCLC: limited (restricted to the primary hemithorax, mediastinum, or supraclavicular lymph nodes), and extensive (spread beyond the supraclavicular areas). Without additional definition, the term "stage" refers to the pre-treatment clinical stage (Lemjabbar-Alaoui, Hassan *et al.* 2015).

1.3 Treatment of early stage (stage I and stage II) NSCLC

In the European Society for Medical Oncology (ESMO) guidelines, Postmus, Kerr *et al.* (2017) recommend surgical resection as the preferred course of action for non-centrally located possibly resectable lung cancer, and should be made available to all patients with stage I and stage II NSCLC, in whom there is no nodal metastasis on both computed tomography (CT) and positron emission tomography (PET) scans, and who are prepared to accept procedure-related risks. Imaging, biopsies, a detailed assessment of cardiac and pulmonary function, as well as an evaluation of other comorbidities, need to be undertaken to calculate the risk of operative morbidity prior to considering surgical resection (Postmus, Kerr *et al.* 2017, Zappa, Mousa 2016). For tumours ≥ 2 cm and with a solid appearance on CT, lobectomy is still regarded as the standard surgical procedure. When possible, full resection is advised for individuals with multifocal lung cancer (Postmus, Kerr *et al.* 2017).

Moreover, ESMO guidelines suggest that patients with stage II and stage III NSCLC who have had resection, and those with resected stage IB illness whose primary tumour is larger than 4 cm, should be offered adjuvant chemotherapy; in such cases a two-drug regimen containing cisplatin is preferred.

1.4 Radiotherapy

Tumours at specific locations in the body may be reduced or removed with the aid of radiotherapy (RT), which utilises high-energy beams that disrupt the DNA of cancer cells and ultimately kill them (Zappa, Mousa 2016). Stereotactic body radiotherapy (SBRT) is the recommended course of treatment for patients with comorbidities or other reasons that render them inoperable, patients who present with stage I NSCLC that is located peripherally, or patients who refuse surgery (Postmus, Kerr *et al.* 2017, Zappa, Mousa 2016). To achieve exact placement of the tracking device, current SBRT practice typically uses small planning margins based on 4-dimensional CT (4DCT), numerous radiation beams or arcs, all of which lower the likelihood of non-malignant organ toxicity. Radical RT utilising more conventional or accelerated schedules is advised for medically inoperable patients whose tumours are larger than 5 cm and/or located in a somewhat central area (Postmus, Kerr *et al.* 2017). In early-stage NSCLC that has been entirely resected, postoperative radiotherapy (PORT) is not advised. In order to improve quality of life for NSCLC patients who do not respond to surgery or chemotherapy, radiotherapy may potentially be included as part of palliative care (Zappa, Mousa 2016).

1.5 Treatment of stage III NSCLC

Stage III NSCLC is a diverse condition that can range from resectable tumours with microscopic lymph node metastases, to untreatable, bulky disease with many nodal sites.

Therefore, the position of the tumour and whether it can be removed surgically are what determine the best treatment plan, which may include surgery, chemotherapy, and radiotherapy (Lemjabbar-Alaoui, Hassan *et al.* 2015). A diagnostic contrast-enhanced CT scan of the chest and upper abdomen, followed by a PET or a PET-CT paired with a CT technique with a sufficiently high resolution for initial staging reasons, is recommended to be performed on all patients who are scheduled for definitive stage III NSCLC treatment (Daly, Singh *et al.* 2022, Postmus, Kerr *et al.* 2017). Furthermore, if N2 disease is only detected after surgery despite acceptable mediastinal staging methods, adjuvant chemotherapy should be administered after surgery. Concurrent definitive chemotherapy and radiation therapy are preferred in cases of multi-station N2 or N3. Additionally, ESMO guidelines advise that patients should be able to receive platinum-based chemotherapy, ideally with cisplatin, for care with a curative objective (Postmus, Kerr *et al.* 2017).

In instances where, even after induction therapy and following a multidisciplinary evaluation, resection is not feasible, the malignancy is referred to as unresectable locally advanced (LA). Recommendations in such cases include concurrent chemoradiation as first line management, whereby, unless contraindicated, and in the absence of conclusive findings in favour of carboplatin as a single agent radiation sensitiser, both Daly, Singh *et al.* (2022) and Postmus, Kerr *et al.* (2017) suggest two to four cycles of a combination of cisplatin-based chemotherapy with radiation, targeting a total cumulative dose of cisplatin of at least 300 mg/m^2. Alternatively, sequential chemotherapy followed by definitive radiotherapy may be another option for patients who are not candidates for concurrent chemoradiation; the most common combinations used are cisplatin + etoposide, cisplatin + vinca alkaloid (usually vinorelbine), or cisplatin + pemetrexed in non-squamous histology (Postmus, Kerr *et al.* 2017).

1.6 Advanced/metastatic (stage IV) NSCLC

Consideration of the patient's age, performance status (PS), any other comorbidities, the patient's preferences, as well as the histology and molecular pathology, need to be addressed when deciding on a management plan of Stage IV NSCLC (Lemjabbar-Alaoui, Hassan *et al.* 2015, Planchard, Popat *et al.* 2018). In the absence of any major comorbidities, both ESMO and the American Society of Clinical Oncology (ASCO) guidelines (Hanna, Schneider *et al.* 2020) recommend that all patients with PS 0 – 2 in stage IV should be given systemic treatment. For patients with a PS of 0 or 1, the first-line therapy is advised to consist of a combination of two cytotoxic medications; given that there are no contraindications to such compounds, doublets of platinum-based chemotherapy (cisplatin or carboplatin), in conjunction with comparable activity taxanes (paclitaxel or docetaxel), antimetabolites (gemcitabine or pemetrexed), or vinca alkaloids (vinblastine or vinorelbine) are the treatment of choice (Hanna, Schneider *et al.* 2020, Planchard, Popat *et al.* 2018). This is to be followed by less toxic maintenance monotherapy. Lemjabbar-Alaoui, Hassan *et al.* (2015) reported that compared to non-platinum combination therapy, platinum-based combination therapies that include cisplatin or carboplatin produce higher response and overall survival (OS) rates.

Similarly, the first line treatment of advanced stage SCC with PS 0 – 2 and without major comorbidities, is based on platinum-based doublets in combination with a third-generation cytotoxic drug, namely gemcitabine or vinorelbine (Planchard, Popat *et al.* 2018). Additionally, for metastatic SCC, ESMO guidelines recommend a combination of the monoclonal antibody pembrolizumab with carboplatin and paclitaxel (or albumin-bound paclitaxel).

1.7 Maintenance

Following first-line chemotherapy, only patients with PS 0 – 1 should be administered maintenance chemotherapy. Histology, response to doublets of platinum-based chemotherapy, residual toxicity from first-line treatment, PS, and the patient's preference should all be taken into account when deciding on maintenance. In cases where control of the disease is achieved with four cycles of cisplatin + pemetrexed, Planchard, Popat *et al.* (2018) recommend that continued maintenance with pemetrexed may be considered. Two randomised Phase III trials conducted by Quoix, Zalcman *et al.* (2011) and Zukin, Barrios *et al.* (2013) report prolonged survival and improved quality of life in patients with PS of 2 who were treated with carboplatin-based combination chemotherapy, when compared to patients treated with a single-agent chemotherapy.

The regulatory circuits that control typical cell growth and homeostasis are damaged in lung cancer cells. It is believed that a number of genetic and epigenetic changes lead to the transformation of a benign lung cancer phenotype into a malignant one, which then progresses to an invasive malignancy via clonal growth. Following the onset of the initial malignancy, clonal expansion-acquired genetic and epigenetic aberrations continue to accumulate, and these affect the processes of invasion, metastasis, and cancer therapy resistance. For better disease prevention, early detection, and treatment, it is crucial to identify and characterise these molecular changes. The individualised prognosis and best course of treatment for each patient will be much improved by knowledge of both the tumour features and genetics of the patient (Lemjabbar-Alaoui, Hassan *et al.* 2015).

As a result of recent developments in molecular profiling, a personalised medicine approach to treatment is now possible for many NSCLCs (Papadimitrakopoulou 2012). With

a better understanding of the molecular changes and genomic biomarkers that promote the development of lung cancer, even the traditional classification of lung cancer into SCLC and NSCLC has been modified (Tan 2020). A crucial regulator of numerous cellular processes which is affected by many of these mutations is the phosphatidylinositol 3-kinase/protein kinase B (PKB, also known as Akt)/mammalian target of rapamycin (PI3K/Akt/mTOR) pathway, whose enhanced activation results in a number of characteristics that distinguish cancer, such as acquired growth signal autonomy, suppression of apoptosis, persistent angiogenesis, increased tissue invasion and metastasis, and insensitivity to antigrowth signals (Cheng, Shcherba *et al.* 2014, Papadimitrakopoulou 2012, Tan 2020).

Physiologically, activation of the PI3K/Akt/mTOR pathway is initiated when extracellular growth factors bind to transmembrane receptor tyrosine kinases (RTKs), such as epidermal growth factor receptor (EGFR), human epidermal growth factor receptor 2 (HER2), insulin-like growth factor receptor (IGFR-1), vascular endothelial growth factor receptor (VEGFR), and platelet-derived growth factor receptor (PDGFR) (Fumarola, Bonelli *et al.* 2014, Papadimitrakopoulou 2012, Yip 2015).

1.8 Components of the PI3K/Akt/mTOR pathway

1.8.1 PI3K

The PI3Ks, which phosphorylate the 3'-hydroxyl group of phosphatidylinositol and phosphoinositides, are a distinct and conserved family of intracellular lipid kinases (Cantley, Engelman *et al.* 2006). Depending on their structure and substrate specificity, PI3Ks are classified into three groups (I-III), each of which plays a unique part in signal transduction

(Solomon, Pearson 2009). There are two types of class I PI3Ks, namely the class IA PI3Ks, that are heterodimers made up of a p110 catalytic subunit and a p85 regulatory subunit, and which are triggered by growth factor RTKs; and class IB PI3Ks, which are triggered by G-protein-coupled receptors (Tewari, Patni *et al.* 2022). Upstream RTKs as well as growth factor stimulation can activate class IA PI3Ks. When the PI3K regulatory subunit (p85) binds to the RTK, the p110 catalytic subunit is released and translocates to the plasma membrane (Papadimitrakopoulou 2012, Tan 2020), where it catalyses the phosphorylation of phosphatidylinositol 4,5-bisphosphate (PIP2) by PI3K, resulting in the production of phosphatidylinositol 3,4,5-trisphosphate (PIP3) (Figure 1.1). At this point, activation of the mitogen-activated protein kinase (MAPK) cascade of the rapidly accelerated fibrosarcoma/MAPK/extracellular signal-regulated kinase (Ras/MAPK/ERK) pathway, may simultaneously take place and through Ras, also activate PI3K (Cheng, Shcherba *et al.* 2014, Papadimitrakopoulou 2012). Subsequently, PIP3 localises Akt to the plasma membrane where it undergoes phosphorylation by 3-phosphoinositide-dependent kinase 1 (PDK1). As shown in Figure 1.1, this activates a cascade of target proteins that promote cell growth, metabolism, survival, mobility, and proliferation (Cheng, Shcherba *et al.* 2014, Papadimitrakopoulou 2012, Yu, Cui 2016).

1.8.2 Akt

The downstream effector kinase of PI3K, Akt, is a serine/threonine-specific protein kinase, and is expressed as the three isoforms Akt 1 (PKBα), Akt 2 (PKBβ) and Akt 3 (PKBγ), each of which has a pleckstrin homolog (PH) domain at the amino-terminus, a serine-threonine catalytic domain in the middle, and a short carboxy-terminal regulatory domain (Yip 2015, Zhao, Liu *et al.* 2009). As mentioned earlier, the translocation of Akt to the plasma

membrane, which is facilitated by the docking of the PH domain to PIP3 on the membrane, is the first step in its activation process (Zhao, Liu *et al.* 2009). The subsequent conformational shift in Akt exposes two essential amino acid residues for phosphorylation that are necessary for its complete activation (Yu, Cui 2016) (Figure 1.1), namely:

- phosphorylation by PDK1 at Thr308 in the catalytic domain, and
- phosphorylation by mammalian target of rapamycin complex 2 (mTORC2) (which will be further discussed in Section 1.8.3.2), at the Ser473 in the C-terminal hydrophobic motif.

The two above processes result in full activation of Akt.

After becoming fully activated and phosphorylated, Akt has a number of potentially significant downstream effects, including:

- phosphorylation and inactivation of tuberous sclerosis complex 1 and 2 (TSC1 & 2) (Ciuffreda, Di Sanza *et al.* 2010, Papadimitrakopoulou 2012). This complex is a critical negative regulator of the multiprotein complex mTORC1 (a primary regulator of cell growth and metabolism – discussed in Section 1.8.3.1). The small G-protein Ras homologue enriched in brain (Rheb), when in its GTP (guanosine 5' triphosphate)-bound form, serves as an activator of mTORC1, and is subject to GTPase-activating protein (GAP) activity by the TSC1 and TSC2 (Ciuffreda, Di Sanza *et al.* 2010, Fumarola, Bonelli *et al.* 2014). As a result, further downstream activation of the eukaryotic initiation factor 4E (eIF4E) complex will promote tumorigenesis, cell cycle regulation, and inhibition of apoptosis (Tan 2020);
- phosphorylation and inhibition of downstream signalling proteins, such as the pro-apoptotic protein BCL2-antagonist of cell death (BAD), forkhead box O (FOXO)

transcription factors, and glycogen synthase kinase 3 (GSK3), hence reducing apoptotic signals that promote cell cycle progression (Fumarola, Bonelli *et al.* 2014, Tan 2020);

- minute double minute 2 (MDM2) is phosphorylated and activated, which results in the downregulation of p53-mediated apoptosis (Tan 2020);
- prevention of the negative regulation of the nuclear factor kappa-light-chain-enhancer of activated B cells (NFκB) transcription factor, which is essential for the effects of PI3K/Akt pathway activation. Numerous genes involved in apoptosis, cell cycle control, immunological modulation, cell survival, adhesion and differentiation are regulated by NFκB. Akt blocks the IκB family, and in particular IκBα, from negatively regulating NFκB (since IκBα takes NFκB out of DNA and returns it to the cytoplasm) (Mills, Hennessy *et al.* 2005, Tan 2020).

1.8.3 mTOR

The 290kDa protein mTOR is a member of the PI3K families of serine-threonine kinases, belonging to the PI3K-related kinase (PIKK) superfamily. It is in fact distinguished by the presence of a carboxy-terminal serine/threonine kinase domain that is comparable to that of PI3K (Dobashi, Watanabe *et al.* 2011).

Although there is only one *MTOR* gene in mammals, the mTOR product makes up the catalytic subunit of two functionally and structurally different multiprotein complexes: mTORC1 and mTORC2 (Krencz, Sebestyen *et al.* 2020), and which between them differ in terms of their protein components, sensitivity to rapamycin, subcellular localisation, upstream regulation, as well as downstream effectors.

1.8.3.1 mTORC1

Krencz, Sebestyen *et al.* (2020) describe mTORC1 as being made up of:

- mammalian lethal with SEC13 protein 8 (mLST8),
- regulatory-associated protein of mTOR (Raptor) – Sengupta, Peterson *et al.* (2010) report that Raptor has a role in controlling mTORC1 assembly, determining the subcellular localisation of mTORC1, recruiting kinase substrates such as eIF4E-binding protein 1 (4E-BP1), and sensing amino acids,
- mTOR as the catalytic subunit, and
- the two inhibitory subunits DEP domain-containing mTOR-interacting protein (Deptor) and proline-rich Akt substrate of 40kDa (PRAS40) – both subunits are phosphorylated upon activation of the mTOR component of mTORC1, weakening their association with the rest of mTORC1, thus increasing the kinase activity of the complex (Sengupta, Peterson *et al.* 2010).

In their review on targeting PI3K/Akt/mTOR pathway in NSCLC, Fumarola, Bonelli *et al.* (2014) explain that mTORC1 plays a crucial role in the management of various metabolic processes; it stimulates cell growth and proliferation by promoting various anabolic processes, such as the biosynthesis of proteins, lipids, and organelles, and inhibits catabolic processes like autophagy. It therefore facilitates the adaptation to shifting environmental conditions by maintaining the balance between anabolism and catabolism (Krencz, Sebestyen *et al.* 2020).

Autophagy is an mTORC1-regulated process which has undergone extensive research due to its relevance to cancer biology and therapy (Fumarola, Bonelli *et al.* 2014); mTOR functions as a tumour suppressor by preventing the accumulation of damaged proteins and

organelles, as well as a cell survival mechanism that gives established tumours an advantage in terms of growth under stressful situations. Fumarola, Bonelli *et al.* (2014) outline the different mechanisms via which mTORC1 inhibits autophagy, namely:

- by inhibiting the interaction between 5' adenosine monophosphate (AMP)-activated protein kinase (AMPK) and the pro-autophagic UNC-51-like kinase 1 (ULK1) at various sites, thus preventing AMPK-dependent activating phosphorylation;
- by direct phosphorylation and inhibition of the coding gene *ATG13* (autophagy-related protein 13), which is a positive regulator of ULK1;
- indirectly, through phosphorylation and inhibition of the nuclear translocation of transcription factor EB (TFEB), which controls the transcription of genes involved in lysosome synthesis.

Another mTORC1 function is the regulation of translation. It is best described with reference to oncogenesis and is regulated by two downstream effectors (Ciuffreda, Di Sanza *et al.* 2010, Hay, Sonenberg 2004, Zhao, Liu *et al.* 2009):

- the phosphorylated 70 ribosomal S6 kinase 1 (p70S6K1, S6K1) – a serine-threonine kinase that is activated by phosphorylation that is mediated by mTORC1. This activation of S6K1 then phosphorylates the 40S ribosomal protein S6 (rpS6), which increases cap-dependent mRNA translation; and
- the 4E-BP1 – by attaching to and inactivating eIF4E, 4E-BP1 prevents the start of protein translation. However, phosphorylation of 4E-BP1 by mTORC1 promotes the dissociation of the 4EB-P1-eIF4E complex, thereby permitting eIF4E-dependent translation.

1.8.3.2 mTORC2

Similar to mTORC1, the core components mLST8, mTOR and the inhibitory subunit Deptor are found in mTORC2. However, instead of Raptor, there is the scaffold protein rapamycin-insensitive companion of mTOR (Rictor), which is essential for the catalytic activity of mTORC2 (Krencz, Sebestyen *et al.* 2020, Sengupta, Peterson *et al.* 2010). Furthermore, there are also the regulatory subunits mammalian stress-activated protein kinase-interacting protein 1 (mSIN1) and protein observed with Rictor-1 (Protor-1) (Sengupta, Peterson *et al.* 2010); by stabilising one another, mSIN1 and Rictor may help mTORC2 maintain structural integrity.

In a review on mTOR signalling, Laplante and Sabatini (2012) explain that AGC subfamily of protein kinases, among which are Akt, serum and glucocorticoid-induced protein kinase 1 (SGK1), and protein kinase C-α (PKC-α), are regulated by mTORC2:

- through the phosphorylation of a number of effectors, Akt is directly activated by mTORC2 and controls cellular activities including growth, metabolism, proliferation, survival, and apoptosis;
- SGK1, which is a kinase that regulates ion transport and growth, is also directly activated by mTORC2, and its activity is totally inhibited in the absence of mTORC2; and
- activation of PKC-α by mTORC2 regulates cytoskeleton organisation in a cell-type-specific fashion.

1.9 mTOR pathway regulation

In response to different external stimuli, mTOR acts as a cellular sensor to growth factors and nutrients to regulate processes such as cell proliferation, survival, and autophagy

(Ciuffreda, Di Sanza *et al.* 2010, Hare, Harvey 2017). The positive and negative regulators of the mTOR pathway that interact with mTOR have an impact on how this same pathway is regulated; for example, numerous growth factors and their corresponding receptors, including vascular endothelial growth factor and related receptor (VEGFR), insulin-like growth factor (IGF-1) and its receptor (IGFR-1), and human epidermal growth factor and human epidermal growth factor receptor (HER), function as positive growth regulators and send signals to mTOR via PI3K-Akt (Tewari, Patni *et al.* 2022). Example of a negative regulator of mTOR is the phosphatase and tensin homolog (PTEN), which prevents signalling by the PI3K-Akt.

mTOR controls homeostasis, both cellular and organismal, by integrating anabolic and catabolic processes with growth factor signalling, energy, nutrients, as well as oxygen availability (Sengupta, Peterson *et al.* 2010). Upstream signalling for regulation of mTORC1 activity takes place principally via two mechanisms:

- direct alteration of the components that make up mTORC1, or
- regulation of Rheb (as outlined in Section 1.8.2).

What follows is a discussion on how upstream signals influence mTORC1 through the above-mentioned mechanisms.

1.9.1 Growth factors and the mTOR pathway

Growth factors such as insulin and IGF-1 are sustained when food is abundant and thus, through mTORC1, work to support anabolic cell functions like translation, lipid biosynthesis, and nutrient storage. Sengupta, Peterson *et al.* (2010) describe the process by which insulin activates PI3K by binding to its tyrosine kinase receptor, then recruits insulin receptor substrate 1 (IRS1) to the receptor and produces PIP3. What follows is the

recruitment of Akt to the plasma membrane, where PDK1 and mTORC2 activate it by direct phosphorylation; growth factor-activated Akt then phosphorylates PRAS40. By coordinating the activation of the mTOR kinase by the TSC/Rheb pathway with the release of PRAS40 from Raptor, phosphorylation of PRAS40 may help activate mTORC1 by giving it access to substrates including 4E-BP1 and S6K1 (Wang, Harris *et al.* 2008). On the other hand, reduced growth factor signalling inhibits mTORC1 activity; this controls the cells' utilisation of nutrients and energy and therefore aids in their ability to withstand starvation and intermittent fasting (Sengupta, Peterson *et al.* 2010).

In the mTOR domain, growth factor activation restricts the amount of growth factor signalling by mTORC1 through a mechanism known as the "negative feedback loop". In this case however, Sengupta, Peterson *et al.* (2010) explain that unlike traditional feedback loops, inhibition does not take place once a threshold is reached, but mTORC1 appears to suppress the signalling of growth factor in a more gradual and continuous manner. As a result, the acute mTOR inhibitor rapamycin therapy increases PI3K signalling, in contrast to the predicted effect of constitutively active mTORC1 signalling which consistently inhibits PI3K signalling (Harrington, Findlay *et al.* 2004). Moreover, Sengupta, Peterson *et al.* (2010) also report that there are other mechanisms that may also initiate this negative feedback loop, including:

- phosphorylation of IRS1 by S6K1; this results in reduced expression and activity of IRS1, thus hindering the binding to its receptor, leading to its degradation, and ultimately reduced levels of its mRNA (Harrington, Findlay *et al.* 2004), and

- phosphorylation of IRS1 through direct interaction with mTORC1 via Raptor, occurring at locations on IRS1 that eventually inhibit its association with PI3K (Tzatsos 2009).

1.9.2 Carbohydrates (glucose)

Growth factor signalling is used by multicellular organisms to transmit signals to their cells on whether the organism is nourished; however individual cells possess mechanisms that detect the presence of specific nutrients like carbohydrates and amino acids. Sengupta, Peterson *et al.* (2010) describe the mechanisms involved through which the mTORC1 pathway detects particular nutrients.

Low glucose levels lead to decreased adenosine triphosphate (ATP) production, which activates AMPK by increasing the AMP/ATP ratio (Sanders, Grondin *et al.* 2007). Consequently, when AMP binds to AMPK, the upstream activating protein kinase liver kinase B1 (LKB1) (also known as serine threonine kinase 11 (STK11)), phosphorylates the kinase subunit, delaying cell growth and other ATP-consuming processes. As a result, in response to energetic stress, AMPK directly phosphorylates and activates TSC2 and hence suppresses mTORC1 (Shaw 2009), which eventually arrests the cell-cycle.

1.9.3 Amino acids

When the intake of amino acids is reduced, there is deprivation of substrates necessary for protein synthesis as well as the intermediates needed to feed the TCA cycle (tricarboxylic acid cycle, Krebs cycle) and other metabolic processes; the cells therefore respond by inducing and suppressing a number of processes (Sengupta, Peterson *et al.* 2010). The Rag GTPases are thought to interact with mTORC1 and facilitate mTORC1 translocation to a

membrane-bound compartment that harbours the mTORC1 activator, Rheb, where it is then believed that the Rag GTPases activate mTORC1 in response to amino acids. Sancak, Bar-Peled *et al.* (2010) demonstrate that amino acids trigger the translocation of mTORC1 to the lysosomal membranes, where the Rag proteins are found. Rag GTPases interact with one another, are attracted to lysosomes, and are necessary for the activation of mTORC1 by a complex Ragulator. The main event in amino acid signalling to mTORC1 is thus Rag-Ragulator-mediated translocation of mTORC1 to lysosomal membranes.

1.9.4 Oxygen

Hypoxia, or low oxygen levels, block mTORC1 signalling in a number of mechanisms. By limiting metabolic processes like oxidative phosphorylation, hypoxia lowers cellular ATP levels (Sengupta, Peterson *et al.* 2010). As a result, AMPK is activated, which, as previously mentioned, suppresses mTORC1 via TSC2 and Raptor phosphorylation (Figure 1.1). The suppression of mTORC1 in hypoxia is quickly reversed upon reoxygenation, demonstrating the very dynamic manner in which changes in oxygen concentrations govern mTORC1 activity. Findings from a study by Tan and Hagen (2013) demonstrate that the transcription factor hypoxia inducible factor-1α (HIF-1α) or its transcriptional targets are not responsible for the fast response of mTORC1 to changes in oxygen concentrations. Furthermore, the authors show that mTORC1 suppression in hypoxia occurs independently of transcription and new protein synthesis, pointing to a post-translational control of mTORC1 activity in response to oxygen concentration changes. Results of the study also indicate that hypoxia directly regulates mTORC1 at the mTORC1 level, and this may involve a protein containing haem.

1.9.5 DNA damage

When DNA is damaged, cells respond by either repairing themselves or initiating programmed cell death. Whereas mTORC1 inhibition is an important cellular mechanism in response to DNA damage, mTORC1 hyperactivation brought on by TSC1 or TSC2 deficiency makes cells more susceptible to the effects of DNA damage (Sengupta, Peterson *et al.* 2010). The tumour suppressor p53 plays a crucial role in the coordination of responses to DNA damage. Inhibition of mTORC1 at various levels by p53 in response to DNA damage has been explained by different mechanisms, namely:

- transcription activation of genes such as *PTEN* and *TSC2* that work together to inhibit mTORC1 (Feng, Zhang *et al.* 2005);
- through AMPK-dependent control of the TSC1/TSC2 complex (Budanov, Karin 2008, Feng, Zhang *et al.* 2005); and
- p53 rapidly decreases translation initiation by controlling the phosphorylation of S6K and 4E-BP1 (Horton, Bushell *et al.* 2002).

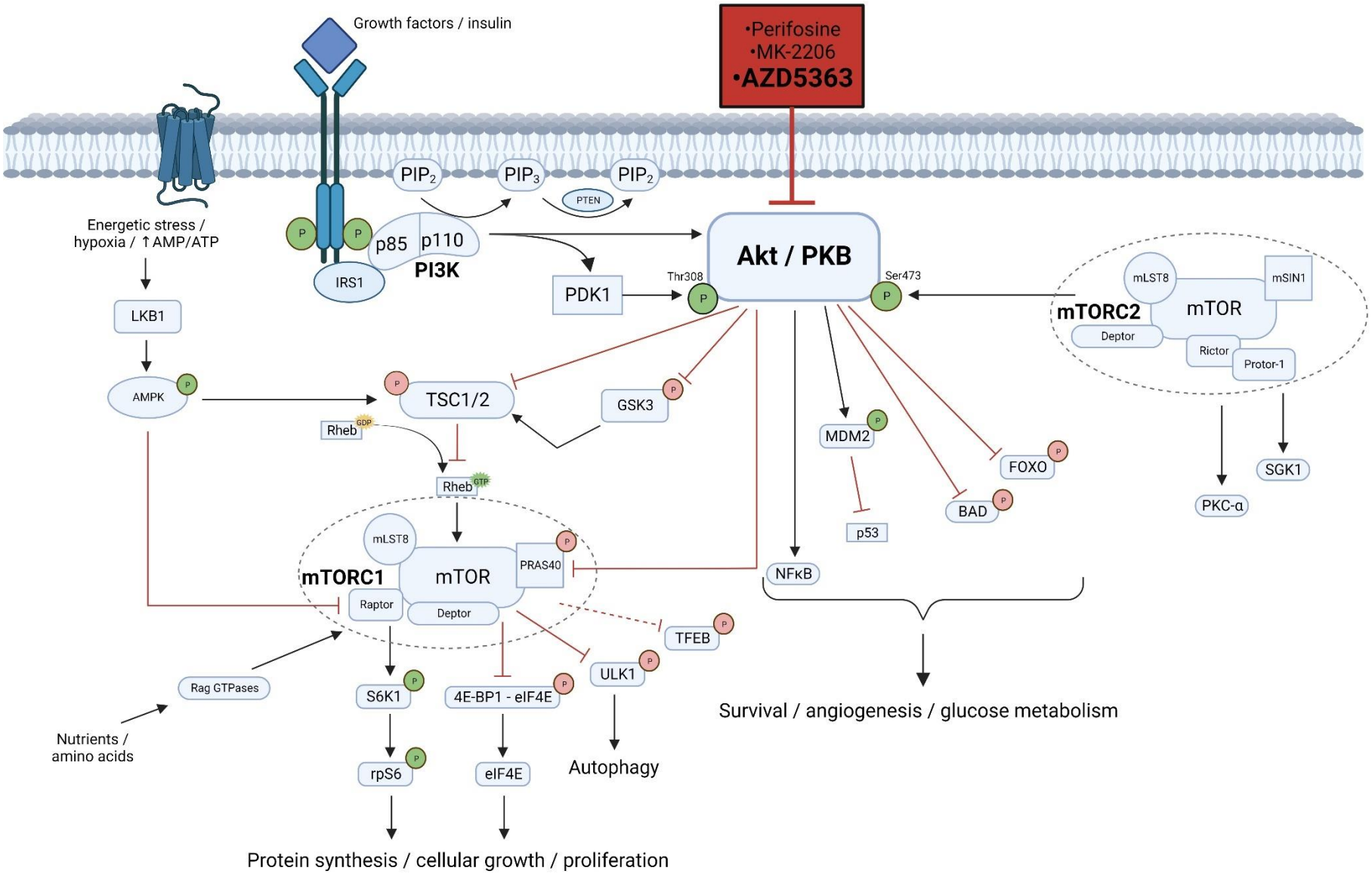
Growth factors / insulin
•Perifosine
•MK-2206
•AZD5363
PIP2
PIP3
PTEN
p85
p110
PI3K
IRS1
Energetic stress / hypoxia / ↑AMP/ATP
LKB1
AMPK
PDK1
Thr308
Ser473
Akt / PKB
mLST8
mSIN1
mTORC2
mTOR
Deptor
Rictor
Protor-1
TSC1/2
GSK3
Rheb
GDP
GTP
MDM2
FOXO
BAD
p53
SGK1
PKC-α
mTORC1
PRAS40
Raptor
NFκB
TFEB
ULK1
Rag GTPases
S6K1
4E-BP1 - eIF4E
Nutrients / amino acids
rpS6
eIF4E
Autophagy
Survival / angiogenesis / glucose metabolism
Protein synthesis / cellular growth / proliferation

Figure 1.1: *A representation of the PI3K/Akt/mTOR pathway. Created with Biorender.com.*

The PI3K/Akt/mTOR pathway is initiated by the activation of growth factor receptor tyrosine kinases. When the PI3K regulatory subunit (p85) binds to the receptor tyrosine kinase, the p110 catalytic subunit is released and translocates to the plasma, where it catalyses the phosphorylation of PIP2 to PIP3. Subsequently, PIP3 localises Akt to the plasma membrane where it undergoes phosphorylation by PDK1. Following a second phosphorylation by mTORC2, the activated Akt separates from the plasma membrane and phosphorylates TSC2, which causes the disassociation and inactivation of the TSC1/2 complex. By associating with different proteins, mTOR forms two physically and functionally distinct complexes, mTORC1 and mTORC2. mTORC1 complex is activated with the loss of the inhibitory effect of the TSC1/2 complex, and the primary mechanism by which the mTORC1 pathway stimulates protein translation and cell proliferation is by activating S6K and blocking eIF4E. The primary downstream targets of the mTORC2 complex are PKC-α, SGK1, and Akt. In addition to mTORC1 activation, Akt enhances cell cycle progression and survival, and inhibits apoptosis through GSK3, FOXO, MDM2, NFκB, and BAD. In conditions of hypoxia and energetic stress, the tumour suppressor LKB1 phosphorylates TSC2 and Raptor to reduce the activity of mTORC1. Directly targeting Akt prevents the PI3K/Akt/mTOR pathway from being abnormally activated by Akt itself, as well as by other sources including PI3K, PTEN, and mTORC2. Arrows represent activating events, whereas bars indicate inhibitory events. 'P' in a green circle signifies activating phosphorylation, and 'P' in a red circle indicates inhibitory phosphorylation.

4E-BP1	Eukaryotic initiation factor 4E-binding protein 1
Akt	Protein kinase B (PKB)
AMP	5' adenosine monophosphate
AMPK	5' adenosine monophosphate-activated protein kinase
ATP	Adenosine triphosphatase
BAD	BCL2-antagonist of cell death
Deptor	DEP domain-containing mTOR-interacting protein
eIF4E	Eukaryotic initiation factor 4E
FOXO	Forkhead box O
GSK3	Glycogen synthase kinase 3
GTP	Guanosine 5' triphosphate
IRS1	Insulin receptor substrate 1
LKB1	Liver kinase B1
MDM2	Minute double minute 2
mLST8	Mammalian lethal with SEC13 protein 8
mSIN1	Mammalian stress-activated protein kinase-interacting protein 1
mTOR	Mammalian target of rapamycin
mTORC1	Mammalian target of rapamycin complex 1
mTORC2	Mammalian target of rapamycin complex 2
NFκB	Nuclear Factor kappa-light-chain-enhancer of activated B cells
PDK1	3-phosphoinositide-dependent kinase 1
PI3K	Phosphatidylinositol 3-kinase
PIP2	Phosphatidylinositol 4,5-bisphosphate
PIP3	Phosphatidylinositol 3,4,5-trisphosphate
PKC-α	Protein kinase C-α
PRAS40	Proline-rich Akt substrate of 40kDa
Protor-1	Protein observed with Rictor-1
PTEN	Phosphatase and tensin homolog
Raptor	Regulatory-associated protein of mTOR
Rheb	Ras homologue enriched in brain
Rictor	Rapamycin-insensitive companion of mTOR
rpS6	Ribosomal protein S6
S6K1	Phosphorylated 70 ribosomal S6 kinase 1
SGK1	Serum and glucocorticoid-induced protein kinase 1
TFEB	Transcription factor EB
TSC	Tuberous sclerosis complex
ULK1	UNC-51-like kinase 1

1.10 Importance of PI3K/Akt/mTOR signalling pathway in cancer

In both physiological and pathological settings, the PI3K/Akt/mTOR signalling pathway is essential, and due to its strong linkages, it is sometimes viewed as a single, distinct route that interacts with a number of other pathways, including Ras, MAPK, and HIFs (Tewari, Patni *et al.* 2022). A competitive growth advantage, metastatic competence, angiogenesis, and therapy resistance are all consequences of the significant disturbance of control over cell growth and survival caused by the activation of this important pathway (Costa, Han *et al.* 2018, Porta, Paglino *et al.* 2014, Rosenberg, Yoon *et al.* 2018).

Different malignancies have been shown to have somatic mutations and gene amplifications that code for the various elements of the PI3K/Akt/mTOR signalling cascade (Tewari, Patni *et al.* 2022), as will be discussed below.

1.10.1 PI3K

With regards to the 1A PI3Ks, Solomon and Pearson (2009) cite numerous studies that have found a relationship between their abnormal activation and cancer development. Samuels, Wang *et al.* (2004) report that the p110α catalytic subunit of the 1A PI3Ks, which is encoded for by the *PIK3CA* gene, is the most common isoform that is implicated in malignancies, where presence of gene mutations or amplifications of *PIK3CA* have been observed; in approximately 80% of the time, such genetic changes occur in the p110α helical and kinase domains (Mayer, Arteaga 2016). While kinase domain mutations improve the retention of p110α at the plasma membrane, helical domain mutations boost catalytic activity by lowering the regulation of p110α by p85 or enhancing the interaction of p110α with IRS1; cellular transformation, growth factor- and anchorage-independent growth, and resistance to programmed cell death (anoikis) are all brought about by these gain-of-function

pathways. Samuels, Wang *et al.* (2004) found that up to 36% of hepatocellular tumours, 26% of breast cancers, and 26% of colon cancers have been shown to have *PIK3CA* mutations; lower incidences of such mutations were reported in ovarian, glioma and gastric malignancies. Amplifications of the *PIK3CA* gene are also frequent, more so in squamous cell carcinomas; Tan (2020) indicates they have been found in up to 69% of cervical malignancies, 66% of lung SCCs, 42% of head and neck cancers, and in appreciable amounts in gastric, thyroid, breast, oesophageal, and lung ACs.

In a review on the roles of PI3K isoforms, Thorpe, Yuzugullu *et al.* (2015) report that human malignancies have also been found to harbour somatic mutations in the genes encoding the regulatory subunits of class I PI3Ks, including *PIK3R1* (which codes for the regulatory subunits p85α, p55α, and p50α), *PIK3R2* (which codes for the regulatory subunit p85β), and *PIK3R5* (which codes for the regulatory subunit p101). Most of these mutations, which have been found in endometrial carcinomas and pancreatic malignancies, among other cancers, affect the inter-SRC homology 2 (iSH2) domain of p85, the area of the protein that interacts with p110, indicating that this domain may be a mutation hot spot. Some of these iSH2 domain mutations retain their ability to stabilise and bind to p110 isoforms, but because they are less capable of inhibiting p110, they promote increased PI3K activity and transformation.

Malignancies such as breast and hepatocellular tumours were reported to have diminished *PIK3R1* expression, with *PIK3R1* mRNA levels being inversely linked to malignancy grade and metastasis (Cizkova, Vacher *et al.* 2013). Moreover, in a study on mice, Taniguchi, Winnay *et al.* (2010) found that ablation of *PIK3R1* exacerbated epithelial neoplasia as a result of PTEN loss and led to the formation of aggressive liver tumours, showing that

p85α can adversely regulate PI3K signalling in cancer and has tumour-suppressing activities in some tissues.

Alterations in additional regulatory isoform-encoding genes have also been identified, namely the documented increase in *PIK3R2* expression in breast and colon malignancies (Cortes, Sanchez-Ruiz *et al.* 2012); *in vivo*, wild-type p85β overexpression boosted PI3K pathway activation in cells and tumour formation in mice. Furthermore, Thorpe, Yuzugullu *et al.* (2015) cite studies that have found somatic *PIK3R2* mutations in endometrial and colorectal malignancies. All reported *PIK3R2* mutations are substitutions with no hotspot regions, and much like some p85α, mutations in p85β boost PI3K activation without impacting p110 binding, implying that PI3K regulatory isoforms contribute to carcinogenesis in multiple mechanisms.

1.10.2 mTOR

Activation of mTOR signalling in cancer is primarily dependent on three levels of mechanisms, as explained by Conciatori, Ciuffreda *et al.* (2018):

- mutations in the *MTOR* gene, which result in a constitutively hyperactive mTOR signalling cascade – When Grabiner, Nardi *et al.* (2014) analysed tumour genome sequencing datasets, they identified 33 *MTOR* mutations that are involved in the hyperactivation of mTOR signalling in distinct cancer types, the majority of which cluster in six distinct areas of the c-terminal region of mTOR in a variety of cancers, whereas one was found to be particularly prevalent in kidney cancer;
- mutations in the components that make up mTORC1 and mTORC2, and which give rise to mTOR signalling activation – In NSCLC, notably in SCC, Cheng, Zou *et al.* (2015) found the mTORC2 component Rictor to be amplified; a similar observation

was reported in breast cancer by Joly, Hicks *et al.* (2016). Such amplification is strongly associated with a poor prognosis and short survival (Conciatori, Ciuffreda *et al.* 2018). Furthermore, nearly 70% of patients with high-Akt-activated gliomas and HER2-positive breast malignancies were shown to have overexpression of Rictor, which increased Akt activity and accelerated tumour progression (Joly, Hicks *et al.* 2016, Masri, Bernath *et al.* 2007); and

- most importantly, aberrant mTOR signalling can also result from mutations in upstream genes, that is, loss-of-function suppressor gene mutations and gain-of-function oncogene mutations – The PI3K signalling pathway, which is upstream of both mTOR complexes, frequently experiences various types of alterations in its constituent parts in cancer, including mutation and amplification of *PIK3CA* (as discussed in Section 1.10.1) and Akt (as will be explained in Section 1.10.3), as well as amplification of growth factor receptors EGFR and IGFR-1 (Guertin, Sabatini 2007, Zhao, Liu *et al.* 2009). Moreover, Efeyan, Sabatini *et al.* (2011) report that in cancer, mTOR activation is caused by the loss of activities in tumour suppressor genes such *PTEN* (see Section 1.10.4), *TP53*, *TSC1/TSC2* (refer to Section 1.10.6), and *STK11*.

Downstream of mTORC1, disruption of protein synthesis plays a critical role in carcinogenesis at the 4E-BP1/eIF4E level; by promoting the translation of specific pro-oncogenic proteins, eIF4E regulates cell survival, cell cycle progression, angiogenesis, energy consumption, and metastasis. Furthermore, in order to keep high levels of cell proliferation, mTOR activation also increases ribosome biogenesis (Laplante, Sabatini 2012). As explained earlier (Section 1.9), nutrient sensing primarily stimulates mTORC1, and metabolic alterations in cancer cells, in turn, sustain mTORC1 activity (Mossmann, Park

et al. 2018, Saxton, Sabatini 2017). In order to drive gene transcription in lipid synthesis, mTORC1 activates the critical transcription factor sterol regulatory element-binding protein 1 (SRE-BP1) via Akt activation and phosphorylation of Lipin1 and S6K1 (Peterson, Sengupta *et al.* 2011); increased levels of SRE-BP mRNA and protein are associated with mTORC1 upregulation in human breast cancer tissues (Ricoult, Yecies *et al.* 2016).

1.10.3 Akt1

In 2007, Carpten, Faber *et al.* (2007) identified a somatic mutation of *AKT1*, involving a substitution of glutamic acid to lysine at amino acid 17 (E17K), and was reported in ovarian, colorectal and breast carcinomas. $AKT1^{E17K}$ effects are more comparable to those brought on by *PTEN* loss. When evaluated on genetically engineered mice models (GEMMs), such mutation activated Akt1 by pathological localisation to the plasma membrane, resulting in downstream signal stimulation, cell transformation, and induced leukaemia. Moreover, in line with what has been seen in human cellular models, Malanga, Belmonte *et al.* (2016) highlight the significance of Akt1 activation as an early event that drives proliferation in the mouse lung and demonstrate that $AKT1^{E17K}$ stimulates bronchial and bronchio-alveolar hyperplasia in mice and collaborates with chemical carcinogens to cause cancer. The type of cell in which the oncogene is expressed possibly influences the reported difference in tumour histotype between human and mouse tumours. Also, Bleeker, Felicioni *et al.* (2008) report that this $AKT1^{E17K}$ variant was only found in ductal and lobular histotypes of breast-originating neoplasms and was mutually exclusive with the *PIK3CA* (E454K or H1047R) alleles. These findings therefore suggest that *AKT1* mutations appear to be tissue-specific, and it is possible that the cell and tissue environment have a direct impact on the activity

of mutant *AKT1* in oncogenic PI3K signalling, an observation which has also been suggested by Mancini, Lien *et al.* (2016).

In addition to the changes outlined above, somatic changes in other components of the PI3K/Akt/mTOR pathway, such as genes of *PTEN*, inositol polyphosphate-4-phosphatase type II B (*INPP4B*), and *TSC1/2*, are found at varying frequencies across a variety of tumour types; all of them lead to abnormal pathway activation based on their functional roles, thus resulting in PI3K dependency in tumours (Efeyan, Sabatini *et al.* 2011, Mayer, Arteaga 2016).

1.10.4 PTEN

Among cancer-related genes that encode signalling molecules for the PI3K/Akt/mTOR pathway, *PTEN* is one of the most frequently mutated (Aoki, Fujishita 2017, Tian, Li *et al.* 2019). The function of the phosphatase PTEN is to dephosphorylate PIP3, thus inhibiting class I PI3Ks; therefore, loss or decrease in levels of *PTEN* gives rise to PI3K/Akt/mTOR pathway activation (Aoki, Fujishita 2017). By using GEMMs, numerous studies have been conducted on the roles of *PTEN* loss or mutation in neoplastic transformation. Milella, Falcone *et al.* (2015) report that a significant number of human malignancies frequently lose PTEN function due to somatic mutations, gene silencing, or epigenetic processes. The authors further explain that the related disorders PTEN hamartoma syndromes (PHTS) are a consequence of *PTEN* germline mutations, which result in uncontrolled cell proliferation, and therefore tumorigenesis; this is brought about by mutations that result in an absent or inactive protein. With over 80% of individuals harbouring hereditary *PTEN* mutations, Cowden syndrome is the PHTS disease that is best documented (Eng 2003). In fact, Mester, Moore *et al.* (2013), in their review on patients with PHTS, report that Cowden syndrome patients have a significant lifetime risk (LR) of developing benign and malignant tumours of

the breast (LR – 85%), thyroid (LR – 35%), kidney (renal cell carcinoma) (LR – 33%) and endometrium (LR – 28%), which all correspond to sporadic cancer types that frequently show somatic *PTEN* inactivation. Furthermore, in several sporadic tumour types, the PTEN tumour suppressor is usually deleted, either completely or partially. Examples include neoplastic conditions, such as melanoma, glioblastoma, colon, and endometrial malignancies, where *PTEN* is somatically inactivated (Bonneau, Longy 2000).

1.10.5 INPP4B

Gewinner, Wang *et al.* (2009) demonstrate that the phosphoinositide phosphatase INPP4B functions similarly to PTEN in inhibiting the PI3K/Akt signalling pathway, which in turn inhibits the growth of tumours. Studies on breast cancer clinical samples revealed that a low level of INPP4B was linked to a higher tumour grade and poorer prognosis. In xenograft experiments on human mammary epithelial cells, INPP4B knockdown led to proliferation that was anchorage-independent and enhanced migratory/invasive behaviour. The authors further indicate that most basal-like breast malignancies, as well as a considerable proportion of ovarian cancers and melanomas, usually lack INPP4B. Although these findings supported INPP4B's role as a tumour suppressor, more recent research suggests that INPP4B also plays an oncogenic role in leukaemia, breast cancer, and colorectal cancer (Dzneladze, He *et al.* 2015, Gasser, Inuzuka *et al.* 2014, Guo, Chi *et al.* 2016). These results therefore imply that, depending on the cellular environment, INPP4B can either promote tumour growth or suppress it.

1.10.6 TSC1/TSC2

Tuberous Sclerosis and subsequently, benign tumorigenesis are caused by the inactivation of TSC1 or TSC2, which are negative regulators of mTORC1. Though mutations in TSC1 and

TSC2 are considerably less common than those in components further upstream in the PI3K/Akt/mTOR signalling pathway, they have been linked to urothelial carcinoma, bladder cancer, pancreatic neuroendocrine tumours, and clear cell renal carcinoma (Jiao, Shi *et al.* 2011, Platt, Hurst *et al.* 2009, Sjödahl, Lauss *et al.* 2011).

1.11 Importance of PI3K/Akt/mTOR signalling pathway in lung cancer

The PI3K/Akt/mTOR pathway has been strongly linked to the development of NSCLC and its progression (Tan 2020), and the most downstream effectors, eIF4E and rpS6, are able to transform cells, are overexpressed in both SCC and AC, and are also poor prognostic markers (Chen, Tan *et al.* 2015, Dobashi, Watanabe *et al.* 2011).

In a review on this signalling cascade, Yip (2015) cites numerous studies which have shown that it is abnormally activated often in NSCLC, with a 50–70% overexpression of phosphorylated Akt. Constitutive activation of the signalling pathway may be caused by *EGFR* mutations and aberrant gene fusions involving echinoderm microtubule-associated protein-like 4 and anaplastic lymphoma kinase (EML4-ALK), that activate both key downstream signalling pathways Ras/MAPK/ERK and PI3K/Akt/mTOR, and which give rise to uncontrolled cell growth and proliferation. Therefore, finding new treatments that target this signalling pathway has garnered significant research interest.

Genetic disorders that contribute to the dysregulation of signal transduction in the PI3K/Akt/mTOR pathway include *PIK3CA* mutation and amplification, *PTEN* loss, and *RICTOR*, *AKT1* and *STK11* mutations (Cheng, Zou *et al.* 2015, Janku, Yap *et al.* 2018, Papadimitrakopoulou 2012); Kirsten rat sarcoma (*KRAS*) mutations also have a role since the Ras/MAPK/ERK pathway interacts with PI3K/Akt/mTOR (Carracedo, Pandolfi 2008). In some histological subtypes of NSCLC, these genetic alterations are more common than in

others. Adenocarcinoma, for example, is more likely to have *EGFR*, *KRAS*, and *EML4-ALK* rearrangements than squamous cell carcinoma (O'Byrne, Gatzemeier *et al.* 2011, Wong, Leung *et al.* 2009, Zhu, Da Cunha Santos *et al.* 2008), whereas SCC is more likely to have *PIK3CA* amplification (Scheffler, Bos *et al.* 2015, Spoerke, O'Brien *et al.* 2012). Moreover, whereas O'Byrne, Gatzemeier *et al.* (2011) report that in both NSCLC with squamous and non-squamous histology, *PTEN* loss is equally prevalent, a study carried out by Spoerke, O'Brien *et al.* (2012) has revealed that SCC may exhibit entire loss of *PTEN* expression more frequently than AC. Additionally, Chaft, Arcila *et al.* (2012) found that in contrast to *KRAS* and *PIK3CA* co-mutations, which are prevalent in adenocarcinoma, *EGFR*, *KRAS*, and *EML4-ALK* rearrangement are mutually exclusive. With regards to *STK11* mutations, both Gao, Sun *et al.* (2010) and Matsumoto, Iwakawa *et al.* (2007) found that these frequently co-occur with *EGFR* and/or *KRAS* mutations and are more prevalent in NSCLC with non-squamous cell histology than squamous cell histology.

Significant numbers of NSCLC tumours have also been shown to exhibit upregulation of the mTOR pathway, with overexpression of phosphorylated (activated) mTOR in up to 90% of patients with AC, 60% of patients with LCC, and 40% of patients with SCC (Dobashi, Suzuki *et al.* 2011). Furthermore, with a higher prevalence in AC, S6K and 4E-BP1, which are downstream products of mTOR activation, have also been found in up to 58% and 25% of NSCLC specimens, respectively (Dobashi, Watanabe *et al.* 2011). Tan (2020) also indicates that in early-stage NSCLC, mTOR activity may also be a poor prognostic factor, and even refers to studies that linked increased mTOR expression to poor survival (Dhillon, Mauri *et al.* 2010, Gately, Al-Alao *et al.* 2011).

According to growing body of research, Rictor is overexpressed in an unfavourable manner across a wide range of cancer types, and this is linked to poor survival (Gkountakos, Pilotto *et al.* 2018). Two potential causes of abnormal Rictor expression in cancer which have been identified to date are gene amplification, and epigenetic control, primarily by microRNAs. The analysis of The Cancer Genome Atlas database revealed that 16% of SCC and 10% of AC, respectively, have *RICTOR* amplification (Lawrence, Sivachenko *et al.* 2012); these findings were corroborated by the evaluation of a separate lung cancer cohort conducted by Cheng, Zou *et al.* (2015). When Krencz, Sebestyén *et al.* (2016) evaluated the expression of Rictor protein in primary and brain metastatic AC, brain metastases were shown to express more Rictor and Rictor/mTOR, when compared to primary AC; the authors also documented a correlation between Rictor expression and a higher stage of AC. Intriguingly, AC with brain metastasis had higher levels of Rictor expression (67%) than those without (28%).

The Akt pathway has also been shown to be upregulated in a substantial portion of NSCLC patients (Tan 2020). In a thorough investigation into the function of Akt signalling, Scrima, de Marco *et al.* (2012) found that in the cohort of NSCLC patients investigated, the Akt pathway was active in 62% of instances, and substantial Ser473 phosphorylation was found more frequently in individuals with advanced disease (TNM stage III vs stage II) and higher grade. They also reported Akt1 and Akt2 to be overexpressed in 16% and 12% of AC, and 19% and 32% of SCC, respectively. Their findings also show that, among all genes, only p110α overexpression was significantly related to Akt activation in NSCLC.

As already indicated above, the participation of the PI3K/Akt/mTOR pathway in tumours with other known activating mutations, such *EGFR* and *KRAS*, also highlights the

significance of this route. According to a study by Dobashi, Koyama *et al.* (2011), the Akt/mTOR pathway is constitutively active in 67% of patients with *EGFR* mutations. Another study by Dobashi, Suzuki *et al.* (2011), in which 18% of specimens had positive staining for activated EGFR, activated Akt and activated mTOR, highlighted the significance of this signalling cascade. The significance of Akt activation may potentially be connected to the emergence of treatment resistance. Furthermore, Jacobsen, Bertran-Alamillo *et al.* (2017) suggest that, according to preclinical data, Akt activation in *EGFR* mutant NSCLC may result in acquired resistance to EGFR inhibitors. The PI3K/Akt/mTOR pathway is therefore a compelling target for anticancer therapy in NSCLC due to the extensive downstream signalling effects it has on the onset and progression of malignancy, as well as its potential impact on response and resistance to conventional therapies (Tan 2020).

1.12 Rationale for combination therapy

Current cancer treatment options include chemotherapy, surgery, radiation, hormone therapy, immunotherapy, and targeted therapy. Though chemotherapy continues to be the mainstay treatment of choice for most tumour types due to its advantages over alternative medicines, including ease of administration, good patient compliance, and superior therapeutic outcomes (Chen, Yang *et al.* 2016), there are still a lot of issues with its practical use. A significant downside is the fact that chemotherapeutic drugs kill cells in both cancer and healthy tissues, with side effects manifesting in immunosuppression, hair loss, and severe gastrointestinal symptoms, among others. The environment surrounding tumours is also a barrier to the effectiveness of chemotherapy. Another important limitation is drug resistance (Holohan, Van Schaeybroeck *et al.* 2013), of which there are two types:

- intrinsic resistance, where cancer cells already contain resistance-mediating factors that render the treatment ineffective before chemotherapy is administered, and
- acquired resistance, which develops in cancers that were initially sensitive to treatment; this may be due to mutations that occur during treatment, as well as other adaptive responses like increased expression of the therapeutic target and activation of substitute compensatory signalling pathways.

Multidrug resistance (MDR), which is typically linked to chemotherapy failure and higher cancer-related mortality, refers to the various mechanisms by which cancer cells exhibit resistance to multiple drug treatments (Holohan, Van Schaeybroeck *et al.* 2013). The active interaction of cancer cells with the extracellular environment leads to the formation of the complex tumour microenvironment, which ultimately may encourage the growth of MDR and tumour metastasis.

Polymorphisms in genes encoding drug targets, drug transporter proteins, and enzymes involved in drug metabolism, are among the most significant genotypic differences for numerous clinical uses (Hamidovic, Hahn *et al.* 2010). Additionally, genetic variations linked to changes in the quantity or activity of transport proteins cause these proteins to lose their physiological purpose and change the way that different medicines are transported. The ATP-binding cassette (ABC) transporters are transmembrane proteins responsible for transporting a wide range of substrates across lipid intracellular and extracellular membranes, including metabolites, carcinogens, and cytotoxic drugs (Zawadzka, Jeleń *et al.* 2020). A clinically significant transport protein that has been thoroughly investigated is p-glycoprotein; it is encoded for by the ABC gene B1 (*ABCB1*), also referred to as the multidrug resistance gene (MDR1), which is polymorphic, and whose variations may be

related to the functioning of p-glycoprotein, with an increased susceptibility to the development of a number of diseases, including cancer, as well as interindividual variances in drug response and toxicity. In fact, when Zhong, Guo *et al.* (2019) assessed the impact of *ABCB1* polymorphism on the response and toxicity to taxane-based chemotherapy in patients with lung cancer, they observed poor response as well as an increased predisposition to neurotoxicity.

The most extensively researched variant of this gene is a frequently synonymous C to T transition at nucleotide position 3435 in exon 26 (3435 C>T), which has been strongly linked to lower mRNA expression and protein stability, and possibly, impaired drug transport capacity (Jeleń, Żebrowska-Nawrocka *et al.* 2023). When Subhani, Jamil *et al.* (2015) investigated the role of *ABCB1* C3435T polymorphisms in lung cancer patients undergoing chemotherapy, they reported a 5.23-fold increased risk of lung cancer development. Though these results differ from those of Sinués, Fanlo *et al.* (2003) and Gervasini, Carrillo *et al.* (2006), who did not find any evidence linking polymorphism at position C3435T to an increased risk of lung cancer, the findings of Subhani and colleagues were corroborated by Zawadzka, Jeleń *et al.* (2020), who suggested that the increased risk is linked to the presence of at least one T allele of polymorphism at the C3435T position. Furthermore, the TT genotype of the investigated polymorphism increased the risk of lung cancer by 5.78 times and was found to be more frequent in the SCC cohort than the AC subgroup.

Drug resistance led to the need to develop a thorough understanding of causes of MDR to increase the effectiveness of cancer treatment. One such method is the clinical use of combinations of anticancer drugs which, when compared to monotherapy, have been found to increase efficiency of treatment for cancer patients (Chen, Jia *et al.* 2009). When

used in an optimal synergistic ratio, reasonable combination treatment can greatly enhance therapeutic benefit (Hu, Sun *et al.* 2016), lowers the therapeutic dose required for treatment, minimises side effects, and prevents the emergence of drug resistance (Chou 2006). In fact, when Wang, Xu *et al.* (2021) investigated the addition of an ALK inhibitor to AZD5363 in gastric cancer, both *in vitro* and *in vivo*, they reported that, with the use of lower doses than those used clinically, there was an increased sensitivity to AZD5363 and a synergistic antitumour effect, as evidenced by the considerable decrease in gastric cancer cell proliferation and an increase in apoptosis.

In the phase I study conducted by Smyth, Tamura *et al.* (2020), patients received either intermittent AZD5363 at a dose of 480 mg twice daily for 4 days, and 3 days off, or a lower intermittent dose of 400mg twice daily for 4 days, and 3 days off, this time in combination with fulvestrant. There were less dose interruptions, reductions, or discontinuations in the combination cohort, due to lower incidences of treatment-related adverse effects. Furthermore, a favourable ORR in patients receiving the combination therapy was also observed. As the combination treatment was better tolerated, the authors attributed the lower dose of AZD5363 in the combination cohort to have contributed to this response. Moreover, in the CAPItello trial (Turner, Oliveira *et al.* 2023), in which participants were administered intramuscular fulvestrant (initially every 14 days for the first 3 doses, and continued every 28 days thereafter), in combination with intermittent AZD5363 (twice daily for 4 days, followed by 3 days off) or matching placebo, the investigators suggested that the selected intermittent schedule may have accounted for the decreased toxic effect profile of AZD5363 and the lower prevalence of hyperglycaemia. Similarly, in a dose-escalation study on patients with metastatic castration-resistance prostate cancer, and who were administered a combination of AZD5363 and enzalutamide, Kolinsky, Rescigno

et al. (2020) reported that despite such a combination resulted in a significant reduction in plasma exposure of AZD5363 (when compared to AZD5363 monotherapy), this did not seem to significantly inhibit the phosphorylation of GSK3β and PRAS40. This study also observed that the typical adverse effects usually associated with AZD5363, including diarrhoea, hyperglycaemia, and maculopapular rash, were indeed lower that those reported in single-agent phase I studies of the drug.

1.13 Combination therapy in advanced/metastatic NSCLC

In a review on metastasis, Steeg (2016) explains that one of the main causes of death of cancer patients is tumour metastasis, which is initiated by the infiltration of cancer cells to surrounding tissues, and that is mediated by a variety of mechanistic routes. However, much like the repertoire of RTKs, where the inhibition of one pathway can be countered by activation of another kinase or a downstream mutation, the inhibition of one metastatic pathway may not be sufficient. The author goes on to point out that the entire metastatic process offers a possible therapeutic target for individuals with localised disease, which unfortunately is of limited application in lung cancer, particularly at diagnosis. In fact, more than 25% of all diagnosed thoracic tumour cases are classified as regional diseases, at which point cancer cells are too small to be captured by imaging, but they would have most likely dispersed throughout the body and are either latent in distant organs or starting to colonise. In a systematic review, Peters, Bexelius *et al.* (2016) explain that the brain or CNS is a common location of metastasis for NSCLC, and treatment further increase its cumulative incidence, thus worsening prognosis and quality of life. Efflux transporters such as the ABCB1, referred to in Section 1.13, may further complicate treatment by restricting drug penetration across the blood-brain barrier, giving rise to intracerebral drug resistance

and pharmacologic failure. In fact, Veerman, Boosman *et al.* (2023) observed significantly lower trough levels of the EGFR-TKI osimertinib in a cohort of patients with *ABCB1* 3435 C>T single nucleotide polymorphism, which may have resulted in lower drug absorption due to compromised drug transport through the basolateral intestinal cell membrane into the systemic circulation.

As already discussed in Section 1.6, systemic therapy is generally made available to patients with stage IV NSCLC and a PS of 0 to 2. In fact, regardless of age, sex, histology, or PS, ESMO clinical practice guidelines refer to two meta-analyses that demonstrated benefits of chemotherapy compared to best supportive care, including a 23% lower risk of death, a 9% increase in 1-year survival, and an improvement in quality of life (Hendriks, Kerr *et al.* 2023), and when compared to chemotherapy alone, a number of combination regimens have effectively shown enhanced OS. Moreover, in patients with a PS of 2, and compared to best supportive care, chemotherapy extends overall survival and improves quality of life. Rather than showing a reduction in the size of known metastatic lesions, most preclinical metastasis therapy investigations indicate a notable delay in the formation of metastases, an endpoint which should be helpful in adjuvant setting trials for the therapeutic prevention of an initial metastasis or the prevention of subsequent metastases in patients with limited, treated metastatic illness (Steeg 2016). Several antimetastatic treatments are being developed, but since they are cytostatic rather than cytotoxic, they disrupt colonisation routes instead of eliminating a cancer cell that is actively growing, such that only in the unlikely event that such agents coincidentally synergise with RT or chemotherapy would an existing lesion diminish. With the use of chemotherapy in advanced lung cancer, the observed positive therapeutic effect is often temporary. Steeg (2016) refers to phase III randomised maintenance treatment trials in which, following

standard initial chemotherapy, patients with advanced cancer were randomised to either a long course of investigational treatment (such as chemotherapy or mutation inhibitor therapy) or placebo until unacceptable toxicity or progression occurred. Prognostic factor included OS or PFS. The author goes on to suggest that similar designs could be adapted to incorporate an agent that prevents metastasis, to stop additional colonisation, or to induce dormancy.

1.14 Inhibitors of the PI3K/Akt/mTOR signalling pathway

As already explained, all the crucial elements of carcinogenesis, including cell proliferation, survival, and motility, are enhanced by activation of the PI3K/Akt/mTOR signalling pathway. Given the significance of this pathway, pharmaceutical companies and academic research facilities are currently collaborating to develop inhibitors, under various categories, that specifically target the key components of the pathway. The classes of drugs known to target the PI3K/Akt/mTOR pathway include pan-class I PI3K inhibitors, isoform-specific inhibitors (such as selective PI3K inhibitors), Akt inhibitors, allosteric mTOR inhibitors, mTOR kinase inhibitors, and dual PI3K/mTOR inhibitors (Fumarola, Bonelli *et al.* 2014, Tarantelli, Lupia *et al.* 2020) (Table 1.1).

Single-agent administration of these inhibitors is associated with stable disease and manageable toxicity in the majority of cancer studies, with fatigue, rash and metabolic abnormalities (such hyperglycaemia) being some of their frequent side effects (Cheng, Shcherba *et al.* 2014). However, there are still many unanswered questions surrounding the use of PI3K/Akt/mTOR pathway inhibitors, including which drugs or classes of drugs should be used in specific cancer contexts, and whether the development of logical combination strategies will improve clinical benefit and lead to eventual approval of such

drugs (Janku, Yap *et al.* 2018). Krencz, Sebestyen *et al.* (2020) refer to early clinical results which indicate that combinations of chemotherapy or other targeted therapies with PI3K/Akt/mTOR pathway inhibitors are more successful than monotherapy alone.

***Table 1.1**: List of PI3K/Akt/mTOR inhibitors, including some examples*

Class of PI3K/Akt/mTOR inhibitor	**Target**	**Examples**
Pan-class I PI3K inhibitors	Catalytic domain of class IA PI3K p100 subunits	GDC-0941 (pictilisib) PX-886 BKM120 (buparlisib) XL-147 (pilaralisib)
Isoform specific inhibitors	Catalytic subunits α, β or γ of the class I PI3K	BLY719 (alpelisib) – inhibits Iα isoform GSK2636771 – inhibits Iβ isoform IPI-549 – inhibits Iγ isoform
Akt inhibitors	Akt proteins – isoenzyme-specific or targeting multiple Akt isoforms	KRX-0401 (perifosine) MK-2206 AZD5363 (capivasertib)
Allosteric mTOR inhibitors	Elevated mTOR signalling	CCI-779 (temsirolimus) RAD001 (everolimus) MK-8669 (ridaforolimus, AP23573)
mTOR kinase inhibitors	Compete with ATP for binding with the mTOR kinase domain	AZD8055 AZD2014 (vistusertib) INK128 (sapanisertib)
Dual PI3K/mTOR inhibitors	Catalytic domains of mTORC1/2 and p110 subunits	NVP-BEZ235 (dactolisib) PKI-587 (PF-05212384, gedatolisib)

For example, targeting multiple PI3K isoforms as well as mTOR is an intriguing alternative to focusing on a single PI3K isoform or mTOR alone (Tarantelli, Lupia *et al.* 2020). Indeed, the structural similarities between the catalytic isoform of the p110 subunit and mTOR suggest that targeting two critical components of the same pathway could increase efficacy, prevent feedback inhibition brought on by mTOR inhibition, and reduce the risk of developing drug resistance that would undoubtedly arise from using drugs that only target one isoform of the p110 subunit. Also, dual PI3K/mTOR inhibitors have demonstrated, at

least in the preclinical environment, an improvement above what was accomplished by targeting separately single PI3K isoforms, all PI3K isoforms, or mTOR (Tarantelli, Lupia *et al.* 2020).

1.14.1 Pan-class I PI3K inhibitors

The target of pan-class I PI3K inhibitors is the catalytic domain of class IA PI3K p110 subunits, the class most frequently associated with cancer. By selectively inhibiting this class, anticancer efficacy may be achieved without causing significant damage by inhibiting other PI3K classes involved in important cellular functions (Papadimitrakopoulou 2012). Pan-class I PI3K inhibitors include GDC-0941 (pictilisib), PX-866, BKM120 (buparlisib), and XL-147 (pilaralisib).

1.14.1.1 GDC-0941

GDC-0941 (pictilisib) has been tested in phase I trials, either as monotherapy, or in combination with chemotherapy. Maculopapular rash was the dose-limiting toxicity in a phase IA dose-escalation trial of individuals with advanced solid tumours (Sarker, Ang *et al.* 2015). Another phase I dose-escalation study found that the combination of GDC-0941 with the EGFR tyrosine kinase inhibitor erlotinib was safe and effective in patients with advanced solid tumours (Leong, Moss *et al.* 2017). In this trial, modest anti-tumour benefits were seen, in that 19 (33.3%) of 57 patients had stable disease and 2 (3.5%) of them experienced partial response. In a phase IB dose-escalation trial, Soria, Adjei *et al.* (2017) investigated the administration of GDC-0941 concurrently with conventional first-line chemotherapy in patients with advanced NSCLC. Bevacizumab was added depending on the histology, and patients were administered GDC-0941 with carboplatin and paclitaxel or cisplatin and pemetrexed. Out of 66 patients, 20 had stable disease, and 29 experienced partial

response. GDC-0941 and first-line chemotherapy were then combined in the phase II FIGARO study conducted by Chen, Chang *et al.* (2019), though early results did not show any appreciable improvement in progression-free survival (PFS) or OS; a phase IA/IB trial with a Japanese patient group reported similar findings (Yamamoto, Fujiwara *et al.* 2016).

1.14.1.2 PX-866

Another pan-class I PI3K inhibitor is PX-866, which binds PI3K irreversibly (Beck, Ismail *et al.* 2014, Fumarola, Bonelli *et al.* 2014). Non-molecularly selected patients with advanced, resistant NSCLC were enrolled in a randomised phase II trial to test PX-866 in conjunction with docetaxel treatment. With the addition of PX-866, there was no improvement in PFS, response rate, or OS (Levy, Spira *et al.* 2014). In their review on antitumour therapies that target the PI3K/Akt/mTOR pathway, Janku, Yap *et al.* (2018) report that development of this drug was eventually terminated following several Phase I and II studies that reported weak antitumour activity of PX-866.

1.14.1.3 BKM120

BKM120 (buparlisib) exhibits at least 50-fold selectivity against several other protein kinases and, without directly inhibiting mTOR, specifically targets all isoforms of Class I PI3K in biochemical experiments; it has demonstrated antiproliferative, pro-apoptotic, and anti-angiogenic characteristics in preclinical cancer models (Hare, Harvey 2017, Maira, Pecchi *et al.* 2012). As it is being tested in a randomised placebo-controlled phase III clinical study in hormone receptor-positive, HER2-negative breast cancer (BKM120 + placebo versus BKM120 + fulvestrant) (Iwata, Baselga *et al.* 2013), this drug has made the most progress in the therapeutic development of all PI3K inhibitors. A combination of BKM120 and trastuzumab was reported to be well tolerated and showed some antitumor effect in

patients with advanced HER2-positive breast cancer that was resistant to trastuzumab-based therapy (Saura, Bendell *et al.* 2014). Furthermore, Yu, Zhao *et al.* (2016) suggest that BKM120 used in combination with everolimus (or trastuzumab) may be able to prevent the development of rapalogue resistance by PI3K inhibition, which also exhibits good *in vivo* growth inhibition. As for lung cancer however, further development of this drug is no longer being researched because of the changing landscape of available treatments and the problematic safety profile seen in the BASALT investigations (Adjei, Bennouna *et al.* 2016). Similarly, a Phase II clinical trial in advanced or recurrent endometrial carcinoma, in which patients were administered BKM120 as monotherapy, was terminated before the end of recruitment as BKM120 was linked to a poor safety profile and little antitumor efficacy (Heudel, Fabbro *et al.* 2017).

1.14.1.4 XL-147

In phase I trials, XL-147 (SAR245408, pilaralisib) was also evaluated as a monotherapy, and one NSCLC patient experienced a partial response (Shapiro, Rodon *et al.* 2014). Patients with advanced endometrial carcinomas were included in a phase II, multicentre, single-arm study carried out by Matulonis, Vergote *et al.* (2015) that found that XL-147 had a favourable safety profile and little antitumor efficacy. XL-147 has also been tested in combination with other drugs, such as letrozole in patients with advanced-stage hormone-receptor positive breast cancer, carboplatin and paclitaxel in patients with advanced-stage solid tumours, and trastuzumab with or without paclitaxel in patients with HER2-positive metastatic breast carcinoma; however, none of these initiatives ultimately aided in the clinical development of XL-147, which is not currently the subject of ongoing research (Janku, Yap *et al.* 2018).

1.14.2 Isoform-specific PI3K inhibitors

The original justification for creating isozyme-specific antagonists was to enable the delivery of anti-p110α, anti-p110β, and anti-p110δ drugs at maximum target-inhibitory concentrations while potentially avoiding the undesirable effects of non-isoform-selective medicines as are the pan-PI3K inhibitors (Beck, Ismail *et al.* 2014, Janku, Yap *et al.* 2018, Mayer, Arteaga 2016).

1.14.2.1 BYL719

BYL719 (alpelisib) selectively inhibits the Iα isoform of the PI3K catalytic subunit and has shown a tolerable safety profile and encouraging preliminary activity in patients with *PIK3CA*-altered solid tumours in a phase IA study (Juric, Rodon *et al.* 2018). Stable disease was attained in 52% of patients, supporting the case for selective PI3K inhibition in combination with other drugs for the treatment of *PIK3CA*-mutant tumours. A combination of BYL719 with letrozole was administered to patients with metastatic oestrogen receptor-positive (ER+), HER2-negative breast cancer who were resistant to endocrine treatment, in a phase IB research led by Mayer, Abramson *et al.* (2017), where the clinical antitumor activity was seen in 20% of *PIK3CA* wild-type tumours and 44% of patients with *PIK3CA* mutations. Notably, the co-administration of BYL719 and trastuzumab emtansine was well tolerated and showed activity in patients with metastatic, HER2-positive breast cancer that was both taxane- and trastuzumab-resistant (Jain, Shah *et al.* 2018). As a result, more research on this combination is anticipated to be successful. Furthermore, in patients with metastatic *BRAF*-mutant colorectal cancer, the triple-combination therapy of encorafenib (a RAF kinase inhibitor), cetuximab (a monoclonal antibody targeting EGFR), and BYL719 showed encouraging clinical activity and tolerability (van Geel, Tabernero *et al.* 2017).

1.14.2.2 GSK2636771

The catalytic subunit β isoform of the class I PI3K, which is frequently activated due to loss of PTEN inhibitory function, is specifically inhibited by PI3Kβ inhibitors. In general, PI3Kβ inhibitors appear to be well tolerated, and they are still being studied in early clinical trials, many of which are including the biomarker-driven patient selection, frequently based on PTEN status and the absence of activating changes in the PI3Kα catalytic subunit (Janku, Yap *et al.* 2018). One such drug is GSK2636771 which, as part of the NCI-MATCH precision medicine study, is currently being tested as a monotherapy in patients with advanced-stage malignancies that have *PTEN* loss or mutations, including NSCLC (Fumarola, Bonelli *et al.* 2014, Tan 2020). It is also being studied in combination with pembrolizumab in patients with PTEN-deficient melanoma, with enzalutamide in PTEN-deficient castration-resistant prostate cancer, and with paclitaxel in gastric carcinomas that have *PTEN*, *PIK3CB*, or *PIK3R1* aberrations (Janku, Yap *et al.* 2018, Yang, Nie *et al.* 2019).

1.14.2.3 IPI-549

PI3Kγ inhibitors specifically inhibit the leukocyte-expressed class I PI3K catalytic subunit γ isoform (Janku, Yap *et al.* 2018). Preclinical research has shown that PI3Kγ is significantly expressed in tumour-associated macrophages and may potentially play a role in immune-checkpoint inhibitor resistance (De Henau, Rausch *et al.* 2016). IPI-549 is an oral, selective PI3Kγ inhibitor that is being studied by Tolcher, Hong *et al.* (2017) in a dose-escalation study in patients with various advanced-stage carcinomas or melanoma, both as a monotherapy as well as in conjunction with immune-checkpoint inhibitor pembrolizumab; treatment seems to be well tolerated in both groups, but outcomes are still to be reported (NCT02637531).

1.14.3 Allosteric mTOR inhibitors

Developments have been made on therapies that utilise mTOR inhibitors which aim to target the elevated mTOR signalling in different cancer types; the first mTOR inhibitor was rapamycin (sirolimus), which is what caused mTOR to be discovered through the target screening process (Tian, Li *et al.* 2019). Rapamycin binds to FK506 Binding Protein 12 (FKBP12), which releases Raptor from mTORC1. Additionally, by preventing phosphorylation, the downstream action inactivates S6K1 and 4E-BP1, which reduces protein synthesis and causes cell cycle arrest in the G1 phase. VEGF, platelet-derived growth factor (PDGF), basic fibroblast growth factor (bFGF), and other transcriptional targets of HIF-1α that are involved in vascular development and cancer progression are likewise negatively regulated by rapamycin (Faivre, Raymond *et al.* 2006). Furthermore, rapamycin might indirectly affect mTORC2 by binding to FKBP12, which causes Rictor to separate from mTOR and lowers the levels of mTORC2, possibly in a cell-type-dependent manner (Sarbassov, Ali *et al.* 2006).

A group of allosteric mTOR inhibitors (semi-synthetic rapamycin analogues), often known as rapalogues, have been created to improve the efficacy in patients due to the low solubility and erratic kinetic and pharmacological features of rapamycin (Benjamin, Colombi *et al.* 2011). Examples of rapalogues include CCI-779 (temsirolimus), RAD001 (everolimus) and MK-8669 (ridaforolimus, AP23573), which have been used in monotherapy or combination therapies in a range of cancer types in various stages of clinical trials (Tian, Li *et al.* 2019).

1.14.3.1 CCI-779

Based on the findings of the phase III Global ARCC trial (Hudes, Carducci *et al.* 2007), CCI-779 was approved by the FDA in 2007 for the treatment of individuals with advanced-stage renal cell carcinoma (RCC). In this study, treatment-naïve patients with metastatic RCC who received CCI-779 monotherapy had a longer OS than those who received interferon alfa (10.9 months vs 7.3 months). However, only 8.6% of patients showed an objective response by the Response Evaluation Criteria in Solid Tumours (RECIST). In a phase II trial, Gandhi, Besse *et al.* (2017) tested patients with advanced NSCLC who had *HER2* mutations, with CCI-779 combined with the oral HER2 inhibitor neratinib; response rate to this combination was 19%.

1.14.3.2 RAD001

The FDA has approved the use of RAD001 (everolimus), an oral rapamycin derivative, to treat a variety of malignancies, including advanced-stage RCC, hormone receptor-positive HER2-negative breast cancer in postmenopausal women, and pancreatic neuroendrocrine tumours (NETs) (Janku, Yap *et al.* 2018). A phase III double-blind, randomised, placebo-controlled trial conducted by Motzer, Escudier *et al.* (2008) reported that in patients with metastatic RCC who had advanced on prior targeted therapy, RAD001 treatment increased PFS in comparison to placebo. However, despite the longer PFS, there was no statistically significant increase in OS, likely due to patient crossover from the placebo arm to the RAD001 arm as the disease advanced. RAD001 was similarly shown to extend the PFS of patients with advanced-stage pancreatic NETs (median PFS 11.0 months vs 4.6 months) in the randomised, phase III RADIANT-3 trial (Yao, Shah *et al.* 2011). The study even reported a lower rate of severe adverse events, however the ORR among patients in the RAD001

arm did not exceed 5%. According to the findings of a randomised trial (BOLERO-2) that included patients with advanced-stage hormone receptor-positive HER2-negative breast cancer who had previously been treated with the nonsteroidal aromatase inhibitors (AIs) letrozole or anastrozole, RAD001 plus the AI exemestane was associated with a significantly higher overall RR (9.5% vs 0.5%) and a longer median PFS duration (6.9 months vs 2.8 months) than placebo plus exemestane (Baselga, Campone *et al.* 2012). The results of BOLERO-2 supported the idea that PI3K/Akt/mTOR signalling activity contributes to the emergence of hormone treatment resistance. Phase II trials have also looked at the combination of RAD001 and EGFR inhibitors in NSCLC patients who had not been chosen for *EGFR* mutation testing. RAD001 with erlotinib (Besse, Leighl *et al.* 2014) or gefitinib (Price, Azzoli *et al.* 2010) combinations both failed to demonstrate enough efficacy to move onto a phase III trial.

1.14.3.3 MK-8669

Riely, Brahmer *et al.* (2012) tested the oral rapalogue MK-8669 (ridaforolimus) in advanced NSCLC patients with the *KRAS* mutation in a phase II trial; compared to placebo, MK-8669 improved PFS by two months. Similarly, in the phase III SUCCEED study, patients with previously treated metastatic soft-tissue sarcomas who received MK-8669 saw a longer PFS than those who received placebo (median PFS 17.7 weeks vs 14.6 weeks) (Demetri, Chawla *et al.* 2013). However, objective responses were rare, with a mean reduction in target lesion size of just 1.3%, and MK-8669 did not significantly increase the median OS (90.6 weeks vs 85.3 weeks). Due to a lack of therapeutic activity, further development of this drug for the treatment of cancer has not been undertaken.

Based on preclinical findings, despite the potential of mTOR inhibition as an anticancer strategy, outcomes from rapalogue clinical trials have not met expectations, at least for single-agent therapy (Fumarola, Bonelli *et al.* 2014). This underwhelming performance of rapalogues could be caused by a number of factors. Firstly, rapalogues partially block mTORC1 activity and, through a negative feedback loop, the PI3K/Akt/mTORC2 cascade is activated, and thus Akt promotes an anti-apoptotic response which will eventually lead to increased cell growth and survival (Fumarola, Bonelli *et al.* 2014, O'Reilly, Rojo *et al.* 2006). The mTOR signal pathway is a complex system with several interactions with other signalling pathways that can interfere with the effects of rapalogues (Mendoza, Er *et al.* 2011). Secondly, rapalogues completely block the phosphorylation of S6K1, but only mildly inhibit the phosphorylation of 4E-BP1. This means that, even in the presence of rapamycin, 4E-BP1-regulated protein synthesis persists at a sufficient level that will promote cell survival and proliferation (O'Reilly, Rojo *et al.* 2006). Additionally, rapalogues up-regulate levels of IRS1 protein, resulting in the activation of Akt signalling and associated downstream pathways. Furthermore, mTORC1 inhibition can increase cell survival through autophagy and stimulate cell proliferation by catabolising extracellular proteins in nutrient-poor environments (Palm, Park *et al.* 2015). These factors led to the development of ATP-competitive mTOR kinase inhibitors that block both mTORC1 and mTORC2, completely inhibiting 4E-BP1 phosphorylation and preventing the feedback activation of AKT.

1.14.4 ATP-competitive mTOR kinase inhibitors

Competitive (non-allosteric) mTOR kinase inhibitors are ATP analogues that limit mTOR kinase activity by competing with the physiological substrate ATP for binding to the mTOR kinase domain (ATP provides mTOR with the phosphate group needed to phosphorylate its

intended target proteins). In general, compared to rapalogues, ATP-competitive inhibitors have demonstrated greater anticancer activity in preclinical contexts. This is caused by efficient rapamycin-insensitive mTORC2 activity inhibition in addition to mTORC1 inhibition, as well as more thorough and prolonged mTORC1 inhibition as seen by greater 4E-BP1 phosphorylation inhibition (Benjamin, Colombi *et al.* 2011). These drugs may therefore stop the feedback loop-based activation of Akt brought on by mTORC1 inhibition but not mTORC2 inhibition. As a result, mTOR kinase inhibitors may suppress PI3K/Akt/mTOR signalling more effectively than mTORC1-selective allosteric mTOR inhibitors, leading to increased anticancer efficacy (Janku, Yap *et al.* 2018).

1.14.4.1 AZD8055

AZD8055, an inhibitor of mTORC1 and mTORC2 (mTORC1/2), has been tested in patients with advanced-stage solid carcinoma or lymphoma, but there were no reported RECIST responses. Transaminitis was the most common grade 3 or 4 adverse event (AE), and this toxicity, together with a lack of clinical activity, prevented AZD8055 from moving forward to phase II trials (Naing, Aghajanian *et al.* 2012).

1.14.4.2 AZD2014

Another mTORC1/2 inhibitor is AZD2014 (vistusertib), which was studied in patients with advanced-stage malignancies in a phase I study, and in the phase II MANTA study, which included postmenopausal women with advanced-stage hormone receptor-positive HER2-negative breast cancer (Janku, Yap *et al.* 2018). The outcomes have been unsatisfactory, although the drug is still being studied in numerous phase I and II trials including patients with prostate cancer, glioblastoma, meningioma, or tumours with *TSC* or *RICTOR* amplification mutations, which are thought to boost the drug's sensitivity by

hyperactivating mTORC1 and/or mTORC2, respectively (Cheng, Zou *et al.* 2015). Moreover, to circumvent resistance mechanisms and enhance patient outcomes, AZD2014 is also being evaluated clinically in rationally planned combinations with other treatments, such as TAX-TORC study, in which AZD2014 administered with paclitaxel showed a 33% response rate in previously treated squamous NSCLC (Krebs, Spicer *et al.* 2017).

1.14.4.3 INK128

The safety and effectiveness of INK128 (sapanisertib, formerly MLN0128) were evaluated in two independent phase I dose-escalation studies in patients with advanced-stage solid tumours (Infante, Tabernero *et al.* 2013), and patients with refractory multiple myeloma, non-Hodgkin's lymphoma, or Waldenström macroglobulinemia (Ghobrial, Siegel *et al.* 2016). The reported drug-related AEs in the latter study were mostly consistent with those of other drugs in the same class. Despite only a few patients from both studies experienced partial response, INK128 has progressed to more clinical trials in a variety of tumour types and combination therapies.

Though it is still unclear whether mTOR kinase (mTORC1/2) inhibitors have any clinically meaningful advantages over allosteric mTORC1 inhibitors, drugs from both classes are still being investigated in phase I and II trials, including — and perhaps most significantly — trials using rationally-designed combinations and investigations utilising biomarker-based patient selection techniques (Janku, Yap *et al.* 2018).

1.14.5 Dual PI3K/mTOR inhibitors

One consequence of selectively blocking only a portion of a signalling system such as mTOR, is the resultant activation of PI3K, which may ultimately promote tumour growth.

Therefore, the simultaneous targeting of PI3K and mTOR may result in more potent suppression (Beck, Ismail *et al.* 2014). Due to the structural similarity of the catalytic domains of mTORC1/2 and the p110 subunits, some second generation mTOR kinase inhibitors, which have been termed as dual PI3K/mTOR inhibitors, have dual activity against both complexes, may provide an advantage of targeting several locations along the PI3K/AKT/mTOR pathway, resulting in a more potent inhibition of the process. Naturally, when there are more targets, there is also a greater chance for increased toxicity, which must be weighed against any potential increase in efficacy (Fumarola, Bonelli *et al.* 2014, Papadimitrakopoulou 2012).

1.14.5.1 NVP-BEZ235

The dual PI3K/mTOR inhibitor NVP-BEZ235 (dactolisib), which is an imidazo [4,5-c] quinoline derivative that binds to the ATP binding site and blocks the activity of several class I PI3K isoforms and mTOR kinase, is currently undergoing Phase I/II clinical studies. In a clinical review, Yang, Nie *et al.* (2019) report that although in preclinical studies NVP-BEZ235 demonstrated good anticancer effects in colorectal cancer, renal cancer, triple-negative breast cancer, lung cancer, lymphoma, melanoma, prostate cancer, and mucinous adenocarcinoma of the ovary, clinical trials of this drug proved unsatisfactory. Clinical studies of NVP-BEZ235 are now being conducted in patients with metastatic breast cancer as well as in individuals with relapsed or refractory acute leukaemia.

1.14.5.2 PKI-587

PKI-587 (PF-05212384, gedatolisib) is another dual PI3K/mTOR inhibitor, and which is administered intravenously. This drug was evaluated in a first-in-human study in heavily pre-treated patients with various advanced-stage solid tumours (Shapiro, Bell-McGuinn *et*

al. 2015). It demonstrated anticancer activity, and clinical benefit was noted in patients with endometrial cancer, granulosa cell tumour of the ovary, as well as metastatic NSCLC. Phase I or Phase II clinical trials are ongoing to investigate the efficacy of PKI-587, both as monotherapy and in combination with other chemotherapeutic drugs, for the treatment of breast, lung, head & neck, ovarian, endometrial, and pancreatic cancers (Wainberg, Shapiro *et al.* 2016, Yang, Nie *et al.* 2019).

1.14.6 Akt inhibitors

Several drugs have the ability to selectively inhibit Akt proteins, by preventing the activation of mTORC1 and consequently modifying the downstream effects of PI3K/Akt/mTOR signalling. Directly targeting Akt prevents the PI3K/Akt/mTOR pathway from being abnormally activated by Akt itself, as well as by other sources including PI3K, PTEN, and mTORC2. Akt inhibitors, of which there are those that target multiple Akt isoforms and those that are isoenzyme-specific, are showing potential to be generally well tolerated both at the research stage as well as early clinical levels (Hare, Harvey 2017, Papadimitrakopoulou 2012, Janku, Yap *et al.* 2018).

1.14.6.1 KRX-0401

KRX-0401 (perifosine) is a lipid-based phosphatidylinositol analogue which targets the pleckstrin homology domain of Akt, inhibiting the binding of Akt to PIP3 and therefore its translocation to the plasma membrane (Zhao, Liu *et al.* 2009). As a result, AKT remains inactive and is prevented from activating the downstream pathways necessary for cell growth, metabolism, survival, and proliferation. In an *in vitro* setting, KRX-0401 exhibited antitumor properties against many cancer types including melanoma, nervous system, breast cancer, prostate, colon, and lung. Its efficacy was shown to be comparable to or

greater than that of its parent drug, miltefosine (Richardson, Eng *et al.* 2012). The drug is being investigated in Phase III trials for multiple myeloma and colorectal cancer, as well as in a Phase I/II trials in patients with NSCLC (Cheng, Shcherba *et al.* 2014). The latter trial is being conducted with the goal of determining the maximum dose of KRX-0401 that can be administered, comparing the gastrointestinal toxicity of various dose-schedules, and obtaining preliminary data on the response rate of the drug in NSCLC. Although the study has be completed, there is no available data yet (NCT00399789).

1.14.6.2 MK-2206

Allosteric inhibitor MK-2206 inhibits the activity of Akt1, Akt2, and, to a lesser extent, Akt3 (Janku, Yap *et al.* 2018), by preferentially binding to the inactive PH conformation at a cavity generated between the PH and kinase domains, thus preventing phosphorylation and activation of Akt (Savill, Lee *et al.* 2022). Several phase I studies have indicated that MK-2206 may have important therapeutic benefits (Hare, Harvey 2017). Although none of the patients experienced an objective response in the initial dose-finding study of this drug, which included 33 patients with advanced-stage solid tumours (Yap, Yan *et al.* 2011), one patient with pancreatic cancer who lacked *PTEN* expression however experienced tumour shrinkage of 23.3%, as well as reduction of about 60% in the serum level of the tumour marker CA19.9. Moreover, in a phase I trial conducted by Yap, Patnaik *et al.* (2010), single-agent MK-2206 caused modest tumour regressions in one patient with melanoma and in one patient with a neuroendocrine tumour. Tumour regressions was also reported in a patient with pancreatic cancer who had loss of *PTEN* expression. A post-treatment reduction in circulating endothelial cells, which is a sign of anti-angiogenic action, was observed in 18 of 23 evaluable patients. Nausea, rash, exhaustion, and hyperglycaemia

were some of the more frequent reversible drug-related toxicities. Following these accomplishments, MK2206 has been examined in several phase I or II studies either alone or in conjunction with other anti-cancer drugs. In one such Phase I trial, MK-2206 was well tolerated when used in conjunction with anastrozole in patients with metastatic ER+ /HER2-negative breast cancer, where 42% of patients experienced a therapeutic benefit (Ma, Sanchez *et al.* 2016). In a Phase Ib study, MK-2206 was similarly well tolerated in combination with paclitaxel and trastuzumab in patients with advanced HER2-amplified solid tumour malignancies, and 63% of patients displayed a clinical response (Chien, Cockerill *et al.* 2016). Furthermore, in a Phase I dosing study, the combination of MK2206 with gefitinib was well tolerated and showed early signs of efficacy in NSCLC patients with acquired resistance to EGFR inhibitors (Lin, Yu *et al.* 2015). In general, preclinical and early clinical findings suggest that MK-2206 has improved efficacy in patients with tumours that harbour *PIK3CA* and *PTEN* changes, as was observed in a Phase Ib study in advanced solid tumours and metastatic breast cancer (Gonzalez-Angulo, Krop *et al.* 2015). However, further clinical trials have yet to confirm the prognostic use of these modifications as biomarkers.

1.14.6.3 AZD5363

The drug investigated in the current study is AZD5363 (capivasertib), which is classified as an ATP-competitive inhibitor; it is a very potent and orally bioavailable pyrrolopyrimidine-derived pan-Akt kinase inhibitor, whereby it competes with ATP for Akt kinase association at the ATP binding site (Andrikopoulou, Chatzinikolaou *et al.* 2022). The compound bears the chemical name 4-amino-N-[(1S)-1-(4-chlorophenyl)-3-hydroxypropyl]-1-(7H-pyrrolo[2,3-d]pyrimidin-4-yl)piperidine-4-carboxamide (National Center for Biotechnology

Information 2023), has a molecular weight of 428.9 g, and its 2D structure is shown in Figure 1.2.

Much like the allosteric inhibitor MK-2206 referred to above (Section 1.12.6.2), AZD5363 inhibits all three isoforms of Akt (Addie, Ballard *et al.* 2013, Davies, Greenwood *et al.* 2012). It is generally well tolerated, and the most commonly reported side effects include hypertension, hyperglycaemia, diarrhoea, rash and fatigue (Smyth, Batist *et al.* 2021).

When AZD5363 was tested on 182 solid and haematologic tumour cell lines, Davies, Greenwood *et al.* (2012) reported that at a potency of ≤ 3 μM, growth inhibition was observed in 41 cell lines, among which breast-cancer-derived cells or those with *PIK3CA* and/or *PTEN* mutations exhibited the greatest sensitivity; this was further corroborated by Li, Davies *et al.* (2013) who investigated the pharmacological Akt inhibition of the drug on gastric cancer cell lines as well as on a cohort of Chinese gastric cancer patients with *PIK3CA* mutations and *PTEN* loss. Since then, AZD5363 has been undergoing several clinical trials.

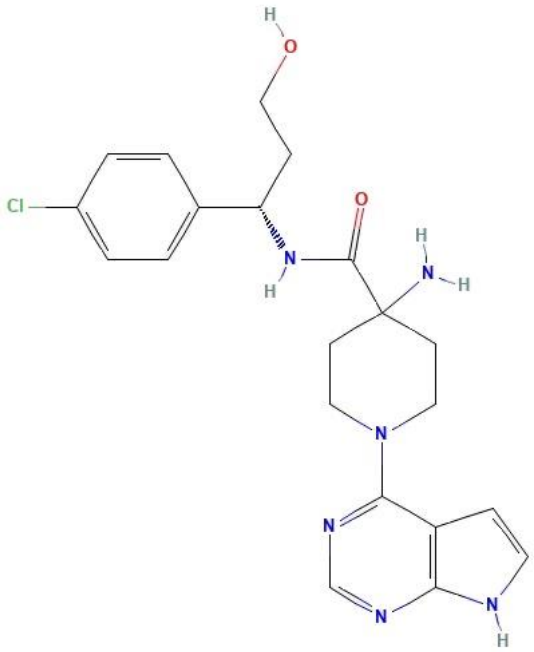

Figure 1.2: *2D structure of the drug AZD5363 (National Center for Biotechnology Information 2023)*

While the BEECH trial (Turner, Alarcón *et al.* 2019) demonstrated no significant improvement in the median PFS of patients with advanced or metastatic ER+/HER2-negative/*PIK3CA*-mutant breast cancer, and who were administered a combination of AZD5363 with paclitaxel, as opposed to paclitaxel monotherapy, a combination of AZD5363 and fulvestrant increased the PFS in patients with aromatase inhibitor-resistant advance breast cancer in the FAKTION trial (Jones, Casbard *et al.* 2020), as well as in patients with hormone receptor-positive, HER2-negative advanced breast cancer who were enrolled in the double-blind phase III CAPItello-291 trial (Turner, Oliveira *et al.* 2023). Additionally, in the PAKT trial, Schmid, Abraham *et al.* (2020) reported a significant improvement in PFS and OS when AZD5363 was added to the first-line paclitaxel therapy for triple-negative breast cancer, with benefits being more noticeable in the *PIK3CA/AKT1/PTEN*-altered subgroup. Following a phase I trial undertaken on patients with prostate cancer using a dose escalation of AZD5363 and enzalutamide, Kolinsky, Rescigno *et al.* (2020) reported a good tolerance limit and increased responsiveness in patients with *PTEN* loss or overexpression of *AKT* mutations.

Other clinical trials have been focusing on cancers with high incidence of *AKT* amplification, namely breast, ovarian, and gastric malignancies. In fact, Hua, Zhang *et al.* (2021) cite a multi-histology basket study on AKT^{E17K}-mutant cancers conducted by Hyman, Smyth *et al.* (2017), and which reported a median PFS ranging from 4.2 to 6.6 months in ER+ breast, gynaecological and other solid tumours. Similarly, in the EAY131-Y non-randomised trial (Kalinsky, Hong *et al.* 2021), where patients harbouring the AKT^{E17K} mutation were administered AZD5363, the ORR was reported to be 28.6%, whereas stable disease was documented in 46% of the patients. Patients with AKT^{E17K}/ER+ metastatic breast cancer

were investigated in a phase I trial (Smyth, Tamura *et al.* 2020), in which an ORR of 20% was reported in those administered AZD5363 as monotherapy; in patients previously treated with fulvestrant, and who were administered a combination of AZD5363 and fulvestrant, the ORR was 36%; the same combination was also administered to fulvestrant-naïve patients, and a 20% ORR was reported.

1.15 Research aim

Among the cell lines tested on AZD5363 by Davies, Greenwood *et al.* (2012), the response frequency of those derived from lung tumours was 12%. Moreover, besides the ongoing National Lung Matrix Trial (Middleton, Fletcher *et al.* 2020), few other investigations have, to date, tested the efficacy of AZD5363 in different types of lung tumours. Therefore, this project aims to investigate the Akt inhibitor AZD5363 on two forms of aggressive non-small cell lung cancer cells.

1.16 Objectives

The aim of this research is going to be achieved through the treatment of H520 (SCC) and A549 (AC) with AZD5363, following which a number of end-point assays shall be implemented:

- Cell viability assays – using PrestoBlue™ reagent, which is a live-cell viability reagent that is made up of cell permeable resazurin-based solution. By using the reducing power of living cells, and following an incubation time, it gives an indication of cell viability by quantitatively measuring cell proliferation. The sensitisation concentration IC_{30} shall be identified from the results obtained. The sensitisation concentration is defined as the concentration at which 30% loss in cell viability is

detected, and that this loss in cell viability is maintained for three further concentrations.

- The use of protein quantification methods – using enzyme-linked immunosorbent assay (ELISA) to quantify how much of the protein eIF4E is being decreased with the sensitisation concentration, IC_{30}.
- Wound healing assays – this will be done using 2-well culture-inserts which, when applied on a confluent cell monolayer, create an artificial gap. Once inserts are removed, cell migration of the cells on the edge of the resulting gap can be observed to test the anti-metastatic potential of the AZD5363.

1.17 Research rationale

This research forms part of a larger project referred to as LCeNT (Lung Cancer enhanced Novel Therapy) that is being undertaken by the Lung Cancer Research Team at the Department of Clinical Pharmacology and Therapeutics within the University of Malta. This project, funded by the Technology Development Programme (TDP) of the Malta Council of Science and Technology (MCST), is investigating combined therapy for the aggressive forms of lung cancer. The novel combination involves the use of a small molecule targeting the mTOR/PI3K pathway, together with the antisense oligonucleotides (ASOs) targeting TCTP and HSP27, the rationale for which lies on the fact that targeting different components with a common target will potentially result in lower required concentrations of each drug, as well as a more efficacious outcome. Thereby, this may in turn lead to reduced adverse effects. Therefore, in context of the LCeNT study, the rationale of the current research to investigate small molecule inhibitors working on the PI3K/Akt/mTOR pathway, is to obtain

the IC_{30} of AZD5363. This result shall then be utilised further in the LCeNT study so as to combine AZD5363 with TCTP and HSP27 ASOs at its IC_{30} concentration.

Chapter 2
Methodology

2 Introduction

The materials used and the methodologies followed for the current research are described in this chapter.

The experiments include treatment of AZD5363 on H520 and A549 cell lines, followed by:

- Cell viability assays
- Enzyme-Linked Immunosorbent Assay (ELISA) for eIF4E
- Wound healing assays.

The protocols for use of the materials, as provided by the respective suppliers, were followed, and where necessary, modifications were employed.

The panel of cells used for treatment with AZD5363 were both purchased from the American Type Culture Collection® (ATCC®). They comprise two different types of NSCLC cell lines, namely:

- H520 (HTB-182™) – an adherent epithelial cell line, derived from a lung mass sample of a male patient with squamous cell carcinoma, and
- A549 (CCL-185™) – an adherent epithelial cell line, derived through explant culture of lung carcinomatous tissue of a 58-year-old Caucasian male.

All the procedures outlined above were done and used entirely for research purposes, on cells *in vitro*. No experiments were carried out *in vivo*; a Research Ethics Review Procedures (REDP) form (reference: MED-2022-00419) was duly submitted.

2.1 Background to cell culture procedures

Subculturing, also known as passaging, is the procedure used to divide a population of cells before transferring them into fresh growth vessels and culture medium. This procedure ensures the proliferation of the cell line and is a crucial component of banking.

Mammal cells grown in culture exhibit a sigmoid growth pattern that is divided into three phases: the Lag Phase, the Exponential (Logarithmic (Log)) Phase, and the Stationary (Plateau) Phase, as shown in Figure 2.1 below.

The cells do not divide but begin to develop slowly after being seeded in the culture vessel (Lag Phase) since they would be recovering from the stress that subculturing induces and start to adjust to the new environment. The duration of this phase will be influenced by the growth stage of the cell line at the time of subculture, as well as the seeding density.

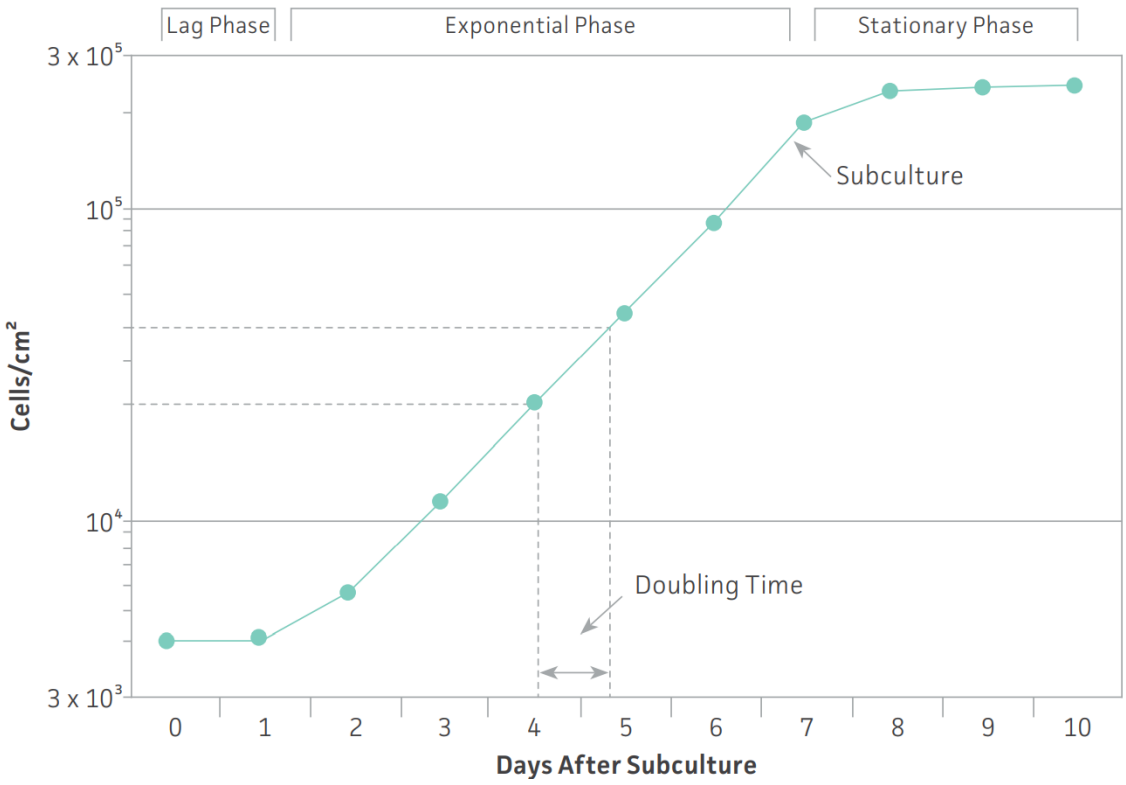

Figure 2.1: *The sigmoid growth pattern and phases of cells grown in culture (ATCC® 2022)*

Subsequently, the rate of cell growth accelerates (Exponential Phase) as the cells adapt to the surroundings. All the experiments in this study were carried out when cells were at this phase, as the Log Phase is considered to be when the cells are at their healthiest. It is also advised to evaluate cellular function at this point. Moreover, the Log Phase is also the best phase for determining the population doubling time, since each cell line will exhibit variable cell proliferation kinetics during this phase.

Adherent cell cultures stop growing (Stationary Phase) when toxic metabolites, such as by-products of cell metabolism accumulate, nutrients and resources are spent, and available space starts to run out. At this point the cells reach the confluent stage (i.e., they completely cover the surface of the cell culture vessel), and if they are left there for a long time, they will almost certainly die. As a result, when adherent cells reach between 70% and 80% confluence (before cells reach the Stationary Phase), a portion of them needs to be passaged and transferred to a new cell culture vessel with fresh culture medium. This confluence range is important since when working with lower cell densities, cell growth would be extremely slow and might even result in cell death. Conversely, a higher cell density will quickly exhaust the nutrients, therefore increasing the likelihood of cell death. This characteristic can be assessed by observing the confluency and the colour of the culture medium, which indicates the amount of metabolites present.

For both personal safety and to avoid contaminating the cell cultures, precautions were followed throughout the entirety of the laboratory activity for the study. All cell culture was carried out in a Class II laminar flow hood (Safe FAST Elite), fitted with a UV lamp and an air filter whereby, through a fan system, 70% of the air is cycled inside the cabinet while only

30% is vented. The purpose of such a cabinet is to safeguard the test sample, the user, as well as the surrounding area.

Before use, every piece of glassware was autoclaved, and any used plastic instruments were also autoclaved prior to disposal. In addition, 70% ethanol was used:

- to clean the laminar flow hood and all the glassware and reagents that were to be utilised in it before every experimental session, and
- before disposing of any biological waste produced during the experiments.

Adherent cells make up the majority of vertebrate cells, including the sample of cells employed in this study. Controlled temperature, a substrate for cell attachment, an adequate growth medium, and an incubator that maintains the proper pH and osmolality are the fundamental environmental needs for cells to proliferate optimally *in vitro* (Meenakshi 2023).

For optimal growth, cells in culture require a controlled temperature of 37 °C. For the present study, the cells were allowed to grow in a carbon dioxide (CO_2) incubator with hot air sterilisation (CB-S 260, Binder GmbH) set at this temperature, and for the regulation of the pH, was configured to keep the level of CO_2 at 5%. The incubator is also equipped with an alarm system to warn against any temperature or CO_2 level fluctuations outside this optimum setting.

2.2 Preparation of cell culture media

The selection of an adequate growth/culture medium for *in vitro* cultivation is the most significant and important phase in cell culture. The majority of cell culture media are made up of components that control the cell cycle and provide an adequate source of energy. A

standard culture medium consists of serum (with the most frequently used in animal cell culture media being Foetal Bovine Serum (FBS)) as a source of growth factors, hormones, and attachment factors, in addition to amino acids, vitamins, inorganic salts, fatty acids and lipids, proteins and peptides, trace elements and carbohydrates. Furthermore, the medium also aids in maintaining pH and osmolality (Meenakshi 2023). Moreover, although they are not necessary for cell growth, antibiotics such as penicillin-streptomycin-amphotericin preparations are frequently added to the cell culture medium to minimise risks of contamination with bacteria and fungi.

The culture medium utilised for the H520 cell line was Roswell Park Memorial Institute medium (RPMI-1640), which was obtained from Sigma-Aldrich® (R6504). For the preparation of 1000 mL of RPMI, 900 mL of tissue culture-grade water at a temperature of between 15 and 20 °C, free from organic, mineral and microbial contaminants including pyrogens, was measured out. While gently stirring the water, the powdered medium was added, and stirring was continued until all powder was dissolved. Any traces of powder were removed from the original package by rinsing with a small amount of water and was added to the solution. Next, for pH adjustment, 2.0 g sodium bicarbonate (S-6297, Sigma-Aldrich®) was added and allowed to dissolve by stirring. More water was added to bring the solution to a final volume of 1000 mL. The medium was then transferred to the laminar flow hood, sterilised by filtration through a 0.22-micron filter membrane into a sterile container. To this basal medium, 10% FBS (P40-37500, PAN™-Biotech GmbH) and 1% antibiotic solution containing penicillin, streptomycin and amphotericin B (pen-strep) (A5955-100ML, Sigma-Aldrich®) were added, and the complete cell culture medium was stored at 2-8 °C in the dark.

The culture medium utilised for the A549 cell line was Dulbecco's Modified Eagle's medium (DMEM) – high glucose, which was obtained from Sigma-Aldrich® (D5648-1L). For the preparation of 1000 mL of DMEM, 900 mL of tissue culture-grade water at a temperature of between 15 and 20 °C, free from organic, mineral and microbial contaminants including pyrogens, was measured out. While gently stirring the water, the powdered medium was added, and stirring was continued until all powder was dissolved. Any traces of powder were removed from the original package by rinsing with a small amount of water and was added to the solution. Next, for pH adjustment, 3.7 g sodium bicarbonate was added and allowed to dissolve by stirring. More water was added to bring the solution to a final volume of 1000 mL. The medium was then transferred to the laminar flow hood, sterilised by filtration through a 0.22-micron filter membrane into a sterile container. This basal medium was supplemented with 10% FBS, 1% pen-strep, and 1% L-glutamine (G6392-1VL, Sigma-Aldrich®), and the complete cell culture medium was stored at 2-8 °C in the dark.

2.3 Other reagents for cell culture

Phosphate Buffered Solution (PBS) is a physiological buffer of balanced salt solution which, owing to its pH and osmolarity, can be used to wash cells without harming them. The PBS utilised in the current research was ROTI® cell 10x concentrate, obtained from Carl Roth GmbH + Co. KG (9150.1). Prior to use, 50 mL from the stock sterile solution was diluted in 500 mL deionised water.

The use of trypsin-ethylenediaminetetraacetic acid (EDTA) is for the detachment of adherent cells from a culture surface, and to disassociate cells from one another. Aliquots of 0.25% concentration were prepared from the stock solution of 0.5% trypsin-EDTA (0.5%) (15400054, Gibco™) by aseptically diluting in equal volume of PBS.

2.4 Cell thawing

Both the A549 and H520 cell lines utilised in this study were cryogenically stored frozen in vapour phase of liquid nitrogen, in 90% FBS and 10% dimethyl sulfoxide (DMSO) (41639, Sigma-Aldrich®). Correct cell thawing is essential for maintaining the culture's viability and facilitating a quicker rate of recovery. It was therefore important to thaw cells rapidly and to dilute them in their respective culture medium to reduce toxic effects since some cryoprotectants, including DMSO, are toxic above 4 °C.

A beaker filled with ice was used to transfer the cryovial containing the cells, from the liquid nitrogen to the laminar flow hood. After allowing the cells to thaw, the contents were decanted into a 15 mL falcon tube, in which 9 mL of complete culture medium was prepared in advance, so as to dilute the DMSO that the cells were frozen in. Subsequently, the tube was carefully balanced in a Biocen 22 R centrifuge (Ortoalresa – Alvarez Redondo, S.A.) and centrifuged for 7 minutes; a relative centrifugal force (RCF) of 330 x g was set for the A549 cell line, whereas an RCF of 120 x g was programmed for the H520 cell line. After centrifugation, the falcon tube was disinfected with 70% ethanol, transferred to the laminar flow hood, and the supernatant was carefully discarded, whilst ensuring that the cell pellet was not dislodged. Next, 6 mL of complete culture medium, supplemented with an additional 10% FBS, was added to the cell pellet and a 10 mL serological pipette was used to facilitate resuspension of the cells. The solution was then pipetted and transferred into a T25 flask and incubated at 37 °C and 5% CO_2.

2.5 Cell passaging

The cell culture in the medium was carefully examined visually for turbidity or any macroscopic particles that would indicate contamination. Attention was taken to observe

the medium-air interface for any floating small fungal colonies, particularly the edges of the flask which may not be obvious through a microscope. The medium was then inspected for signs of microbial contamination using an inverted phase contrast microscope (Olympus IX50) and the morphology of the cells was also checked. The crevices between the cells will show up as tiny, shimmering black dots when there is bacterial infection. Whereas fungi have thin filamentous mycelia, yeast contamination will appear as spherical or budding particles (American Type Culture Collection® 2022). The majority of adherent cells have to be firmly affixed to the surface of the vessel, and occasionally may round up and detach a little bit during mitosis but reattach after this phase. On the other hand, dead cells frequently round up and separate from the monolayer, and under the microscope are observed as darker and smaller in size than healthy cells. The above explained observation and examination were carried out before each experiment conducted during the entire investigation.

The passaging procedure followed after the visual and microscopic examination of both culture medium and the cells. The flask was thoroughly disinfected with 70% ethanol and transferred to the laminar flow hood. The spent medium was carefully decanted from the flask into a waste bottle, and by means of a serological pipette, 6 mL of PBS was added to wash the cells in the flask and then discarded. The following step entailed the addition of 0.25% trypsin-EDTA to the flask: 2 mL were added to cells in a T25 flask, whereas 4 mL were added to the cells in a T75 flask. For both A549 and H520 cell lines, the flasks were then transferred to the incubator and were allowed to sit for 5 minutes at 37 °C and 5% CO_2.

Upon removal from the incubator, the flasks were observed under the microscope to ensure that all the cells were disaggregated and detached from the culture surface, and then were

again disinfected with 70% ethanol and transferred to the laminar flow hood. The trypsin in the culture flask was neutralised by the addition of complete medium in double the volume of trypsin, such that 4 mL of complete medium was added to the T25 flask, and 8 mL to the T75 flask. The cell suspension was then aspirated from the flask and transferred to a falcon tube and centrifuged at the same setting described in the cell thawing procedure (Section 2.4). After centrifugation, the falcon tube was disinfected with 70% ethanol, transferred to the laminar flow hood, and the supernatant was carefully discarded, whilst ensuring that the cell pellet was not dislodged. Next, 6 mL of complete culture medium was added to the cell pellet and a pipette was used to facilitate resuspension of the cells. The solution was then split by pipetting a fraction of the solution depending on the required split ratio and was transferred into a T75 flask. The remaining volume up to 12 mL was topped up with the respective complete medium depending on the cell line being handled and incubated at 37 °C and 5% CO_2. A very common split ratio selected is 1:3, such that from a 6 mL of resuspended cell solution, the passaged cell culture in a T75 flask would contain 2 mL of cell suspension and 10 mL of fresh complete medium.

2.6 Cell counting

Cell counts are required for both the establishment and monitoring of growth rates as well as for the generation of fresh cultures with known cell numbers. Improved Neubauer chamber haemocytometers are often used to count cells and assess their viability. A haemocytometer is a rather thick glass slide with two counting chambers, one on each side. The sides of the chambers are elevated such that a coverslip will fit inside precisely 0.1 mm above the chamber floor.

For the cell counting process, the same procedure of cell passaging, as described in Section 2.5 above, was followed up till the resuspension of cells after centrifugation. The haemocytometer (Weber Scientific) and its cover slip were thoroughly disinfected, dried, transferred into the laminar flow hood and assembled. Using a micropipette, 10 µL of cell suspension was introduced through the edge of the counting chamber of the haemocytometer. A few seconds were allowed for the cell suspension to be drawn into the counting chamber via capillary action. The haemocytometer was then placed under the inverted microscope, and focused on the quadrants labelled 1, 2, 3, and 4, as in Figure 2.2, each of which holds a volume of 0.0001 mL. The number of cells in each quadrant was recorded, averaged, and finally multiplied by the dilution factor, that is 'average cell count x 10^4 cells/mL'.

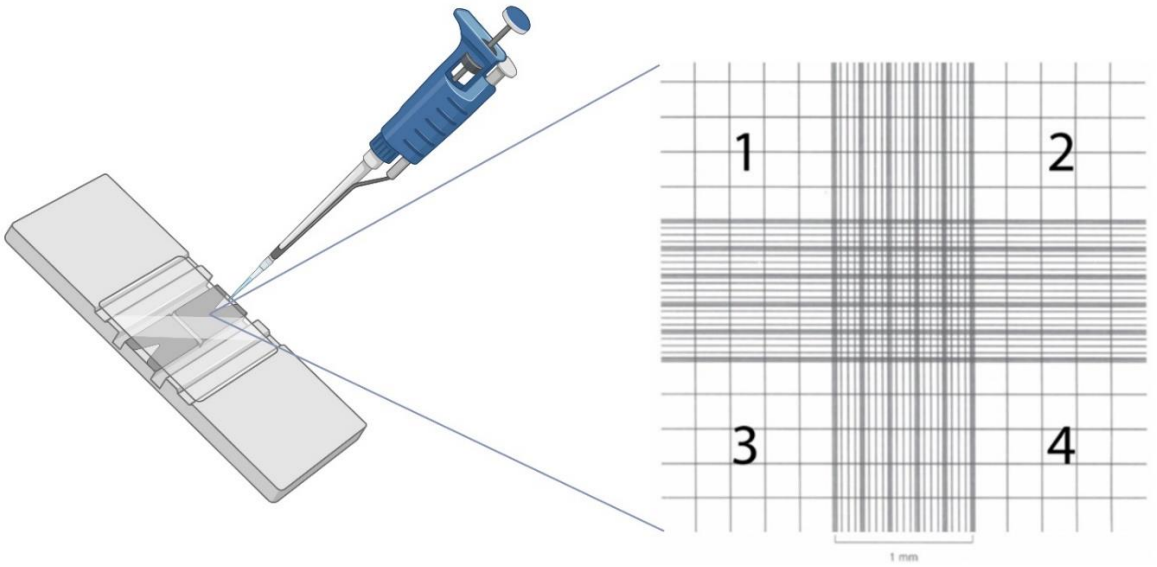

Figure 2.2: *Haemocytometer and Neubauer grid. Created with BioRender.com*

2.7 Cell seeding

Depending on the type of treatment, the investigations for this study involved seeding a known concentration of cells in culture dishes and multi-well plates. Since cell culture

dishes provide optimum access to the growth surface, they were the vessels of choice for manipulations such as scraping where direct access to the monolayer was required. Drug treatment assays, such a PrestoBlue™ cell viability assays which require a large number of treatment wells, were however performed in 96-well plates, which offer convenient handling and significant space, media, drug and reagent savings. The volume needed per well or cell culture dish was determined by the size of the well or culture dish, in accordance with the recommendations of the suppliers.

The initial cell suspension was prepared as described above in Section 2.5 and was then counted to establish the cell density. The total volume and number of cells required for cell treatment was calculated depending on the type of experiment and the number of wells or cell culture dishes to be seeded, and by considering the required cell density for each respective treatment. Finally, the volume of medium to be added to the initial cell suspension to achieve the final cell suspension was also worked out.

The final cell suspension was carefully seeded into the wells or culture dishes, and gently agitated to ensure homogeneity and maintain cell clumping to a minimum. Furthermore, to reduce evaporation of the test cultures during incubation, the border wells of the 96-well plates were seeded with PBS. The seeded cells were then incubated at 37 °C and 5% CO_2.

2.8 Treatment with AZD5363 in preparation for viability assays

AZD5363 was purchased from Cayman Chemical Company (Item Number: 15406), and was presented as a crystalline solid, stored at -20 °C. Prior to use, the drug (10mg) was allowed to acclimatise to room temperature, and was then dissolved in 2mL of DMSO to achieve a concentration of 5 mg/mL.

Both H520 and A549 cell lines were cultured using the respective culture media as described in Section 2.2. Each was then seeded in 96-well plates and treated with varying concentrations of AZD5363 to ultimately determine, through viability assays, the concentration at which 30% loss in cell viability was attained.

To achieve this, 111.5 µL from the 5 mg/mL (11660 µM) drug solution was diluted in 13000 µL of culture medium (according to the cell line being handled). This dilution resulted in a 100 µM drug solution, from which further dilutions were made to attain the different concentrations of AZD5363 needed for the investigation, as shown in Table 2.1, below.

Table 2.2: *The range of AZD5363 concentrations used for treatment on A549 and H520 cell lines in 96-well plates.*

AZD5363 concentration (µM)	**Volume from the 100 µM drug solution (µL)**	**Volume of culture medium (µL)**
10	200	1800
20	400	1600
30	601	1399
35	699	1301
40	800	1200
45	901	1099
50	1000	1000
55	1099	901
60	1198	802
65	1299	701
70	1399	601
75	1504	496
80	1600	400
85	1695	305
90	1800	200
100	2000	0

The culture media used for the test-drug treatment on the two cell lines investigated were both prepared in the same way as described in Section 2.2; they were however supplemented with 1% FBS (instead of 10%) and were left devoid of the antibiotic

component. The 1% FBS supplementation (instead of 10%) was carried out due to the high protein-binding capacity of the drug, in order to minimise loss of drug availability to the cells, due to its binding to serum proteins. Previous studies in our lab, carried out over 5 days, have established that growth patterns and viability of these cell lines cultured with 1% FBS-containing medium, do not differ from the 10% FBS-containing medium.

Treatment with the test drug was carried out 24 hours after the seeding process. The organisation of the 96-well plate and a sample of the concentrations of AZD5363 used is shown in Figure 2.3, below. Four wells in each plate were seeded with culture medium only so that this could serve as a 'blank', whereas another four wells were seeded with DMSO (vehicle) control solution, which was prepared by using the same concentration of DMSO present in 100 µM of AZD5363 solution (approximately 0.8% v/v).

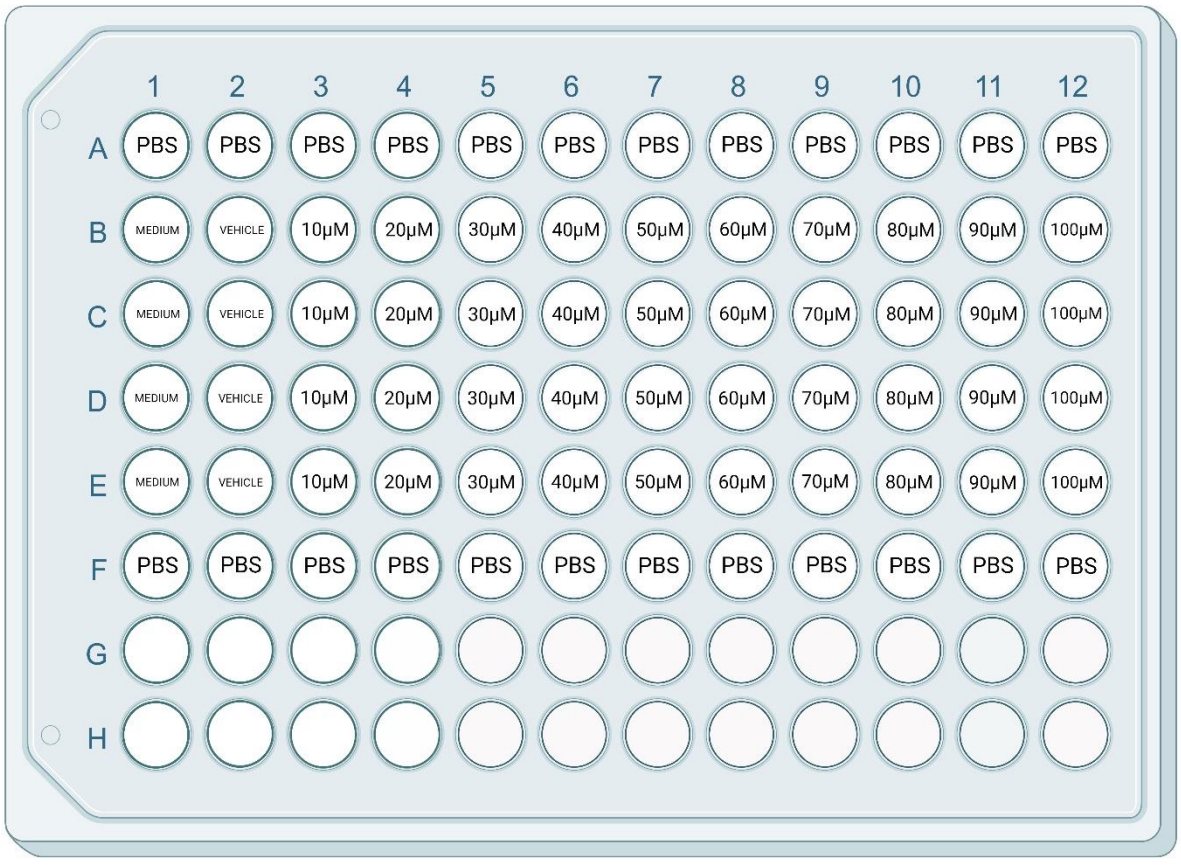

Figure 2.3: *The organisation of the 96-well plate and concentrations of AZD5363 used. Created with BioRender.com*

2.8.1 PrestoBlue™ cell viability assay

Changes in cell viability were measured using the PrestoBlue™ cell viability assay, which utilises a resazurin-based reagent. Upon entering living cells, this blue, cell-permeable and non-toxic compound is reduced to a red, highly fluorescent compound resorufin as a result of the reducing environment within the cells. Since the amount of resorufin corresponds to the number of viable cells present in the cell culture medium, the more viable cells are present in a culture medium, the more the cell suspension becomes red and highly fluorescent and can be measured through fluorescence or end-point measurements. In this study, absorbance measurements at 570 nm were carried out as per manufacturer's guidelines.

A seeding density of 1 x 10^5 cells/mL for the A549 cell line and 4 x 10^5 cells/mL for the H520 cell line were used for the PrestoBlue™ cell viability assays, as was established in earlier projects carried out within the Department of Clinical Pharmacology and Therapeutics at the University of Malta. The seeding density ensured that the untreated cell confluency of around 80% would be attained after 72 hours, thus ensuring that the cell population would remain in an active growth phase for the duration of the experiment. High confluency was avoided as this leads to contact growth inhibition, with subsequent growth retardation which can confound experimental data. Three 96-well plates were seeded for each biological repeat of the viability assay and each cell line investigated.

After 24 hours of treatment with AZD5363, one of the plates was taken out of the incubator and examined under the microscope for any contamination. It was then disinfected, transferred to the laminar flow hood, and the culture/treatment medium was carefully aspirated from the wells containing the cells. Using a multichannel pipette, 90 µL of culture

medium was added to the wells, followed by 10 µL of PrestoBlue™ (A13262, Invitrogen™) reagent. To attain a homogenous solution, the 96-well plate was placed in a plate shaker (ThermoMixer® Comfort, Eppendorf) for 1 minute at 300 revolutions per minute (rpm), after which it was incubated at 37 °C for 2 hours.

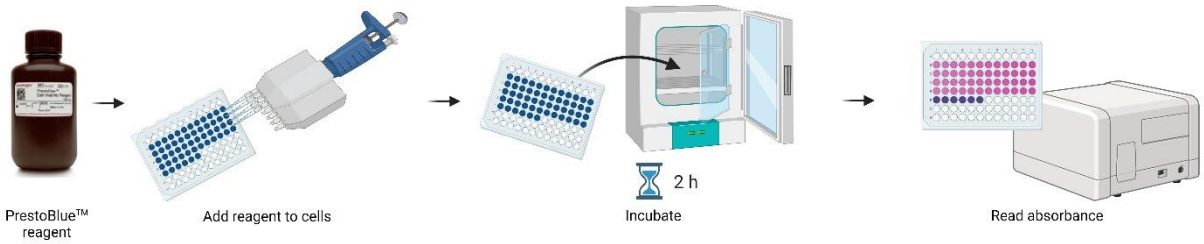

Figure 2.4: *PrestoBlue™ assay process. Created with Biorender.com*

At the end of the two-hours, the plate was taken out of the incubator and inserted into a microplate spectrophotometer (Mithras LB 940, Berthold Technologies GmbH) to capture and record the absorbance of each well at a wavelength of 570 nm, using the MicroWin 2010 software.

This same procedure (Figure 2.4) was repeated using plate 2 after 48 hours of AZD5363 treatment and using plate 3 after 72 hours of test-drug treatment.

2.9 Treatment of A549 cells with AZD5363 in preparation for eIF4E ELISA assay

In vitro eIF4E protein in human cell and tissue extracts can be quantitatively measured using the SimpleStep ELISA® (Enzyme-Linked Immunosorbent Assay) kit, in which the sample analyte is immunocaptured in solution using an affinity tag labelled capture antibody and a reporter coupled detecting antibody.

For this investigation, the A549 cell lines were treated with 55 µM of AZD5363, which was the concentration that yielded a 30% loss in cell viability in the PrestoBlue™ viability assays described above (Section 2.8.1). The rationale for this experiment was to determine if the loss in cell viability is due to the PI3K/Akt/mTOR pathway inhibition.

Due to the amount of sample required for the ELISA assays, these experiments were carried out in 10 cm diameter treated tissue cell culture dishes, having a growth surface area of 55 cm^2.

Following trypsinisation of A549 cells and resuspension in DMEM supplemented with 10% FBS, 1% pen-strep, and 1% L-glutamine, a cell count was carried out. More complete medium was subsequently added to achieve a final seeding density of 2 x 10^5 cells/mL. The culture dishes were then seeded with 10 mL of cell suspension and transferred into the incubator set at 37 °C and 5% CO_2.

After 24 hours, the following solutions were prepared:

- DMEM supplemented with 1% FBS and 1% L-glutamine
- 55 µM solution of AZD5363 in the prepared DMEM, from the drug stock solution
- DMSO control solution in the prepared DMEM, to be equivalent to the DMSO concentration present in the 55 µM AZD5363 solution (approximately 0.4% v/v).

The cell culture dishes were subsequently taken out of the incubator and were visually and microscopically inspected for any contamination. They were then transferred to the laminar flow hood and the culture medium was carefully aspirated. In four of the cell culture dishes, the aspirated medium was replaced with 10 mL of DMEM supplemented with 1% FBS and 1% L-glutamine, to serve as the 'untreated' control. Four culture dishes were each treated with 10 mL of the 55 µM AZD5363 solution, whereas the remaining four culture dishes were

treated with 10 mL of the DMSO control solution. Following this process, the culture dishes were again transferred to the incubator. The schematic representation in Figure 2.5 shows a sample of the cell culture dishes prepared for the treatment of AZD5363 on A549 cell lines in preparation for eIF4E ELISA.

Figure 2.5: *Sample of cell culture dishes prepared for the treatment of AZD5363 on A549 cell lines in preparation for eIF4E ELISA. Created with BioRender.com*

2.9.1 Cell lysate collection in preparation for the eIF4E ELISA

Following the treatment described in the previous section, two cell culture dishes from each of the three test samples were used for the collection of cell lysate at the 6-hour and 10-hour time points, respectively. This was done using the Human eIF4E SimpleStep ELISA® Kit (ab214564, Abcam). For this step, a 10 mL 1X cell extraction buffer was prepared by combining 2 mL of 5X cell extraction buffer and 200 µL of 50X cell extraction enhancer solution, both supplied in the kit, and diluted in 7.8 mL deionised water.

Figure 2.6 below describes the process for the collection of cell lysate for the eIF4E ELISA. Each culture dish was taken out of the incubator, observed under the microscope for any possible contaminations, and was then transferred to the laminar flow hood. The solution in the cell culture dish was carefully aspirated and any remaining solution was washed off twice with 5 mL PBS. The cells were then solubilised by the addition of 750 µL 1X cell extraction buffer to the dish and were scraped off the bottom by the use of a cell scraper.

The resulting cell lysate was carefully pipetted into a pre-labelled microcentrifuge tube and was then incubated for 15 minutes on ice. Next, the tube was centrifuged for 20 minutes at 18,000 x g at 4 °C, following which the supernatant was carefully pipetted and transferred into a clean pre-labelled microcentrifuge tube and stored at -80 °C for subsequent ELISA analysis.

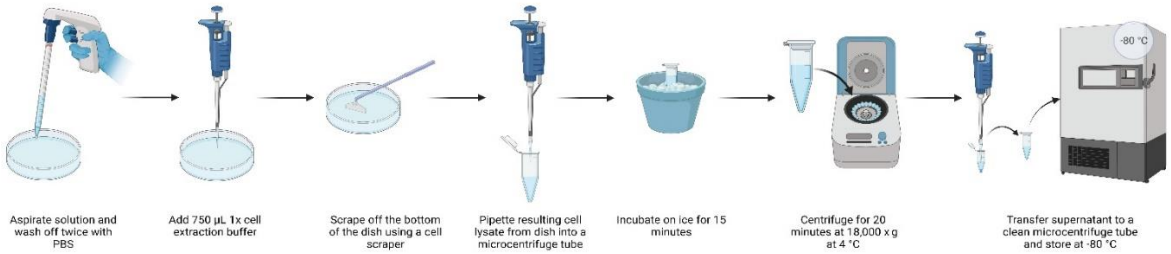

Figure 2.6: *The process for the collection of cell lysate for eIF4E ELISA. Created with BioRender.com*

2.9.2 ELISA assay

All reagents required for the ELISA assay were equilibrated to room temperature and freshly prepared prior to the analysis, as described below.

- An aliquot of 50 mL 1X wash buffer PT was prepared by diluting 5mL of 10X wash buffer PT with 45 mL deionized water, and gently mixed.
- 6 µL of detector antibody concentrate were added to 369 µL of sample diluent NS, to achieve an aliquot of 375 µL 10X detector antibody.
- For the preparation of a 3 mL aliquot of antibody cocktail, 300 µL 10X capture antibody and 300 µL 10X detector antibody were gently and thoroughly mixed with 2.4 mL antibody diluent 5BR.

For the preparation of the eIF4E standards, 100 µL water was initially added to the protein standard vial, allowed to stand for 10 minutes at room temperature, and then mixed gently;

this yielded the 100,000 pg/mL stock standard solution. Next, eight microcentrifuge tubes were prepared and labelled 1 – 8; 1X cell extraction buffer PTR was then added into each of the tubes as follows: 344 µL into tube 1, and 150 µL into each of tube numbers 2 – 8. Subsequently, for the preparation of the dilution series, 56 µL stock standard was added into tube 1, and 150 µL from the resulting solution was then added into tube 2; this procedure was repeated sequentially from tubes 2 to 7. Tube 8 did not contain any protein and thus served as the blank control; the resulting concentrations ranged from 0 to 14,000 pg/mL as shown in Figure 2.7, below.

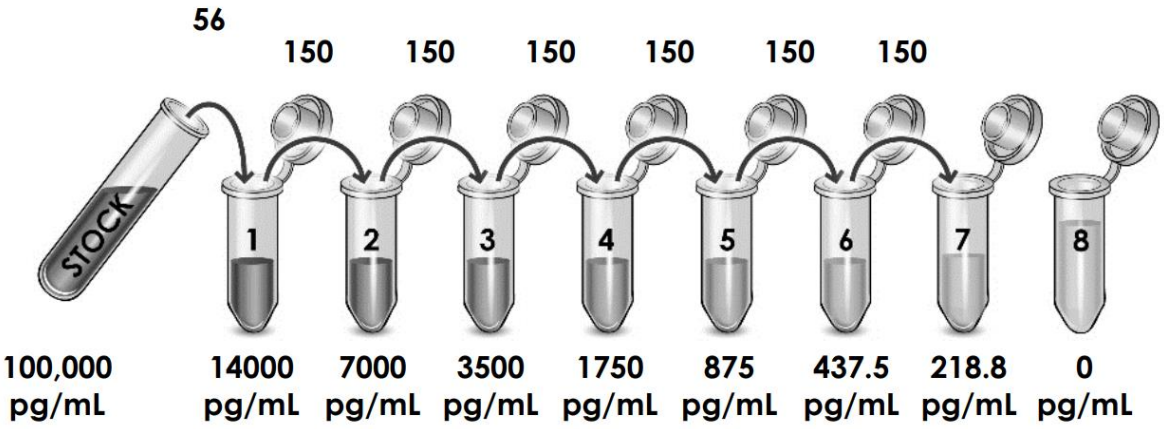

Figure 2.7: *Preparation of Standards for the eIF4E ELISA assay. (Abcam 2021)*

Excess microplate strips were removed from the 96-well plate frame, placed back into the foil pouch holding the desiccant pack, sealed, and stored at 4 °C. Next, the appropriate wells were filled with 50 µL of each sample or standard, in duplicate, followed by 50 µL of the antibody cocktail. The plate was then sealed and allowed to sit at room temperature on a plate shaker set at 400 rpm for one hour.

Each well was then washed three times with 350 µL 1X wash buffer PT. With each wash, it was ensured that the wash buffer PT was left in the wells for at least 10 seconds before

being aspirated completely. Following this step, 100 µL TMB development solution was added to each well and the plate was then sealed again and incubated in the dark for 10 minutes on a plate shaker set at 400 rpm.

The plate was inspected for development of blue colour in the standard solutions, and more time was allowed until a gradient could be observed. At this point 100 µL stop solution were added to each well, and the plate was returned to the plate shaker to mix for one minute. Using a microplate reader, the absorbance was then measured at 450 nm.

2.9.2.1 Calculations to plot a standard curve

The average absorbance value of the blank control standards (represented by well 8, where concentration of eIF4E was 0 pg/mL) was calculated, and the value obtained was then subtracted from the absorbance values of the rest of the readings. These corrected values were utilised for the remainder of the calculations, which consisted of the average absorbance of the other seven eIF4E standards, followed by their log, as well as the log eIF4E concentrations.

A standard curve of the Log_{10} eIF4E concentration of the standards (x-axis) against the Log_{10} average absorbance standard values (y-axis) was plotted to fit a linear trendline, as shown in Section 3.2 (Figure 3.4).

A total of 4 values per condition were obtained because testing was done utilising 2 biological repeats, each with 2 analytical repeats. Each result acquired from the spectrophotometer output was converted to a Log_{10} scale. All of the data was backfitted using the trendline equation $y = 1.0387x – 4.3112$. The amount of eIF4E protein (in pg/mL) in each sample was then determined by calculating the antilog to base 10 of the values obtained after backfitting.

2.9.3 The Bradford protein assay

The Bradford protein assay is a quick and precise method for measuring the concentration of solubilised protein. It entails the addition of an acidic dye, Coomassie® Brilliant Blue G-250, to a protein solution; this subsequently gives rise to a colour change as a result of binding of this dye to protein, which is then recorded through absorbance measurement at 595 nm, using a microplate reader.

Below is the Bradford protein assay procedure, carried out as per manufacturer's instructions:

- The lyophilised bovine gamma globulin and bovine serum albumin standards were dissolved in 20 mL deionised water.
- An aliquot of dye reagent was prepared by diluting 1 part dye reagent concentrate in 4 parts deionised water and filtered to get rid of any particulate matter.
- Ten dilutions of protein standard ranging from 50 µg/mL to 450 µg/mL, intended to be representative of the protein solution to be analysed, were prepared as per Table 2.2, below.

Table 3.2: *Dilutions of protein standards, in preparation for the Bradford protein assay.*

Standard	1	2	3	4	5	6	7	8	9	10
Protein concentration (µg/mL)	0	50	100	150	200	250	300	350	400	450

- Using a 96-well plate, 10 µL of each standard was pipetted into separate wells.
- 5 µL of each test sample, together with 5 µL of 1X cell extraction buffer PTR were added, in duplicates, into separate wells.
- 10 µL of 1X cell extraction buffer PTR were pipetted, in duplicate, into two separate wells, to serve as sample blanks.

- Using a multichannel pipette, 200 µL of dye reagent were added into each well containing the standards, test samples, and sample blanks.
- The plate was allowed to incubate at room temperature for 5 minutes, and once the development of a clear colour gradient could be observed, absorbance was then measured at 595 nm.

2.9.3.1 Calculations to plot a standard curve

The mean absorbance value of standard 1 (Table 2.2), in which protein concentration was 0 µg/mL, was calculated, and the value obtained was then subtracted from the absorbance values of the rest of the standard readings. These corrected values were utilised for the calculation of the mean absorbance values. A standard curve, plotting the standard concentrations (x-axis) against the respective standard mean absorbance values (y-axis), was generated, and is shown in Section 3.2 (Figure 3.5).

A total of 4 values per condition were obtained because testing was done utilising 2 biological repeats, each with 2 analytical repeats. The mean absorbance value of the sample blanks, corresponding to 1X cell extraction buffer PTR alone, was calculated, and the value obtained was then subtracted from the absorbance values of the rest of the sample readings. These corrected values were utilised for the calculation of the mean absorbance values. Next, all the data was backfitted using the trendline equation $y = 0.001x + 0.0547$, and the result obtained was multiplied by the dilution factor of 2, to determine the amount of protein (in µg/mL) in each sample.

2.9.4 Normalisation of eIF4E to total protein

The concentration of eIF4E of each test sample was normalised to the total amount of protein, by dividing the concentration values (pg/mL) obtained in the ELISA assay (Section 2.9.2.1) by the corresponding protein concentration values (µg/mL) obtained in the Bradford protein assay (Section 2.9.3.1). This was done to account for discrepancies in eIF4E concentrations as a result of differences in cell numbers.

2.10 Wound healing assays

The wound healing collective migration cell protocol was carried out to investigate cell migratory behaviour of A549 cells, utilising Culture-insert 2 Wells (80209, ibidi® GmbH), each comprised of two cell culture reservoirs that are separated by a 500 µm thick wall. Cell growth is only permitted in the designated areas of the reservoirs by filling cell suspension in both wells. Following appropriate cell attachment and removal of culture-inserts, a cell-free gap on a confluent monolayer will be created. Cells on the edge of the generated artificial gap will then start migrating inward until they establish new cell-cell connections, the latter being assessed by time-lapse microscopy.

For this investigation, the A549 cell lines were treated with 55 µM of AZD5363, which was the concentration that yielded a 30% loss in cell viability in the PrestoBlue™ viability assays described above.

Following trypsinisation of A549 cells and resuspension in DMEM supplemented with 10% FBS, 1% pen-strep, and 1% L-glutamine, a cell count was carried out. More complete medium was subsequently added to achieve a final seeding density of 2.5 x 10^5 cells/mL; this density was selected so that a 100% optically confluent cell layer could be reached 24 hours post-seeding.

A culture-insert was carefully placed in the centre of 6 chambers of a 24-well plate (Figure 2.8), following which 75 µL cell suspension was added to each of the culture-insert wells. Shaking was avoided to ensure the maintenance of a homogenous cell distribution. Another 700 µL complete medium was added to the wells enclosing the culture-inserts. Next, the chambers surrounding the seeded wells were seeded with 1 mL PBS to reduce evaporation of the test cultures during incubation. The seeded cells were then incubated at 37 °C and 5% CO_2.

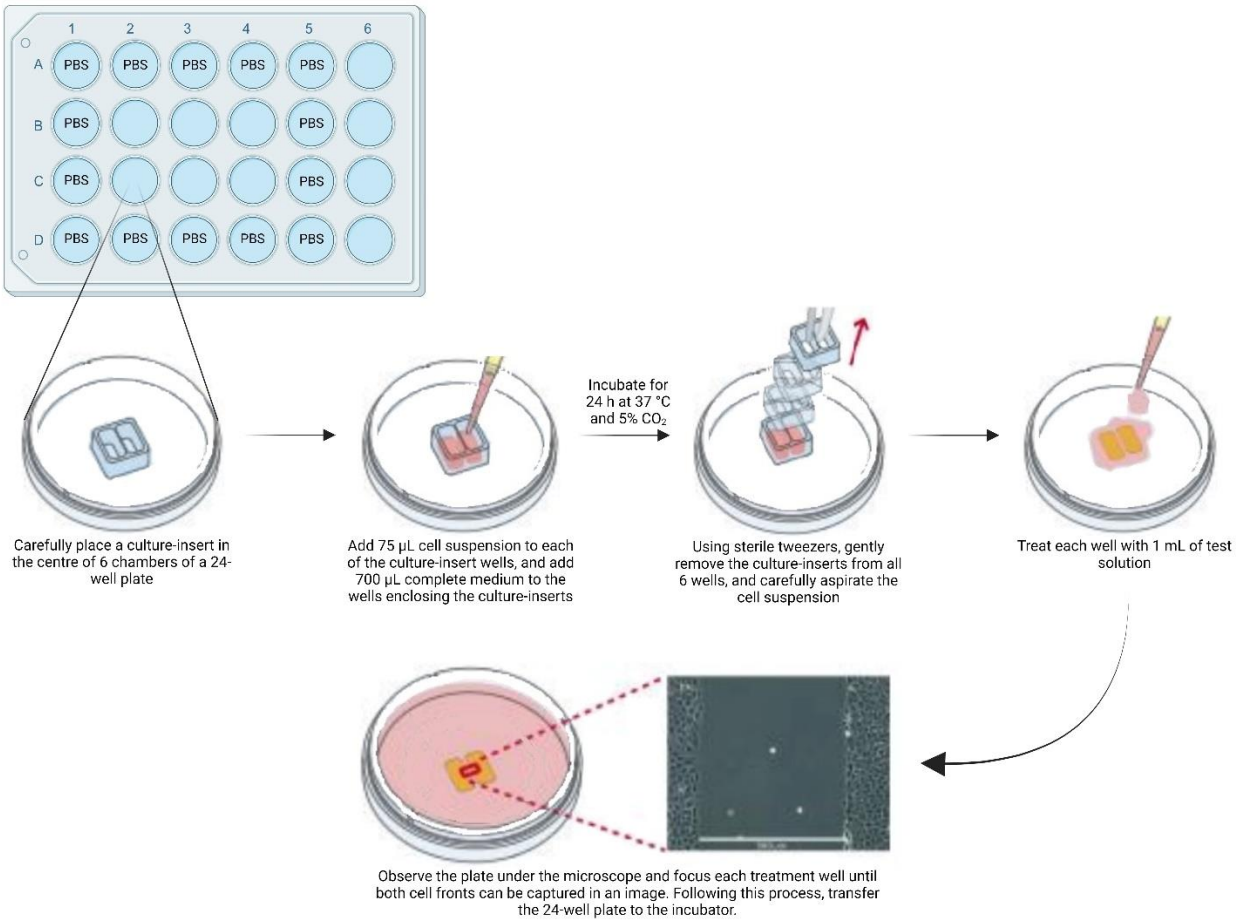

Figure 2.8: *The treatment of A549 cells for the wound healing assay. Created with BioRender.com. Adapted from ibidi (2021)*

After 24 hours, the cell culture plate was taken out of the incubator and inspected under the microscope to ensure that a 100% confluent cell layer was achieved. It was then

transferred to the laminar flow hood and, using sterile tweezers, the culture-inserts were gently removed from all 6 wells. Next, the cell suspension was carefully aspirated. In two of the wells, the aspirated medium was replaced with 1 mL of DMEM supplemented with 1% FBS and 1% L-glutamine, to serve as the 'untreated' control. Two wells were each treated with 1 mL of the 55 µM AZD5363 solution, whereas the remaining two wells were treated with 1 mL of the DMSO control solution (equivalent to the DMSO concentration present in the 55 µM AZD5363 solution (approximately 0.4% v/v)). The plate was then observed under the inverted Nikon Ti-S microscope in brightfield mode, and each treatment well was focused until both cell fronts could be captured in an image. Following this process, the 24-well plate was transferred to the incubator.

The same procedure of image capturing was repeated at 48, 72, and 96 hours after the start of the experiment.

2.11 Statistical analysis

Data was analysed using SPSS for Windows v.25.

2.11.1 Cell viability assays

For each individual cell line, drug concentration and time point, the percentage cell viability values (normalised to 100% vehicle control) from the biological and technical repeats were grouped together and analysed for normality of distribution using the Shapiro-Wilk test. Depending on the outcomes of these analyses, it was decided whether to proceed via parametric or non-parametric analysis. In the case of normally distributed data, comparisons of percentage viability changes for the same drug concentration at different time points were carried out by Analysis of Variance (ANOVA), followed by *post-hoc*

pairwise-comparison with Tukey correction for multiple analysis. In the case of data that was not normally distributed, statistical analysis was carried out using Kruskal-Wallis testing with *post-hoc* pairwise-comparison with Bonferroni-Dunn correction for multiple analysis. Results were considered significant at a *p*-value of less than 0.05.

2.11.2 ELISA assays

ELISA assays were carried out in order to determine eIF4E concentrations at two time points, post exposure to the drug under study, compared to a vehicle-treated control. eIF4E concentrations were first normalised to total protein content as determined by Bradford assays. The normalised values (4 repeats of each sample) were then analysed for distribution normality using Shapiro-Wilk testing. Normally distributed data was analysed at each of the two time points, for differences in eIF4E concentrations between vehicle control and cells treated with IC_{30}, 6 hours and 10 hours post treatment, using the independent sample t-test. In the case of data that was not normally distributed, statistical analysis was carried out using the Mann Whitney U test. Results were considered significant at a *p*-value of less than 0.05.

2.11.3 Wound healing assays

The wound areas for each sample were quantified using TScratch software for Windows. Loss in wound area for drug-treated cells was expressed as a percentage of the vehicle control wound area for each time point.

The normalised values were then analysed for distribution normality using Shapiro-Wilk testing. Normally distributed data was analysed for differences in wound closure between 24, 48 and 72 hours. For data that showed a normal distribution, analysis was carried out

using the independent sample t-test to compare migration differences between vehicle control and treated cells. In the case of data that was not normally distributed, statistical analysis was carried out using the Mann Whitney U test. Results were considered significant at a *p*-value of less than 0.05.

Chapter 3

Results

3 Introduction

All results obtained from this present study, together with the respective statistical analyses carried out for each experiment are presented in this chapter as follows:

- results of cell viability assays following the treatment of AZD5363 on H520 and A549 cells,
- results of eIF4E ELISA following the treatment of AZD5363 on A549 cells, and
- results of wound healing assays following the treatment of AZD5363 on A549 cells.

3.1 PrestoBlue™ cell viability assays

3.1.1 Results following the treatment of AZD5363 on H520 cells

For the first experimental procedure, H520 cell lines were treated with various concentrations of AZD5363 ranging from 10 µM to 100 µM, at 10 µM increments, as described in Sections 2.8 and 2.8.1. The dose-response curves that represent the cell viabilities following such increasing concentrations of AZD5363 treatment at 24-, 48-, and 72-hour time points are shown in Figure 3.1, below.

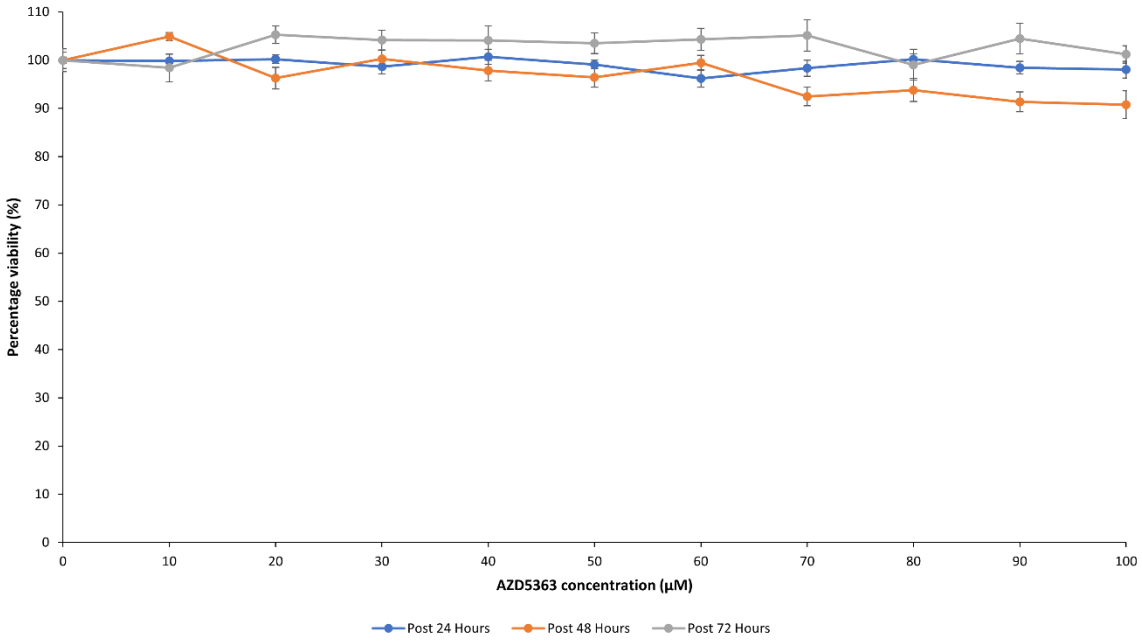

Figure 3.1: *Dose response curves at 24-, 48-, and 72-hour time points, following the treatment of H520 cells with AZD5363 at concentrations from 10 µM to 100 µM. The calculation of the percentage cell viability was carried out by quantifying the blank-corrected mean absorbance values obtained from PrestoBlue™ cell viability assays in relation to the blank-corrected mean absorbance values obtained from the DMSO vehicle control (approx. 0.8% v/v). n=4 for DMSO control, blank, and all AZD5363 concentrations. Error bars represent SEM. DMSO: Dimethyl sulfoxide; SEM: Standard Error of the Mean.*

For the current study, the point of interest is the concentration of AZD5363 that results in a loss of 30% in cell viability. When H520 cells were treated with the drug at concentrations ranging from 10 to 100 µM, a cell viability of 70% was not achieved at any of the time points

investigated. In fact, the lowest mean cell viability that was recorded is 96.2%; for this reason, no further investigations were conducted with the H520 cell line.

3.1.2 Results following the treatment of AZD5363 on A549 cells

Figure 3.2 below shows the dose-response curves that represent the resulting cell viabilities following the treatment of A549 cells with concentrations of AZD5363 ranging from 10 µM to 100 µM, at 10 µM increments.

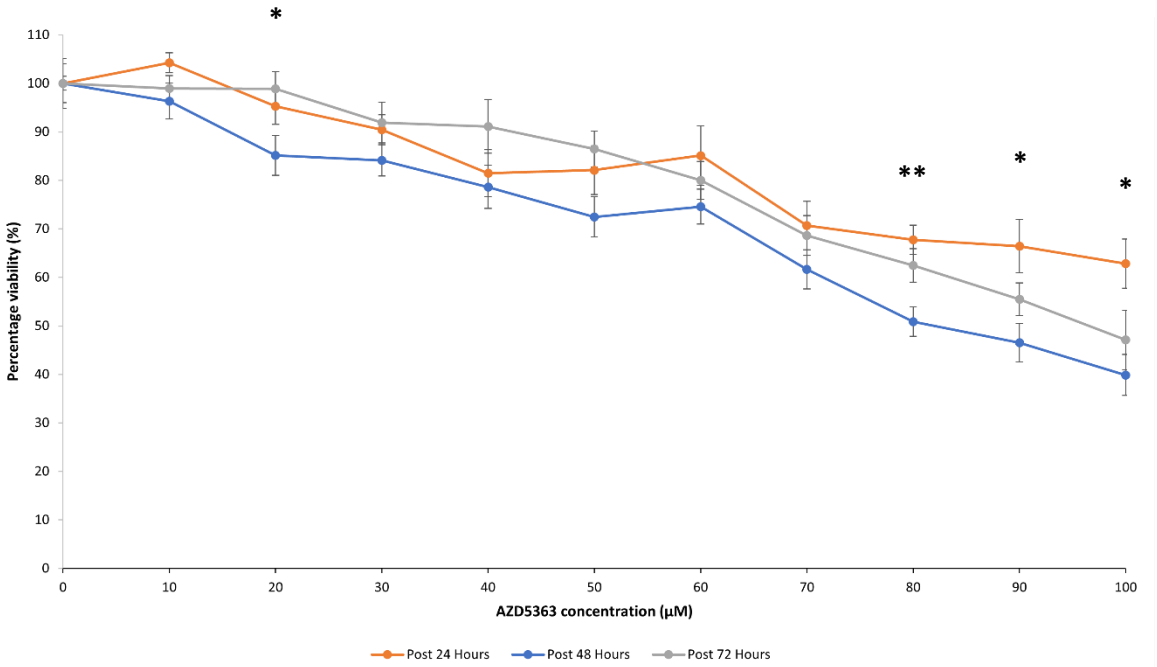

Figure 3.2: *Dose response curves at 24-, 48-, and 72-hour time points, following the treatment of A549 cells with AZD5363 at concentrations from 10 µM to 100 µM.* *The calculation of the percentage cell viability was carried out by quantifying the blank-corrected mean absorbance values obtained from PrestoBlue™ cell viability assays in relation to the blank-corrected mean absorbance values obtained from the DMSO vehicle control (approx. 0.8% v/v). n=4 for DMSO control, blank, and all AZD5363 concentrations. Error bars represent SEM. DMSO: Dimethyl sulfoxide; SEM: Standard Error of the Mean.*

With respect to A549 cells, a general decrease in cell viability was observed with increasing AZD5363 concentration, at almost all time points. Analysis of the three biological repeats carried out resulted in an approximate 70% cell viability at AZD5363 concentrations between 40 µM and the 90 µM. To achieve a more accurate concentration, the

experimental procedure was therefore repeated, and this time the concentration range of drug treatment was further narrowed down from 35 µM to 90 µM and using 5 µM increments; the yielded dose-response curves are shown in Figure 3.3, below.

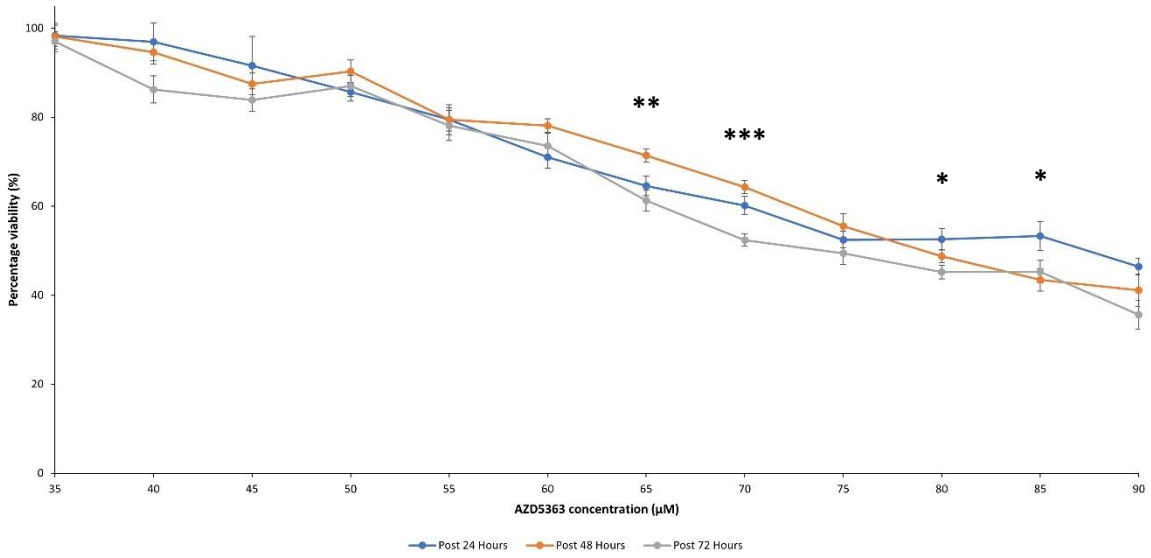

Figure 3.3: *Dose response curves at 24-, 48-, and 72-hour time points, following the treatment of A549 cells with AZD5363 at concentrations from 35 µM to 90 µM. The calculation of the percentage cell viability was carried out by quantifying the blank-corrected mean absorbance values obtained from PrestoBlue™ cell viability assays in relation to the blank-corrected mean absorbance values obtained from the DMSO vehicle control (approx. 0.8% v/v). n=4 for DMSO control, blank, and all AZD5363 concentrations. Error bars represent SEM. DMSO: Dimethyl sulfoxide; SEM: Standard Error of the Mean.*

When taking into account the viability results at the 24-hour time point, it can be observed that 70% cell viability of A549 cells was achieved with AZD5363 concentrations ranging from 55 to 65 µM; cell viability plummeted further with increasing AZD5363 concentrations, reaching a mean viability of 46% with 90 µM drug concentration.

At the 48-hour time point, AZD5363 concentrations ranging from 55 to 75 µM yielded a 30% decrease in cell viability of A549 cells. Similar to what was observed after 24 hours, a trend of further decrease in cell viability with increasing drug concentration can also be seen after 48 hours; this time however, the mean cell viability at 90 µM AZD5363 was 41%.

A 30% decrease in A549 cell viability at the 72-hour time point was achieved with AZD5363 concentrations ranging from 55 to 65 µM, which was a similar concentration range yielded after 24 hours of drug treatment. This time the mean A549 cell viability reached with the treatment of 90 µM AZD5363 was 36%.

3.1.3 Shapiro-Wilk test

The analysis for normality between each of the three data sets of absorbance per concentration was carried out using the Shapiro-Wilk test, the results of which are tabulated below (Tables 3.1 and 3.2).

Table 3.1: *Result of the Shapiro-Wilk test which analysed the normality between each data set of absorbance at concentrations from 10 µM to 100 µM investigated. Results were considered significant at a p-value < 0.05.* *NS = Not significant.*

AZD5363 concentration (µM)	Time point (Hours)	*p*-value	Normal distribution (Yes/No)
40	24	NS	Yes
	48	0.047 *	No
	72	NS	Yes

The test for normality comparing the AZD5363 concentration range between 10 µM and 100 µM against different time points for the initial viability assays yielded a normal distribution, except for the 40 µM AZD5363 concentration at the 48-hour time point.

The second viability assay on A549 cells, where AZD5363 was tested at concentrations ranging from 35 µM to 90 µM, yielded a normal distribution at the 24-hour time point except for the 45 µM. A similar trend of normal distribution resulted at the 48-hour time point, where only the 70 µM and 80 µM concentrations did not follow a normal distribution. At the 72-hour time point, the 75 µM, 85 µM and 90 µM concentrations did

not follow a normal distribution. In view of the above results, it was therefore decided to proceed with the parametric analysis using ANOVA.

Table 3.2: *Result of the Shapiro-Wilk test which analysed the normality between each data set of absorbance at concentrations from 35 µM to 90 µM investigated. Results were considered significant at a p-value < 0.05.* NS = Not significant.

AZD5363 concentration (µM)	Time point (Hours)	*p*-value	Normal distribution (Yes/No)
45	24	0.012 *	No
	48	NS	Yes
	72	NS	Yes
70	24	NS	Yes
	48	0.038 *	No
	72	NS	Yes
75	24	NS	Yes
	48	NS	Yes
	72	0.024 *	No
80	24	NS	Yes
	48	0.009 **	No
	72	NS	Yes
85	24	NS	Yes
	48	NS	Yes
	72	0.040 *	No
90	24	NS	Yes
	48	NS	Yes
	72	0.016 *	No

3.1.4 ANOVA with Tukey correction

The absorbance of each drug concentration at the analysed three different time points was compared using the ANOVA with *post-hoc* Tukey correction to yield corrected values for pairwise comparison; this was done for the two viability assays carried out on the A549 cells, and results are presented in Tables 3.3 and 3.4, below.

For the initial viability assay using AZD5363 concentrations ranging from 10 µM to 100 µM (Table 3.3), there was a significant difference in cell viability between the 48-hour and 72-

hour time points at the 20 µM concentration, with a *p*-value of 0.041. At the 90 µM and 100 µM concentration, there was a significant difference between the 24-hour and 48-hour time points, with *p*-values of 0.011 and 0.012, respectively. The 80 µM concentration yielded a highly significant difference ($p = 0.002$) in cell viability at the 48-hour time point with both the 24- and 72-hour time points. There was no significant difference in cell viability between the different time points at the rest of the concentrations tested.

Table 3.3: *ANOVA with post-hoc Tukey correction comparing the absorbance of AZD5363 drug concentrations ranging from 10 µM to 100 µM at 24-, 48-, and 72-hour time points. Results were considered significant at a p-value < 0.05.* NS = *Not significant.*

AZD5363 concentration (µM)	ANOVA	Time point comparison (Hours)	*Post-hoc* Tukey *p*-value
20	0.041 *	24 vs 48	NS
		24 vs 72	NS
		48 vs 72	0.040 *
80	0.002 **	24 vs 48	0.002 *
		24 vs 72	NS
		48 vs 72	0.038 *
90	0.011 *	24 vs 48	0.008 *
		24 vs 72	NS
		48 vs 72	0.325
100	0.012 *	24 vs 48	0.010 *
		24 vs 72	NS
		48 vs 72	NS

The second viability assay that investigated the A549 cells to AZD5363 concentrations from 35 µM to 90 µM (Table 3.4) resulted in a highly significant difference in cell viability at the 65 µM concentration between the 48- and 72-hour time points ($p = 0.005$). A significant difference in cell viability between the 24- and 72-hour time points was recorded at concentrations 80 µM ($p = 0.028$) and 90 µM ($p = 0.052$), whereas at a concentration of 85 µM, a significant difference in cell viability resulted between the 24- and 48-hour time

points (p = 0.044). The 70 µM concentration yielded a very highly significant difference (p = < 0.001) in cell viability at the 72-hour time point with both the 24- and 48-hour time points.

Table 3.4: *ANOVA with post-hoc Tukey correction comparing the absorbance of AZD5363 drug concentrations ranging from 35 µM to 90 µM at 24-, 48-, and 72-hour time points. Results were considered significant at a p-value < 0.05.* *NS = Not significant.*

AZD5363 concentration (µM)	ANOVA	Time point comparison (Hours)	*Post-hoc* Tukey *p*-value
65	0.005 **	24 vs 48	NS
		24 vs 72	NS
		48 vs 72	0.004 **
70	< 0.001 ***	24 vs 48	NS
		24 vs 72	0.007 **
		48 vs 72	< 0.001 ***
80	0.028 *	24 vs 48	NS
		24 vs 72	0.021 *
		48 vs 72	NS
85	0.044 *	24 vs 48	0.049 *
		24 vs 72	NS
		48 vs 72	NS
90	0.052	24 vs 48	NS
		24 vs 72	0.041 *
		48 vs 72	NS

Based on the cell viability results obtained, a concentration of 55 µM AZD5363 was therefore chosen for subsequent investigations carried out.

3.2 Result of ELISA for eIF4E following treatment of A549 cells with AZD5363

The calibration curve of the ELISA assay described in Section 2.9.2.1 is shown in Figure 3.4, below.

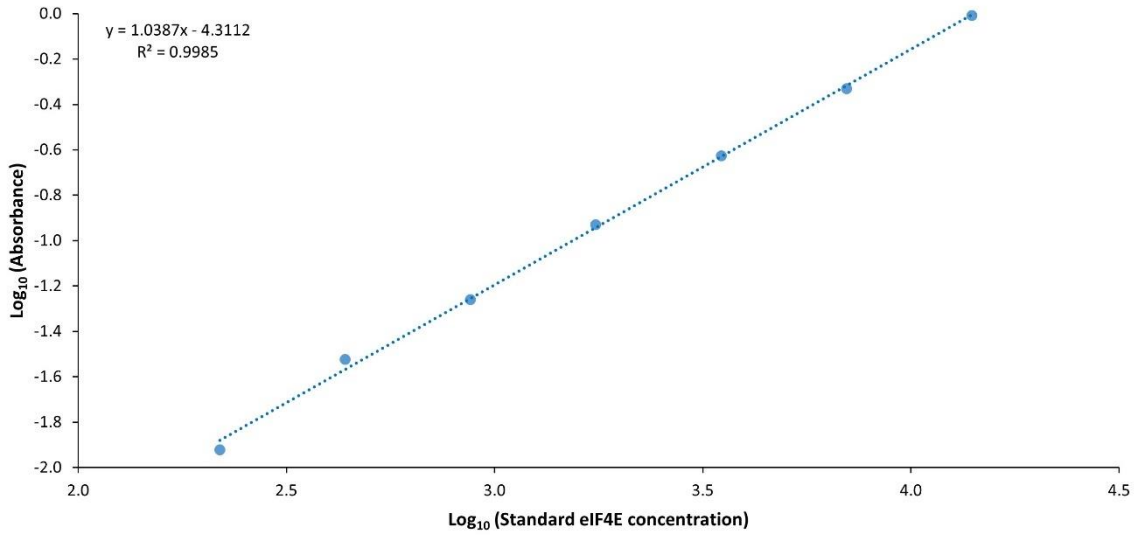

Figure 3.4: *A standard curve of the log10 eIF4E standard concentrations against the average Log10 absorbance standard values.*

Figure 3.5 below shows the calibration curve of the Bradford protein assay, as described in Section 2.9.3.1.

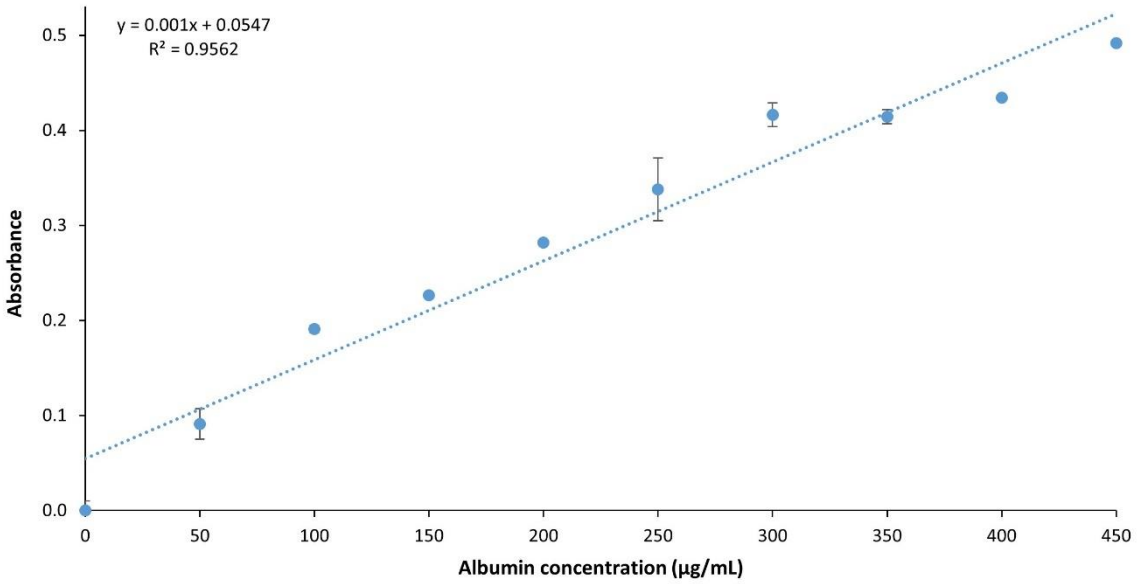

Figure 3.5: *A standard curve of the albumin concentrations against the average absorbance standard values.*

A549 cells were treated with 55 µM AZD5363, and an ELISA for eIF4E was carried out to determine the levels of eIF4E, as per procedure described in Section 2.9. The normalisation

of treated samples to their respective vehicle controls generated a box plot, as shown in Figure 3.6, below.

The mean normalised eIF4E concentration of the test samples at the 6-hour time point was 22% less than that of the vehicle control, whereas at the 10-hour time point, the mean normalised eIF4E concentration was 29% lower than the eIF4E concentration of the vehicle control.

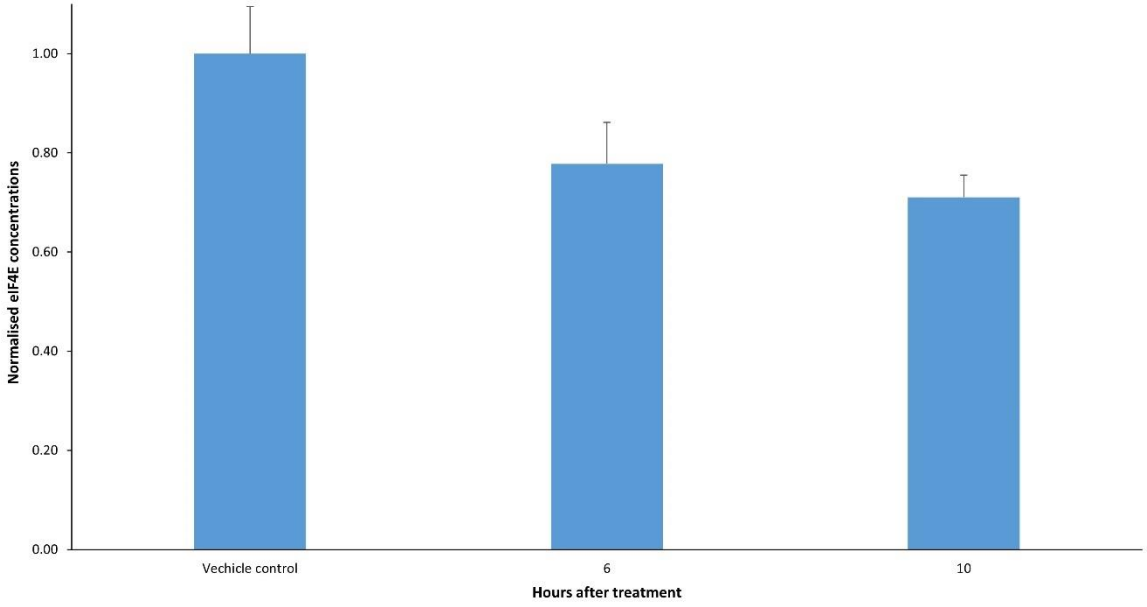

Figure 3.6: *A box plot of normalised eIF4E concentrations of A549 cells treated with 55 µM AZD5363, at 6 hours, and 10 hours post-treatment, as compared with vehicle control.* *n=4 for vehicle control, blank, and 55 µM AZD5363 concentration utilised to treat the cells. Error bars represent SEM. SEM: Standard Error of the Mean.*

3.2.1 Shapiro-Wilk test

The analysis for normality between the two time points for each data set was carried out using the Shapiro-Wilk test, the results of which are tabulated below (Table 3.5).

Table 4.5: *Result of the Shapiro-Wilk test which analysed the normality between 6- and 10- hour time points, for A549 cells treated with vehicle control solution, and cells treated with 55 µM AZD5363. Results were considered significant at a p-value < 0.5.* *NS = Not significant*

Cell treatment	Time point (Hours)	*p*-value	Normal distribution (Yes/No)
Vehicle control	6	NS	Yes
	10	NS	Yes
55 µM AZD5363	6	NS	Yes
	10	NS	Yes

The tests for normality of distribution of repeats of the same time points and treatment conditions yielded a normal distribution, since the *p*-value of all the data points showed no significant difference between the data sets of each experiment as they ranged from 0.167 to 0.858. It was therefore decided to proceed with the parametric analysis using the independent sample t-test.

3.2.2 Independent sample t-test

An independent sample t-test was carried out to compare the difference in normalised eIF4E concentrations between vehicle control and the two time points investigated. Results are tabulated in Table 3.6, below. Despite the consistent downward trend observed, there was no significant difference between the values obtained (p = > 0.05).

Table 3.6: *Result of the independent sample t-test, comparing the difference in normalised eIF4E concentrations between cells treated with vehicle control solution, and cells treated with 55 µM AZD5363, at the 6- and 10-hour time points. Results were considered significant at a p-value < 0.05.* *NS = Not significant.*

		Time (h)	
		6	**10**
Normalised eIF4E concentration	**Vehicle Control**	1.00	1.00
	55 µM AZD5363	0.78	0.71
***p*-value**		**NS**	**NS**

3.3 Results of the wound healing assays

For this experimental procedure, A549 cells were treated with 55 µM AZD5363, as described in Section 2.10. The figures that follow show the gap areas at the time of treatment (0 h), and 24, 48, and 72 hours after treatment – for cells treated with the vehicle control solution (Figure 3.7), untreated cells (Figure 3.8), and cells treated with 55 µM AZD5363 (Figure 3.9), as captured by TScratch for Windows.

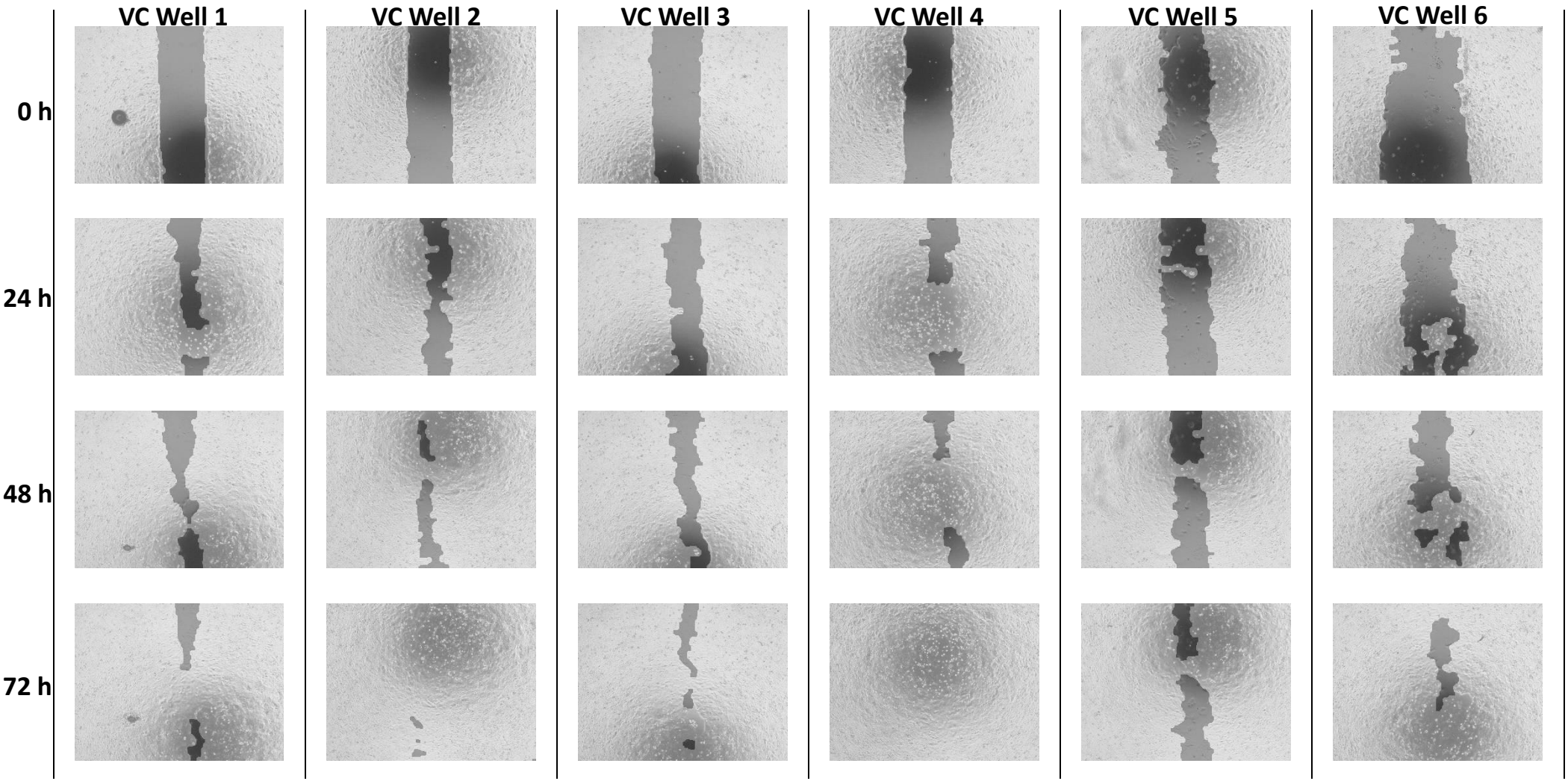

Figure 3.7: *Results of wound healing assays performed on A549 cells treated with vehicle control solution, showing the gap areas at the time of treatment (0 h), and 24, 48, and 72 hours after treatment, as captured by TScratch for Windows.*

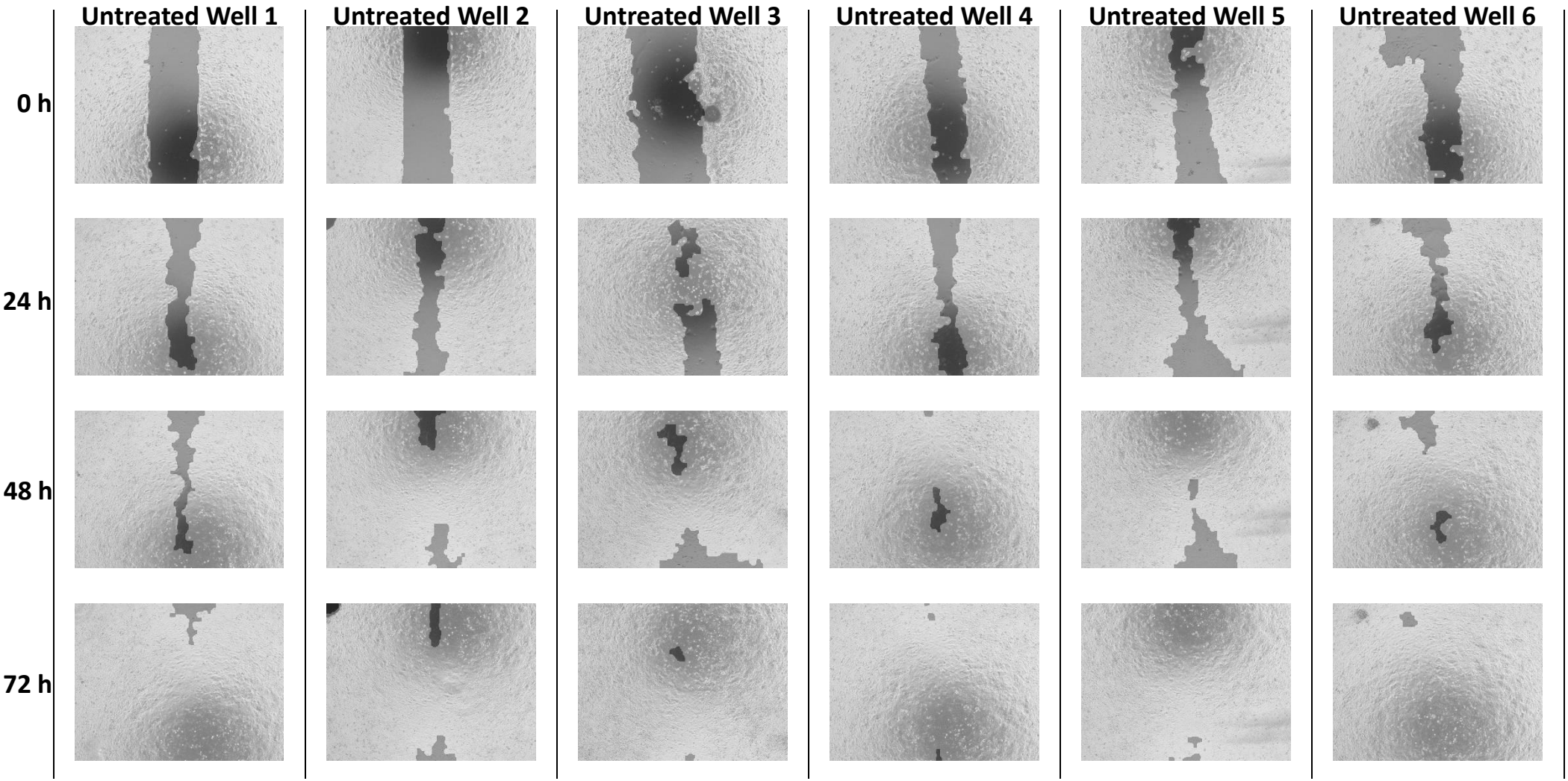

Figure 3.8: *Results of wound healing assays performed on untreated A549 cells, showing the gap areas at the time of treatment (0 h), and 24, 48, and 72 hours after treatment, as captured by TScratch for Windows.*

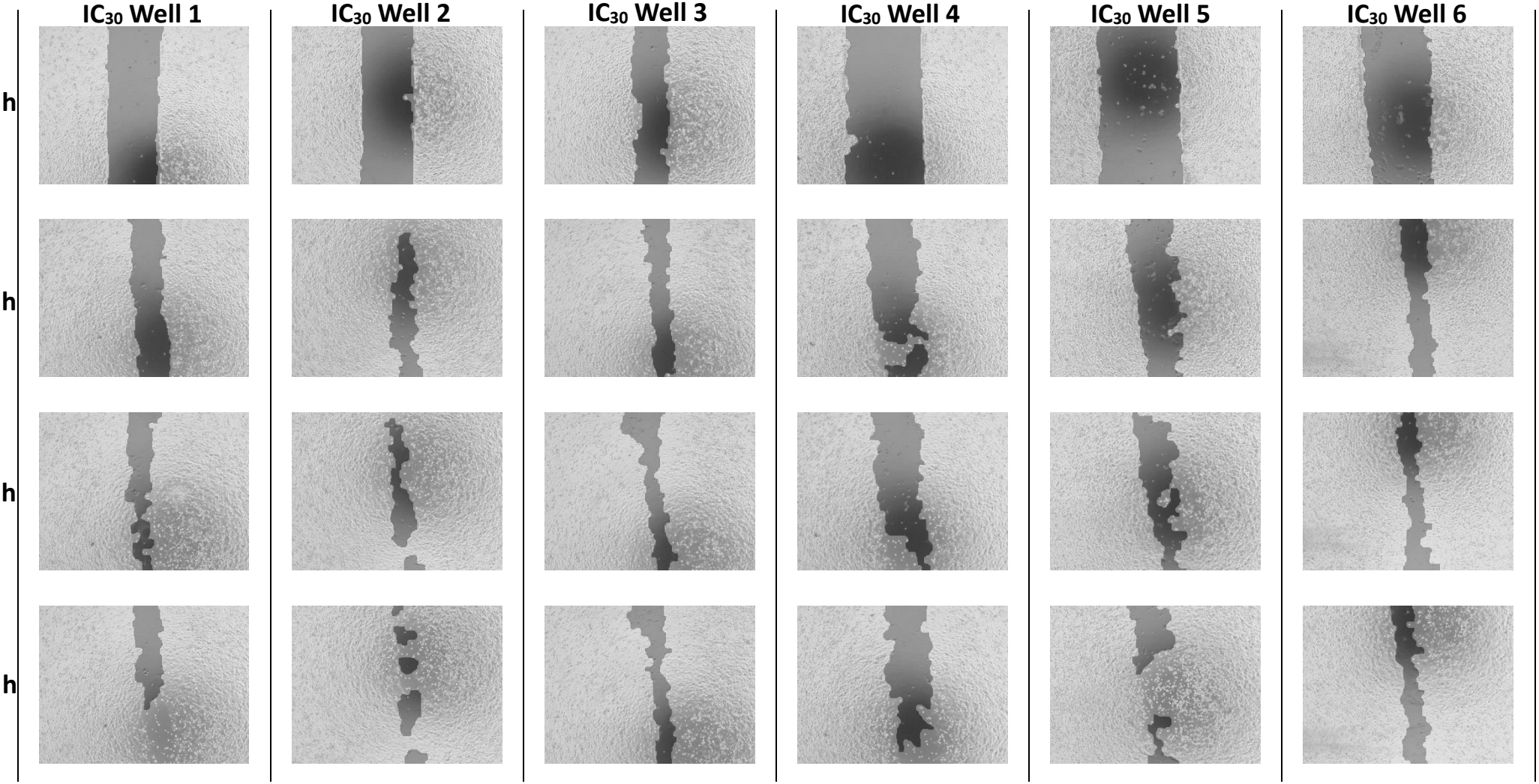

Figure 3.9: *Results of wound healing assays performed on A549 cells treated with 55 µM (IC_{30}) AZD5363, showing the gap areas at the time of treatment (0 h), and 24, 48, and 72 hours after treatment, as captured by TScratch for Windows.* *IC_{30} = 30% inhibitory concentration*

Untreated cells were used as a visual cue that cell culture was successful; they were therefore eliminated from analysis. The captured percentage mean gap area at the investigated different time points, for the cells treated with 55 µM AZD5363 and for those treated with the DMSO vehicle control solution, were plotted in a percentage-response curve, as shown in Figure 3.10, below.

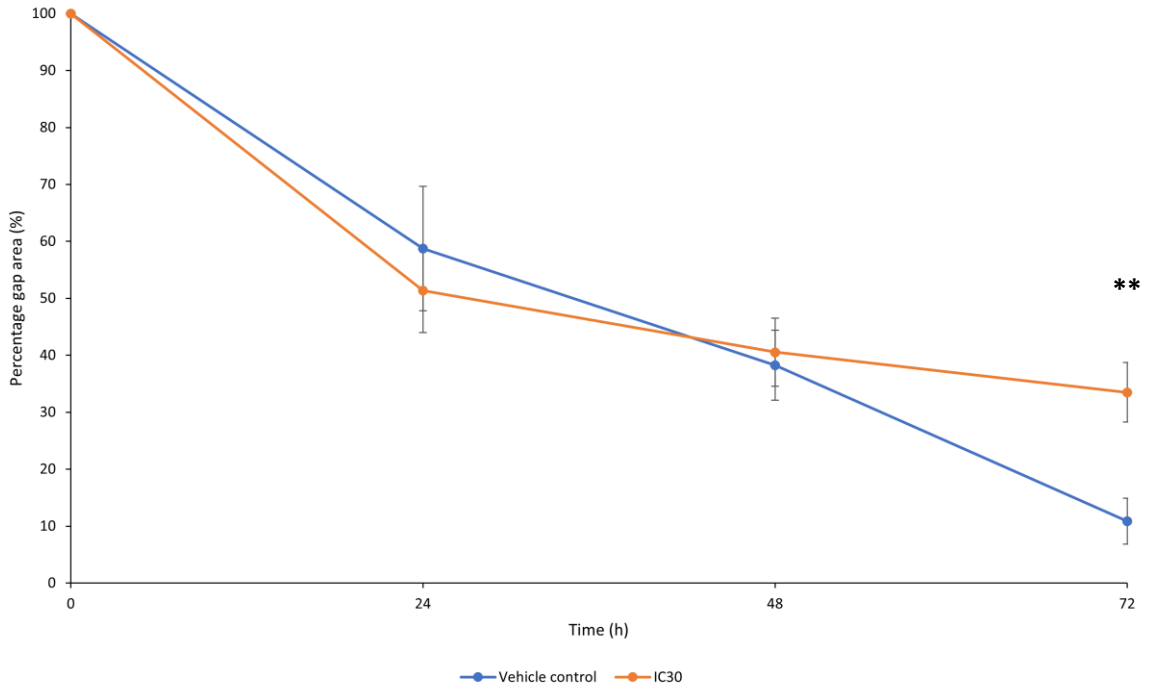

Figure 3.10: *Percentage-response curve of captured percentage mean gap area against time for A549 cells treated with 55 µM AZD5363 and those treated with vehicle control solution.* *n=6 for DMSO vehicle control, blank, and 55 µM AZD5363 concentration utilised to treat the cells. Error bars represent SEM. DMSO: Dimethyl sulfoxide; SEM: Standard Error of the Mean.*

The percentage wound closure of the cells treated with the vehicle control decreased to an average of 59% at the 24-hour time point; it plummeted steadily to 38% for the following 24 hours and reached 11% at the 72-hour time point.

A similar trend in the decrease in percentage gap area at the 24-hour time point was observed for the cells treated with 55 µM AZD5363 (51%). Subsequently however, the

wound closure was less steady and was down to 41% at the 48-hour time point and 33% after 72 hours.

3.3.1 Shapiro-Wilk test

The analysis for normality between each of the three time points for each data set was carried out using the Shapiro-Wilk test, the results of which are tabulated below (Table 3.7).

Table 3.7: *Result of the Shapiro-Wilk test which analysed the normality between 24-, 48-, and 72- hour time points, for A549 cells treated with vehicle control solution, and cells treated with 55 µM AZD5363. Results were considered significant at a p-value < 0.05.* NS = Not significant

Cell treatment	Time point (Hours)	*p*-value	Normal distribution (Yes/No)
Vehicle control	24	NS	Yes
	48	NS	Yes
	72	NS	Yes
55 µM AZD5363	24	NS	Yes
	48	NS	Yes
	72	NS	Yes

The tests for normality of distribution of repeats of the same time points and treatment conditions yielded a normal distribution, since the *p*-value of all the data points showed no significant difference between the data sets of each experiment as they ranged from 0.265 to 0.414. It was therefore decided to proceed with the parametric analysis using the independent sample t-test.

3.3.2 Independent sample t-test

Migration differences between vehicle control and treated cells at the investigated three different time points were compared using the independent sample t-test, and results are tabulated below (Table 3.8).

Table 3.8: *Result of the independent sample t-test, comparing the difference in migration between cells treated with vehicle control solution, and cells treated with 55 µM AZD5363. Results were considered significant at a p-value < 0.05.* NS *= Not significant.*

		Time (h)		
		24	**48**	**72**
Percentage mean gap closure (%)	**Vehicle Control**	58.73	38.22	10.83
	55 µM AZD5363	51.34	40.53	33.49
***p*-value**		**NS**	**NS**	**0.009 ****

There was no significant difference in percentage mean gap closure between the vehicle control and the cells treated with 55 µM AZD5363 at the 24-hour (p = > 0.05) and 48-hour (p = > 0.05) time points. However, at the 72-hour time point, the difference in percentage mean gap closure was highly significant (p = 0.009).

Chapter 4

Discussion and Conclusion

4 Introduction

As outlined in Section 1.17, this current study is part of a larger research project LCeNT, which is investigating combined therapy for aggressive forms of lung cancer. It is funded by the MCST and is being conducted at the Department of Clinical Pharmacology and Therapeutics within the University of Malta. The aim of the present study is to investigate the *in vitro* effects of the small molecule inhibitor AZD5363, which targets the PI3K/Akt/mTOR pathway, and is tested on two forms of aggressive NSCLC cells with the aim of achieving a 30% reduction in cell viability, such that cells are sensitised. Sensitisation, for the purpose of the current research, is defined as being the use of small molecule inhibitors to reach a 30% loss in cell viability. Following such treatment, ASOs will be added as part of a combination treatment.

AZD5363 is an ATP-competitive inhibitor, which is a very potent, orally bioavailable pan-Akt kinase inhibitor, and inhibits all three isoforms of Akt. The drug exhibited growth inhibition on 41 cell lines when it was tested on a panel of 182 solid and haematologic tumour cells *in vitro* (Davies, Greenwood *et al.* 2012). Among those that demonstrated the most sensitivity are cells derived from breast cancer or those with mutations in *PIK3CA* and/or *PTEN*. The drug has since been undergoing further investigations on breast cancer cells harbouring *AKT* mutations (Shrestha Bhattarai, Shamu *et al.* 2022), liver cell lines (Zhang, Zheng *et al.* 2016), and lung tumour cells (Jacobsen, Bertran-Alamillo *et al.* 2017, Puglisi, Thavasu *et al.* 2014), among others.

As discussed in Section 1.11, Tan (2020) documents a strong link between the PI3K/Akt/mTOR pathway and the development and progression of NSCLC. Furthermore, the downstream effectors of this cascade, eIF4E and rpS6, besides being capable of

transforming cells, are overexpressed in AC and SCC, and are poor prognostic markers (Chen, Tan *et al.* 2015, Dobashi, Watanabe *et al.* 2011). Additionally, *PIK3CA* mutations and amplifications, *PTEN* loss, as well as mutations in *RICTOR*, *AKT1* and *STK11*, have all been described as genetic disorders contributing to the dysregulation of the signal transduction in the same mTOR pathway (Cheng, Zou *et al.* 2015, Janku, Yap *et al.* 2018, Papadimitrakopoulou 2012). For these reasons, the present study investigated AZD5363 on two NSCLC cell lines, namely H520, derived from squamous cell carcinoma, and A549, originating from adenocarcinomic human alveolar basal epithelial cells. Research consisted of treatment of both cell lines using drug concentrations from 10 to 100 µM, followed by PrestoBlue™ viability assays to determine the approximate concentration that will result in a 30% loss in viability. Subsequent tests entailed the quantification of the protein eIF4E through ELISA, as well as would healing assays for the investigation of the anti-metastatic potential of AZD5363 at the determined concentration.

4.1 Treatment of AZD5363 on H520 and A549 cells

As shown in Figure 3.1, the treatment of AZD5363 at concentrations from 10 to 100 µM on the H520 cells failed to result in a decrease in cell viability. Conversely, the same treatment on A549 cells decreased the cell viability in a concentration-dependent fashion (Figures 3.2 and 3.3), such that 55 µM AZD5363 was selected as the 30% inhibitory concentration (IC_{30}) for the subsequent investigations carried out on this cell line. Therefore, this drug can be further investigated in the LCeNT study in order to be used in combination with the two antisense oligonucleotides.

4.1.1 Sensitivity of A549 cells to AZD5363 treatment

The dose- and time- dependent sensitivity of A549 cells to treatment with AZD5363 (Figures 3.2 and 3.3) is in line with what was observed in an investigation undertaken by Zhang, Zheng *et al.* (2016) on a panel of two liver cancer cell lines, Hep-G2 (hepatoblastoma) and Huh-7 (adult hepatocellular carcinoma), exposed to AZD5363 concentrations ranging from 5 to 30 µM for 24, 48 and 72 hours; both cells exhibited a similar dose-dependent growth inhibition. Furthermore, the authors reported that the 50% inhibitory concentration (IC_{50}) of the drug on both cell lines decreased in a time-dependent manner, such that at the 72-hour time point the IC_{50} of the Huh-7 cells and Hep-G2 was 17.80 µM and 18.476 µM, respectively. Further investigation led to the observation that despite that the drug increased the phosphorylation of Akt in a dose-and time-dependent fashion in both cell lines, it inhibited the phosphorylation of GSK3. It was therefore concluded that AZD5363 resulted in the suppression of Akt kinase activity. Furthermore, the authors suggest that, since there were also differing reactions to the mTOR pathway by the cells investigated, they highlight that it is therefore essential to ascertain whether traits such as *PIK3CA* mutation, *PTEN* loss, Ras mutations and *ERBB2* (HER2) amplification, are present in liver cancer cells, as certain tumour types may be enriched for responders to Akt inhibitors, such as AZD5363.

Jacobsen, Bertran-Alamillo *et al.* (2017) analysed the use of Akt inhibitors on NSCLC cells with acquired resistance to EGFR tyrosine kinase inhibitor (TKI) treatment, and in which phosphorylated Akt, its downstream effector, phosphorylated PRAS40, as well as phosphorylated FOXO were all elevated. When AZD5363 was used as a single agent, the drug inhibited cell growth at concentrations ranging from 5 to 15 µM. Moreover, when

compared to EGFR-TKI sensitive cells, treatment with a combination of AZD5363 and EGFR TKI on the same cells resulted in a significant increase in growth inhibition after 72 hours. The authors thus indicated that sensitisation of the EGFR-TKI resistant cells to the addition of AZD5363 may be due to reduced Akt pathway activation and subsequent inhibition of PRAS40 phosphorylation and FOXO activation, strongly suggesting that Akt kinase activity is being inhibited. A similar observation was noted by Ribas, Pancholi *et al.* (2015) who investigated the effect of AZD5363, alone or in combination with endocrine therapy, on endocrine sensitive and resistant breast cancer cells. The examined cell lines exhibited different levels of sensitivity towards the drug; at concentrations above 10 μM, HCC1428 (breast adenocarcinoma) and their long-term oestrogen deprivation (LTED) derivative were resistant to treatment, whereas T47D and their LTED derivative, and ZR75-LTED (two invasive breast cancers of no special type) were sensitive to concentrations as low as approximately 100 nM. In combination with endocrine therapy (fulvestrant, anastrozole or tamoxifen) however, AZD5363 was more efficacious on both endocrine-sensitive and -resistant cell lines, particularly those with *PIK3CA* mutations and/or *PTEN* loss.

Other PI3K/Akt/mTOR effectors may also be responsible, and thus explain the sensitivity of tumour cells to AZD5363. In a study that evaluated the prevention or delay of resistance to enzalutamide in prostate cancer, Toren, Kim *et al.* (2015) observed a dose-dependent reduction in cell viability of the enzalutamide-resistant MR49C and MR49F cells (both originating from prostate carcinoma) after 48 hours of treatment of AZD5363 at concentrations from 0.005 to 5 μM, and reported the drug to cause a buildup of inactive phosphorylated Akt, as shown by subsequent decreases in S6K1 and 4E-BP1. A similar significant response was seen *in vivo*, where the administration of lower doses of AZD5363

were observed to decrease tumour growth, and the concomitant administration of enzalutamide appeared to function as an agonist.

4.1.2 Resistance of H520 cells to AZD5363 treatment

The resistance of H520 cells to the drug (Figure 3.1) might confirm what Davies, Greenwood *et al.* (2012) reported when they carried out proliferation assays on a panel of 182 cell lines from haematologic and solid tumours. The authors classified sensitivity to the drug using a cut-off of $IC_{50} \leq 3$ μM AZD5363. They reported 88% of lung cancer cells to be resistant to such treatment. Since in the present investigation, a maximum concentration of 100 μM did not result in any loss in cell viability of H520 cells, it may mean that either a higher concentration of the drug than what was tested is required to sensitise the cells, or lung SCC cells are resistant to such treatment altogether. A plausible explanation could be that, as was discussed in Section 1.11, squamous cell tumours tend to have an increased likelihood of *PTEN* loss (Spoerke, O'Brien *et al.* 2012) and *PIK3CA* amplification (Scheffler, Bos *et al.* 2015), both of which give rise to Akt hyperphosphorylation, and possibly unpredictable sensitivity and response to drug treatment. In fact, when Wang, Xu *et al.* (2021) evaluated the cell survival of gastric tumour cell lines with hyperphosphorylated Akt following treatment with Akt inhibitors, one of which was AZD5363, they observed variable sensitivity, suggesting that the therapeutic effect of Akt inhibitors on cells may be impaired. Their research also revealed a correlation between the susceptibility to Akt inhibitors and the reduced levels of phosphorylated GSK3, the downstream target protein of Akt. Following this observation and further investigations on the least sensitive cell lines, cell sensitisation only occurred when a combination of AZD5363 and ALK inhibitors was used. This however contrasts with the highly significant correlation that Davies, Greenwood *et*

al. (2012) reported between sensitivity to AZD5363 and *PIK3CA* mutation as well as *PTEN* mutations. Instead, the authors described a significant correlation between resistance to AZD5363 and the presence of Ras mutations.

Another possible explanation for the marked resistance to treatment of AZD5363 on H520 cells may be an elevation of *SGK1* mRNA expression, as was reported by Sommer, Dry *et al.* (2013) who, following the treatment of AZD5363 on 21 breast cancer cell lines, identified low *SGK1* mRNA expression in a number of highly AZD5363-sensitive cells, as opposed to high *SGK1* mRNA expression on resistant cells. They proposed that the monitoring of SGK1 levels to Akt inhibitor treatment may play a role in predicting tumour sensitivity to drugs that target Akt.

4.2 Quantification of eIF4E protein

Eukaryotic initiation factor 4E is essential for promoting mRNA translation (Xu, Zong *et al.* 2016). As a component of the eIF4F complex, which also includes eIF4G and eIF4A, it binds to the 5' cap structure. For cap-dependent translation initiation, the assembly of eIF4F is typically regarded as limiting, and it is principally controlled by variations in eIF4E availability. The activity of the eIF4F complex is especially sensitive to a subset of mRNAs encoding factors that promote survival and proliferation, such as *MCL1*, *MYC*, *VEGF* and *CCND1* (Robichaud, Hsu *et al.* 2018, Sonenberg, Hinnebusch 2009). Given this, it is not surprising that eIF4E is overexpressed in a variety of malignancies, including breast (Heikkinen, Korpela *et al.* 2013), gastric (Liang, Guo *et al.* 2013), lung (Li, Fan *et al.* 2012), and prostate (Graff, Konicek *et al.* 2009) cancers. In fact, breast cancer patients who had high levels of eIF4E expression had worse survival and a higher rate of cancer recurrence

(Heikkinen, Korpela *et al.* 2013), whereas overexpression of eIF4E is linked to vascular invasion in gastric cancer (Liang, Guo *et al.* 2013).

Lu, Zang *et al.* (2020) and Tang, Luo *et al.* (2022) investigated the correlation between the expression of phosphorylated conformations of Akt, mTOR and eIF4E with clinicopathological features in NSCLC and non-cancer lung tissues. Their findings show that, after surgical resection, increased levels of these proteins were associated with metastasis and poor OS in NSCLC patients. Additionally, SCC and, more notably AC, were found to significantly increase eIF4E phosphorylation levels; high levels of phosphorylated eIF4E were also associated with poor prognosis.

In line with these findings, when Xu, Zong *et al.* (2016) evaluated eIF4E levels in colorectal cancer (CRC) tissues, they found the protein level of eIF4E to be higher in colorectal liver metastasis (CLM) and non-CLM tissues as compared to matched non-tumour tissues. Since there was a significantly greater eIF4E overexpression rate in the CLM group (82.5%) compared to the non-CLM group (65%), the authors thus indicated that the raised eIF4E expression is linked to increased liver metastasis in CRC patients. They further corroborated these results by following 80 CRC patients who had surgically resected tumours; after two years, liver metastasis was found in 27 patients who had high eIF4E expression, while only three patients in the low eIF4E expression group had liver metastasis. Furthermore, through loss-of-function assays, the researchers reported that, following the knockdown of eIF4E, proliferation, migration and invasion was inhibited in both low and highly metastatic CRC cells. When looking into the underlying mechanism in more detail, they identified *CCND1*, *VEGF*, *MMP2* and *MMP9* as important components that regulate tumour metastasis; since their expression levels were observed to be reduced with downregulation

of eIF4E, they suggested that metastasis of CRC cells may be limited in part through the regulation of expression of these mRNAs encoding factors.

In view of the above observations, together with the results obtained in the current study, in which a reduction of 29% in mean eIF4E concentration was noted 10 hours after treatment of A459 cells with 55 µM AZD5363 (Figure 3.6), the role of the drug in regulating the expression of eIF4E, studied in combination with other treatment regimens, may be further investigated.

4.3 Investigation of the anti-metastatic potential of AZD5363 on A549 cells

The effect of AZD5363 on the Akt signalling pathway was investigated in a study on vascular smooth muscle cells undertaken by Lu, Liu *et al.* (2016). They initially transfected the cells with proteins that promote Akt phosphorylation, subsequent proliferation and migration, and which ultimately led to narrowing of the vascular lumen. Next, they performed a scratch-induced would healing assay using a concentration of 5 µM AZD5363. The authors observed that the drug caused a significant inhibition of wound closure rate at 12- and 24-hours post treatment, thus confirming the involvement of the Akt through the deactivation of GSK3 phosphorylation.

Şanli, Barlak *et al.* (2020) investigated the migration potential of AZD5363 on larynx cancer cells at concentrations of 1-5-10 µM. Their findings showed that, after 24 hours of treatment, whereas cells exposed to 1 µM AZD5363 did not change in terms of their ability to migrate, those treated with 5 and 10 µM AZD5363 covered a much smaller fraction of the wound, in comparison to control cells. More than 50% of the wound could be closed by control cells. The authors thus demonstrated the drug's potential to impede larynx cancer

cell migration, thus explaining the involvement of the Akt signalling pathway in the regulation of cell migration.

Kano, Izumi *et al.* (2023) studied prostate cancer cells and the influence of chemokines, namely CCL20 and its receptor CCR6, which are suggested to be associated with the Akt pathway and have a role in the development of cancer microenvironment and are involved in the migration and infiltration of both inflammatory and tumour cells. This phenomenon is also documented to occur in gastric (Han, Wu *et al.* 2015), kidney (Kadomoto, Izumi *et al.* 2019), breast (Marsigliante, Vetrugno *et al.* 2016), and lung (Wang, Shi *et al.* 2016) cancers. The researchers performed a cell migration assay on prostate cancer cells, and after 48 hours metastasis was observed to be inhibited more effectively with 1 µM AZD5363 than the inhibition of CCL20-CCR6 axis alone. A similar migration assay was conducted by Kadomoto, Izumi *et al.* (2019) on renal cell carcinoma cells, where the addition of AZD5363 also contributed to a decrease in cell migration. The authors suggest that, since the Akt pathway serves as a channel for a variety of cytokine signals, such a response may be due to other upstream signals also being suppressed, as is CCL20.

The cells' response in the present study was in such a manner that up to 48 hours post treatment, wound closure in both the vehicle control and treated cells was somewhat parallel (Figure 3.10, and Table 3.8). However, at the 72-hour time point, there seemed to be a plateau in gap closure in the treated cells which was highly significant to that of the vehicle control. This observation indicates that AZD5363 still has the potential to effectively regulate cell migration of the cell line investigated, however at a slower rate than that observed on other cells.

4.4 Limitations and sources of error

- Investigations in the current study entailed experimental procedures carried out on cells *in vitro*, such that cell processes and subsequent response to treatment was studied in a controlled environment. Thus, cells were grown in a monolayer in culture flasks or petri dishes, as adherent 2D cell cultures which, though simple and inexpensive to maintain, do not mimic the natural conformation of tissues and tumours (Kapałczyńska, Kolenda *et al.* 2018). As a result, there may be differences in the physiology, biochemistry and morphology of cells when compared to *in vivo* testing since, in contrast to 2D conformations, cells in 3D culture methods have variable access to nutrients, oxygen, metabolites and signalling molecules. Additionally, there is the formation of cell-cell and cell-extracellular environment interactions. The results obtained in the present study may, therefore, not necessarily represent what occurs in similar scenarios in animal models, or in the human body, and thus the use of 3D models may be a more effective model in the pursuit of novel therapeutic approaches.
- Given that *in vitro* investigations are performed on live cells, high error bars and subsequently high SEMs (Standard Error of the Mean) arise due to the variability that is associated with living cells. Increasing the number of replicates of the experimental processes undertaken may have reduced the SEMs; a solution which was not feasible due to time constraints.
- Despite that one or two biological repeats were performed for most of the experiments, each procedure involved a small number of technical repeats, resulting in relatively small sample sizes. When analysed, not all data fit a normal distribution; however further analysis was still undertaken using parametric tests.

Having utilised more technical repeats may have achieved normally distributed data; this, however, was not possible due to time and financial limitations.

- The ELISA assay that was performed in the current study determined the total eIF4E concentration, which does not distinguish between the phosphorylated and the unphosphorylated protein. Running an assay that quantifies the phosphorylated eIF4E would have yielded a more accurate reading, and ultimately be more relevant to the present investigation undertaken.

4.5 Conclusions

- Treatment of 10 to 100 µM AZD5363 on the H520 cells failed to result in a decrease in cell viability. Conversely, similar treatment on A549 cells achieved a decrease in the cell viability in a concentration-dependent fashion, such that 55 µM AZD5363 was selected as the IC_{30} for the subsequent investigations carried out on this cell line. Therefore, this drug can be further investigated in the LCeNT study, to ultimately be used in combination with the two antisense oligonucleotides.
- Since a reduction of 29% in mean eIF4E concentration was noted 10 hours after treatment of A459 cells with 55 µM AZD5363, the role of the drug in regulating the expression of eIF4E, studied in combination with other treatment regimens, may be further investigated.
- The significant difference in gap closure observed after 72 hours post-treatment, between cells treated with AZD5363 and those treated with vehicle control solution indicates that AZD5363 still has the potential to effectively regulate cell migration of the cell line investigated, however at a slower rate than that observed on other cells.

- The results obtained in the present study offer a compelling justification for future investigations of AZD5363, both in combination with established treatment options, as well as in combination with ASOs, in addressing the sensitisation of NSCLC cells, to ultimately increase therapy efficacy.
- The results obtained in the current study, where migration of A549 cells was somewhat regulated by treatment with AZD5363, may be further investigated for the role in advanced stages of NSCLC, in combination with standard chemotherapy or other investigational therapy, to potentially improve quality of life and survival.

4.6 Future work

It is proposed to carry out quantification of phosphorylated and non-phosphorylated eIF4E using phosphorylated-specific antibodies, either in an ELISA or Western Blot experiment. Such experiments can be carried out on AZD5363-treated cells, as well as cells treated with AZD5363 in combination with other molecules.

Further investigations of the drug AZD5363 may be carried out as part of the ongoing LCeNT study in combination with the two antisense oligonucleotides targeting TCTP and HSP27, combined with established treatment options for lung cancer, and for the role in advanced stages of NSCLC, in combination with standard chemotherapy or other investigational treatment.

The experimental conditions that yielded the optimum profile can be tested in primary patient-derived lung cancer cells, and the results compared to experimental data derived from normal healthy primary airway cells.

It is important to elucidate the complex pathways of multiple therapy, in order to identify mechanisms of action which can lead to further optimisation of drugs and their targets.

One way of doing this is to carry out RNA-Seq analysis to study transcriptomic changes between treated and untreated cells. The differential gene expression profiles generated will then be processed through gene pathway analysis software, to identify molecular pathways that are modified by the combination of drugs.

Furthermore, in the longer term, drug combinations can be studied in an animal model of human lung cancer, such as rodents xenografted with human lung cancer cells.

References

ABCAM, 2021-last update, ab214564 Human eIF4E SimpleStep ELISA® Kit, [Online]. Available: https://www.abcam.com/ps/products/214/ab214564/documents/Human-eIF4E-ELISA-Kit-protocol-book-v3-ab214564%20(website).pdf [02 May, 2023].

ABDULKADER, R.S., ABERA, S.F., ACHARYA, D., AICHOUR, I., AICHOUR, M.T.E., AKSEER, N., AL-MEKHLAFI, H., ALJUNID, S.M., ALTIRKAWI, K., AYER, R., BANOUB, J.A.M., BEURAN, M., BHATTARAI, S., BLEYER, A., BRAUER, M., BRAZINOVA, A., BREITBORDE, N.J.K., BUCHBINDER, R., CASTILLO RIVAS, J., CHANG, H., COOPER, C., DACHEW, B.A., DE LEO, D., DEIPARINE, S., DOKU, D.T., ELYAZAR, I.R., ENAYATI, A., ESTEP, K., FARO, A., FAY, K.A., FINGER, J.D., FULLMAN, N., GEBREMEDHIN, A.T., GEBREMICHAEL, T.G., GODWIN, W.W., GRAMS, M.E., HAO, Y., HARIKRISHNAN, S., HEDAYATIZADEH-OMRAN, A., HERTELIU, C., HOY, D.G., HSIAO, T., HUSSEN, M.A., IRVINE, C.M.S., JHA, R.P., KARAMI MATIN, B., KEREN, A., KOPEC, J.A., KOUL, P.A., LARSON, S.L., LI, Y., LOGROSCINO, G., LOPEZ, A.D., LOTUFO, P.A., MANGUERRA, H., MARTINS-MELO, F., MCGRATH, J.J., MEKONNEN, F.A., MIRICA, A., MOHAMMADNIA-AFROUZI, M., MORADI, G., MOUSAVI, S.M., NAIK, G., NISHI, N., NIXON, M.R., NOWROOZI, M.R., ORTIZ, A., PARK, E., PATIL, S.T., PEREIRA, D.M., RAHIMI-MOVAGHAR, V., RAHMAN, M.A., RANABHAT, C.L., REINER, R.C., RODRÍGUEZ-RAMÍREZ, S., SAFDARIAN, M., SALIMI, Y., SALIMZADEH, H., SALOMON, J.A., SANTOS, J.V., SARKER, A.R., SATPATHY, M., SAWANT, A.R., SCHÖTTKER, B., SIDDIQI, T.J., SORIANO, J.B., STARODUBOV, V.I., STECKLING, N., SULO, G., TEKLE, M.G., THOMAS, M.L., TO, Q.G., TUDOR CAR, L., UKWAJA, K.N., VILLAFAINA, S., WALLER, S.G., ZAIDI, Z., ZAMAN, S.B., ZHOU, M. and MURRAY, C.J.L., 2018. Global, regional, and national comparative risk assessment of 84 behavioural, environmental and occupational, and metabolic risks or clusters of risks for 195 countries and territories, 1990–2017: A systematic analysis for the Global Burden of Disease Study 2017. *The Lancet (British edition),* 392(10159), pp. 1923-1994.

ADDIE, M., BALLARD, P., BUTTAR, D., CRAFTER, C., CURRIE, G., DAVIES, B.R., DEBRECZENI, J., DRY, H., DUDLEY, P., GREENWOOD, R., JOHNSON, P.D., KETTLE, J.G., LANE, C., LAMONT, G., LEACH, A., LUKE, R.W.A., MORRIS, J., OGILVIE, D., PAGE, K., PASS, M., PEARSON, S. and RUSTON, L., 2013. Discovery of 4-Amino-N-[(1S)-1-(4-chlorophenyl)-3-hydroxypropyl]-1-(7H-pyrrolo[2,3-d]pyrimidin-4-yl)piperidine-4-carboxamide (AZD5363), an orally bioavailable, potent inhibitor of Akt kinases. *Journal of Medicinal Chemistry,* 56(5), pp. 2059-2073.

ADJEI, A.A., BENNOUNA, J., LEIGHL, N.B., FELIP, E., CORTINOVIS, D.L., ALT, J., SCHAEFER, E.S., THOMAS, M., CHOUAID, C., MORABITO, A., DE CASTRO, J., GROSSI, F., PAZ-ARES, L., DE PAS, T.M., MAIER, J., CHAKRAVARTTY, A., CHOL, M., AIMONE, P. and PLANCHARD, D., 2016. Safety and efficacy of buparlisib (BKM120) and chemotherapy in advanced, squamous non-small cell lung cancer (sqNSCLC): Results from the phase Ib/II BASALT-2 and BASALT-3 studies. *Journal of Clinical Oncology,* 34(15_suppl), pp. e20522.

AMERICAN TYPE CULTURE COLLECTION®, 2022-last update, ATCC animal cell culture guide, [Online]. Available: https://www.atcc.org/resources/culture-guides/animal-cell-culture-guide [15 February, 2023].

ANDRIKOPOULOU, A., CHATZINIKOLAOU, S., PANOURGIAS, E., KAPARELOU, M., LIONTOS, M., DIMOPOULOS, M. and ZAGOURI, F., 2022. The emerging role of capivasertib in breast cancer. *Breast (Edinburgh),* 63, pp. 157-167.

AOKI, M. and FUJISHITA, T., 2017. Oncogenic roles of the PI3K/AKT/mTOR axis. *Current Topics in Microbiology and Immunology,* 407, pp. 153-189.

BASELGA, J., CAMPONE, M., PICCART, M., BURRIS, H.A., RUGO, H.S., SAHMOUD, T., NOGUCHI, S., GNANT, M., PRITCHARD, K.I., LEBRUN, F., BECK, J.T., ITO, Y., YARDLEY, D., DELEU, I., PEREZ, A., BACHELOT, T., VITTORI, L., XU, Z., MUKHOPADHYAY, P., LEBWOHL, D. and HORTOBAGYI, G.N., 2012. Everolimus in postmenopausal hormone-receptor–positive advanced breast cancer. *The New England Journal of Medicine,* 366(6), pp. 520-529.

BAUM, P., WINTER, H., EICHHORN, M.E., ROESCH, R.M., TABER, S., CHRISTOPOULOS, P., WIEGERING, A. and LENZI, J., 2022. Trends in age- and sex-specific lung cancer mortality in Europe and Northern America: Analysis of vital registration data from the WHO Mortality Database between 2000 and 2017. *European Journal of Cancer (1990),* 171, pp. 269-279.

BECK, J.T., ISMAIL, A. and TOLOMEO, C., 2014. Targeting the phosphatidylinositol 3-kinase (PI3K)/AKT/mammalian target of rapamycin (mTOR) pathway: An emerging treatment strategy for squamous cell lung carcinoma. *Cancer Treatment Reviews,* 40(8), pp. 980-989.

BENJAMIN, D., COLOMBI, M., MORONI, C. and HALL, M.N., 2011. Rapamycin passes the torch: A new generation of mTOR inhibitors. *Nature Reviews. Drug discovery,* 10(11), pp. 868-880.

BESSE, B., LEIGHL, N., BENNOUNA, J., PAPADIMITRAKOPOULOU, V.A., BLAIS, N., TRAYNOR, A.M., SORIA, J.-., GOGOV, S., MILLER, N., JEHL, V. and JOHNSON, B.E., 2014. Phase II study of everolimus–erlotinib in previously treated patients with advanced non-small-cell lung cancer. *Annals of Oncology,* 25(2), pp. 409-415.

BLEEKER, F.E., FELICIONI, L., BUTTITTA, F., LAMBA, S., CARDONE, L., RODOLFO, M., SCARPA, A., LEENSTRA, S., FRATTINI, M., BARBARESCHI, M., DEL GRAMMASTRO, M., SCIARROTTA, M.G., ZANON, C., MARCHETTI, A. and BARDELLI, A., 2008. AKT1 (E17K) in human solid tumours. *Oncogene,* 27(42), pp. 5648-5650.

BONNEAU, D. and LONGY, M., 2000. Mutations of the human PTEN gene. *Human Mutation,* 16(2), pp. 109-122.

BUDANOV, A.V. and KARIN, M., 2008. p53 target genes Sestrin1 and Sestrin2 connect genotoxic stress and mTOR signaling. *Cell,* 134(3), pp. 451-460.

CANTLEY, L.C., ENGELMAN, J.A. and LUO, J., 2006. The evolution of phosphatidylinositol 3-kinases as regulators of growth and metabolism. *Nature Reviews. Genetics,* 7(8), pp. 606-619.

CARPTEN, J.D., FABER, A.L., HORN, C., DONOHO, G.P., BRIGGS, S.L., ROBBINS, C.M., HOSTETTER, G., BOGUSLAWSKI, S., MOSES, T.Y., SAVAGE, S., UHLIK, M., LIN, A., DU, J., QIAN, Y., ZECKNER, D.J., TUCKER-KELLOGG, G., TOUCHMAN, J., PATEL, K., MOUSSES, S., BITTNER, M., SCHEVITZ, R., LAI, M.T., BLANCHARD, K.L. and THOMAS, J.E., 2007. A transforming mutation in the pleckstrin homology domain of AKT1 in cancer. *Nature,* 448(7152), pp. 439-444.

CARRACEDO, A. and PANDOLFI, P.P., 2008. The PTEN-PI3K pathway: Of feedbacks and cross-talks. *Oncogene,* 27(41), pp. 5527-5541.

CHAFT, J.E., ARCILA, M.E., PAIK, P.K., LAU, C., RIELY, G.J., CATHERINE PIETANZA, M., ZAKOWSKI, M.F., RUSCH, V., SIMA, C.S., LADANYI, M. and KRIS, M.G., 2012. Coexistence of PIK3CA and other oncogene mutations in lung adenocarcinoma-rationale for comprehensive mutation profiling. *Molecular Cancer Therapeutics,* 11(2), pp. 485-491.

CHEN, B., TAN, Z., GAO, J., WU, W., LIU, L., JIN, W., CAO, Y., ZHAO, S., ZHANG, W., QIU, Z., LIU, D., MO, X. and LI, W., 2015. Hyperphosphorylation of ribosomal protein S6 predicts unfavorable clinical survival in non-small cell lung cancer. *Journal of Experimental & Clinical Cancer Research,* 34(1), pp. 126.

CHEN, S., YANG, K., TUGUNTAEV, R.G., MOZHI, A., ZHANG, J., WANG, P.C. and LIANG, X., 2016. Targeting tumor microenvironment with PEG-based amphiphilic nanoparticles to overcome chemoresistance. *Nanomedicine,* 12(2), pp. 269-286.

CHEN, X., CHANG, C., SPOERKE, J.M., YOH, K.E., KAPOOR, V., BAUDO, C., AIMI, J., YU, M., LIANG-CHU, M.M.Y., SUTTMANN, R., HUW, L., GENDREAU, S., CUMMINGS, C. and LACKNER, M.R., 2019. Low-pass whole-genome sequencing of circulating cell-free DNA demonstrates dynamic changes in genomic copy number in a squamous lung cancer clinical cohort. *Clinical Cancer Research,* 25(7), pp. 2254-2263.

CHEN, Y., CUI, X., WANG, D., XIA, G., XING, M., CHENG, L., SHENG, L. and DU, X., 2022. Molecular characterization and prognostication of large cell neuroendocrine carcinoma and large cell carcinoma. *Frontiers in Oncology,* 11, pp. 664397.

CHEN, Y.Z., JIA, J., ZHU, F., MA, X., CAO, Z.W. and LI, Y.X., 2009. Mechanisms of drug combinations: Interaction and network perspectives. *Nature Reviews. Drug Discovery,* 8(2), pp. 111-128.

CHENG, H., SHCHERBA, M., PENDURTI, G., LIANG, Y., PIPERDI, B. and PEREZ-SOLER, R., 2014. Targeting the PI3K/AKT/mTOR pathway: Potential for lung cancer treatment. *Lung Cancer Management,* 3(1), pp. 67-75.

CHENG, H., ZOU, Y., ROSS, J.S., WANG, K., LIU, X., HALMOS, B., ALI, S.M., LIU, H., VERMA, A., MONTAGNA, C., CHACHOUA, A., GOEL, S., SCHWARTZ, E.L., ZHU, C., SHAN, J., YU, Y., GRITSMAN, K., YELENSKY, R., LIPSON, D., OTTO, G., HAWRYLUK, M., STEPHENS, P.J., MILLER, V.A., PIPERDI, B. and PEREZ-SOLER, R., 2015. RICTOR amplification defines a novel subset of patients with lung cancer who may benefit from treatment with mTORC1/2 inhibitors. *Cancer Discovery,* 5(12), pp. 1262-1270.

CHIEN, A.J., COCKERILL, A., FANCOURT, C., SCHMIDT, E., MOASSER, M.M., RUGO, H.S., MELISKO, M.E., KO, A.H., KELLEY, R.K., KORN, W.M., ESSERMAN, L.J., VAN'T VEER, L., YAU, C., WOLF, D.M. and MUNSTER, P.N., 2016. A phase 1b study of the Akt-inhibitor MK-2206 in combination with weekly paclitaxel and trastuzumab in patients with advanced HER2-amplified solid tumor malignancies. *Breast Cancer Research and Treatment,* 155(3), pp. 521-530.

CHOU, T., 2006. Theoretical basis, experimental design, and computerized simulation of synergism and antagonism in drug combination studies. *Pharmacological Reviews,* 58(3), pp. 621-681.

CIUFFREDA, L., DI SANZA, C., INCANI, U.C. and MILELLA, M., 2010. The mTOR Pathway: A new target in cancer therapy. *Current Cancer Drug Targets,* 10(5), pp. 484-495.

CIZKOVA, M., VACHER, S., MESEURE, D., TRASSARD, M., SUSINI, A., MLCUCHOVA, D., CALLENS, C., ROULEAU, E., SPYRATOS, F., LIDEREAU, R. and BIÈCHE, I., 2013. PIK3R1 underexpression is an independent prognostic marker in breast cancer. *BMC Cancer,* 13(1), pp. 545.

COGLIANO, V.J., BAAN, R., STRAIF, K., GROSSE, Y., LAUBY-SECRETAN, B., EL GHISSASSI, F., BOUVARD, V., BENBRAHIM-TALLAA, L., GUHA, N., FREEMAN, C., GALICHET, L. and WILD, C.P., 2011. Preventable exposures associated with human cancers. *JNCI: Journal of the National Cancer Institute,* 103(24), pp. 1827-1839.

CONCIATORI, F., CIUFFREDA, L., BAZZICHETTO, C., FALCONE, I., PILOTTO, S., BRIA, E., COGNETTI, F. and MILELLA, M., 2018. MTOR cross-talk in cancer and potential for combination therapy. *Cancers (Basel),* 10(1), pp. 23.

CORTES, I., SANCHEZ-RUIZ, J., ZULUAGA, S., CALVANESE, V., MARQUES, M., HERNANDEZ, C., RIVERA, T., KREMER, L., GONZALEZ-GARCIA, A. and CARRERA, A.C., 2012. p85β phosphoinositide 3-kinase subunit regulates tumor progression. *Proceedings of the National Academy of Sciences – PNAS USA,* 109(28), pp. 11318-11323.

COSTA, R.L.B., HAN, H.S. and GRADISHAR, W.J., 2018. Targeting the PI3K/AKT/mTOR pathway in triple-negative breast cancer: A review. *Breast Cancer Research and Treatment,* 169(3), pp. 397-406.

COURAUD, S., SOUQUET, P., PARIS, C., DÔ, P., DOUBRE, H., PICHON, E., DIXMIER, A., MONNET, I., ETIENNE-MASTROIANNI, B., VINCENT, M., TRÉDANIEL, J., PERRICHON, M., FOUCHER, P., COUDERT, B., MORO-SIBILOT, D., DANSIN, E., LABONNE, S., MISSY, P., MORIN, F., BLANCHÉ, H. and ZALCMAN, G., 2015. BioCAST/IFCT-1002:

Epidemiological and molecular features of lung cancer in never-smokers. *The European Respiratory Journal,* 45(5), pp. 1403-1414.

DALY, M.E., SINGH, N., ISMAILA, N., ANTONOFF, M.B., ARENBERG, D.A., BRADLEY, J., DAVID, E., DETTERBECK, F., FRÜH, M., GUBENS, M.A., MOORE, A.C., PADDA, S.K., PATEL, J.D., PHILLIPS, T., QIN, A., ROBINSON, C. and SIMONE II, C.B., 2022. Management of stage III non-small-cell lung cancer: ASCO Guideline. *Journal of Clinical Oncology,* 40(12), pp. 1356-1384.

DAVIES, B.R., GREENWOOD, H., DUDLEY, P., CRAFTER, C., YU, D., ZHANG, J., LI, J., GAO, B., JI, Q., MAYNARD, J., RICKETTS, S., CROSS, D., COSULICH, S., CHRESTA, C.C., PAGE, K., YATES, J., LANE, C., WATSON, R., LUKE, R., OGILVIE, D. and PASS, M., 2012. Preclinical pharmacology of AZD5363, an inhibitor of AKT: Pharmacodynamics, antitumor activity, and correlation of monotherapy activity with genetic background. *Molecular Cancer Therapeutics,* 11(4), pp. 873-887.

DE HENAU, O., RAUSCH, M., WINKLER, D., CAMPESATO, L.F., LIU, C., CYMERMAN, D.H., BUDHU, S., GHOSH, A., PINK, M., TCHAICHA, J., DOUGLAS, M., TIBBITTS, T., SHARMA, S., PROCTOR, J., KOSMIDER, N., WHITE, K., STERN, H., SOGLIA, J., ADAMS, J., PALOMBELLA, V.J., MCGOVERN, K., KUTOK, J.L., WOLCHOK, J.D. and MERGHOUB, T., 2016. Overcoming resistance to checkpoint blockade therapy by targeting PI3Kγ in myeloid cells. *Nature (London),* 539(7629), pp. 443-447.

DEMETRI, G.D., CHAWLA, S.P., RAY-COQUARD, I., LE CESNE, A., STADDON, A.P., MILHEM, M.M., PENEL, N., RIEDEL, R.F., BINH BUI-NGUYEN, CRANMER, L.D., REICHARDT, P., BOMPAS, E., ALCINDOR, T., RUSHING, D., SONG, Y., LEE, R., EBBINGHAUS, S., EID, J.E., LOEWY, J.W., HALUSKA, F.G., DODION, P.F. and BLAY, J., 2013. Results of an international randomized phase III trial of the mammalian target of rapamycin inhibitor ridaforolimus versus placebo to control metastatic sarcomas in patients after benefit from prior chemotherapy. *Journal of Clinical Oncology,* 31(19), pp. 2485-2492.

DHILLON, T., MAURI, F.A., BELLEZZA, G., CAGINI, L., BARBARESCHI, M., NORTH, B.V. and SECKL, M.J., 2010. Overexpression of the mammalian target of rapamycin: A novel biomarker for poor survival in resected early stage non-small cell lung cancer. *Journal of Thoracic Oncology,* 5(3), pp. 314-319.

DOBASHI, Y., KOYAMA, S., KANAI, Y. and TETSUKA, K., 2011. Kinase-driven pathways of EGFR in lung carcinomas: Perspectives on targeting therapy. *Frontiers in Bioscience,* 16(5), pp. 1714-1732.

DOBASHI, Y., SUZUKI, S., KIMURA, M., MATSUBARA, H., TSUBOCHI, H., IMOTO, I. and OOI, A., 2011. Paradigm of kinase-driven pathway downstream of epidermal growth factor receptor/Akt in human lung carcinomas. *Human Pathology,* 42(2), pp. 214-226.

DOBASHI, Y., WATANABE, Y., MIWA, C., SUZUKI, S. and KOYAMA, S., 2011. Mammalian target of rapamycin: A central node of complex signaling cascades. *International Journal of Clinical and Experimental Pathology,* 4(5), pp. 476-495.

DZNELADZE, I., HE, R., WOOLLEY, J.F., SON, M.H., SHAROBIM, M.H., GREENBERG, S.A., GABRA, M., LANGLOIS, C., RASHID, A., HAKEM, A., IBRAHIMOVA, N., ARRUDA, A., LÖWENBERG, B., VALK, P., MINDEN, M.D. and SALMENA, L., 2015. INPP4B overexpression is associated with poor clinical outcome and therapy resistance in acute myeloid leukemia. *Leukemia,* 29(7), pp. 1485-1495.

EAPEN, M.S., HANSBRO, P.M., LARSSON-CALLERFELT, A., JOLLY, M.K., MYERS, S., SHARMA, P., JONES, B., RAHMAN, M.A., MARKOS, J., CHIA, C., LARBY, J., HAUG, G., HARDIKAR, A., WEBER, H.C., MABEZA, G., CAVALHERI, V., KHOR, Y.H., MCDONALD, C.F. and SOHAL, S.S., 2018. Chronic obstructive pulmonary disease and lung cancer: Underlying pathophysiology and new therapeutic modalities. *Drugs (New York, N.Y.),* 78(16), pp. 1717-1740.

EFEYAN, A., SABATINI, D.M. and ZONCU, R., 2011. mTOR: From growth signal integration to cancer, diabetes and ageing. *Nature Reviews. Molecular Cell Biology,* 12(1), pp. 21-35.

ENG, C., 2003. PTEN: One gene, many syndromes. *Human mutation,* 22(3), pp. 183-198.

FAIVRE, S., RAYMOND, E. and KROEMER, G., 2006. Current development of mTOR inhibitors as anticancer agents. *Nature Reviews. Drug Discovery,* 5(8), pp. 671-688.

FENG, Z., ZHANG, H., LEVINE, A.J. and JIN, S., 2005. The coordinate regulation of the p53 and mTOR pathways in cells. *Proceedings of the National Academy of Sciences – PNAS USA,* 102(23), pp. 8204-8209.

FUMAROLA, C., BONELLI, M.A., PETRONINI, P.G. and ALFIERI, R.R., 2014. Targeting PI3K/AKT/mTOR pathway in non-small cell lung cancer. *Biochemical Pharmacology,* 90(3), pp. 197-207.

GANDHI, L., BESSE, B., MAZIERES, J., WAQAR, S., CORTOT, A., BARLESI, F., QUOIX, E., OTTERSON, G., ETTINGER, D., HORN, L., MORO-SIBILOT, D., SOCINSKI, M., GOLD, K., GRAY, J., OTON, A., HEIST, R.S., COSTA, D., MCCULLOCH, L., BEBCHUK, J., BRYCE, R. and KRIS, M., 2017. MA04.02 neratinib ± temsirolimus in HER2-mutant lung cancers: An international, randomized phase II study. *Journal of Thoracic Oncology,* 12(1), pp. S358-S359.

GAO, B., SUN, Y., ZHANG, J., REN, Y., FANG, R., HAN, X., SHEN, L., LIU, X., PAO, W., CHEN, H. and JI, H., 2010. Spectrum of LKB1, EGFR, and KRAS mutations in Chinese lung adenocarcinomas. *Journal of Thoracic Oncology,* 5(8), pp. 1130-1135.

GASSER, J.A., INUZUKA, H., LAU, A.W., WEI, W., BEROUKHIM, R. and TOKER, A., 2014. SGK3 mediates INPP4B-dependent PI3K signaling in breast cancer. *Molecular cell,* 56(4), pp. 595-607.

GATELY, K., AL-ALAO, B., DHILLON, T., MAURI, F., CUFFE, S., SECKL, M. and O'BYRNE, K., 2011. Overexpression of the mammalian target of rapamycin (mTOR) and

angioinvasion are poor prognostic factors in early stage NSCLC: A verification study. *Lung Cancer (Amsterdam, Netherlands),* 75(2), pp. 217-222.

GERVASINI, G., CARRILLO, J.A., GARCIA, M., SAN JOSE, C., CABANILLAS, A. and BENITEZ, J., 2006. Adenosine triphosphate-binding cassette B1 (ABCB1) (multidrug resistance 1) G2677T/A gene polymorphism is associated with high risk of lung cancer. *Cancer,* 107(12), pp. 2850-2857.

GEWINNER, C., WANG, Z.C., RICHARDSON, A., TERUYA-FELDSTEIN, J., ETEMADMOGHADAM, D., BOWTELL, D., BARRETINA, J., LIN, W.M., RAMEH, L., SALMENA, L., PANDOLFI, P.P. and CANTLEY, L.C., 2009. Evidence that inositol polyphosphate 4-phosphatase type II is a tumor suppressor that inhibits PI3K signaling. *Cancer Cell,* 16(2), pp. 115-125.

GHOBRIAL, I.M., SIEGEL, D.S., VIJ, R., BERDEJA, J.G., RICHARDSON, P.G., NEUWIRTH, R., PATEL, C.G., ZOHREN, F. and WOLF, J.L., 2016. TAK-228 (formerly MLN0128), an investigational oral dual TORC1/2 inhibitor: A phase I dose escalation study in patients with relapsed or refractory multiple myeloma, non-Hodgkin lymphoma, or Waldenström's macroglobulinemia. *American Journal of Hematology,* 91(4), pp. 400-405.

GKOUNTAKOS, A., PILOTTO, S., MAFFICINI, A., VICENTINI, C., SIMBOLO, M., MILELLA, M., TORTORA, G., SCARPA, A., BRIA, E. and CORBO, V., 2018. Unmasking the impact of Rictor in cancer: Novel insights of mTORC2 complex. *Carcinogenesis (New York),* 39(8), pp. 971-980.

GONZALEZ-ANGULO, A.M., KROP, I., AKCAKANAT, A., CHEN, H., LIU, S., LI, Y., CULOTTA, K.S., TARCO, E., PIHA-PAUL, S., MOULDER-THOMPSON, S., VELEZ-BRAVO, V., SAHIN, A.A., DOYLE, L.A., DO, K., WINER, E.P., MILLS, G.B., KURZROCK, R. and MERIC-BERNSTAM, F., 2015. SU2C phase Ib study of paclitaxel and MK-2206 in advanced solid tumors and metastatic breast cancer. *JNCI: Journal of the National Cancer Institute,* 107(3), pp. 1.

GRABINER, B.C., NARDI, V., BIRSOY, K., POSSEMATO, R., SHEN, K., SINHA, S., JORDAN, A., BECK, A.H. and SABATINI, D.M., 2014. A diverse array of cancer-associated MTOR mutations are hyperactivating and can predict rapamycin sensitivity. *Cancer Discovery,* 4(5), pp. 554-563.

GRAFF, J.R., KONICEK, B.W., LYNCH, R.L., DUMSTORF, C.A., DOWLESS, M.S., MCNULTY, A.M., PARSONS, S.H., BRAIL, L.H., COLLIGAN, B.M., KOOP, J.W., HURST, B.M., DEDDENS, J.A., NEUBAUER, B.L., STANCATO, L.F., CARTER, H.W., DOUGLASS, L.E. and CARTER, J.H., 2009. eIF4E activation is commonly elevated in advanced human prostate cancers and significantly related to reduced patient survival. *Cancer Research,* 69(9), pp. 3866-3873.

GUERTIN, D.A. and SABATINI, D.M., 2007. Defining the role of mTOR in cancer. *Cancer Cell,* 12(1), pp. 9-22.

GUO, S.T., CHI, M.N., YANG, R.H., GUO, X.Y., ZAN, L.K., WANG, C.Y., XI, Y.F., JIN, L., CROFT, A., TSENG, H.-., YAN, X.G., FARRELLY, M., WANG, F.H., LAI, F., WANG, J.F., LI, Y.P., ACKLAND, S., SCOTT, R., AGOULNIK, I.U., HONDERMARCK, H., THORNE, R.F., LIU, T., ZHANG, X.D. and JIANG, C.C., 2016. INPP4B is an oncogenic regulator in human colon cancer. *Oncogene,* 35(23), pp. 3049-3061.

HAMIDOVIC, A., HAHN, K. and KOLESAR, J., 2010. Clinical significance of ABCB1 genotyping in oncology. *Journal of Oncology Pharmacy Practice,* 16(1), pp. 39-44.

HAN, G., WU, D., YANG, Y., LI, Z., ZHANG, J. and LI, C., 2015. CrkL meditates CCL20/CCR6-induced EMT in gastric cancer. *Cytokine (Philadelphia, Pa.),* 76(2), pp. 163-169.

HANNA, N.H., SCHNEIDER, B.J., TEMIN, S., BAKER, S., BRAHMER, J., ELLIS, P.M., GASPAR, L.E., HADDAD, R.Y., HESKETH, P.J., JAIN, D., JAIYESIMI, I., JOHNSON, D.H., LEIGHL, N.B., PHILLIPS, T., RIELY, G.J., ROBINSON, A.G., ROSELL, R., SCHILLER, J.H., SINGH, N., SPIGEL, D.R., STABLER, J.O., TASHBAR, J. and MASTERS, G., 2020. Therapy for stage IV non-small-cell lung cancer without driver alterations: ASCO and OH (CCO) joint Guideline update. *Journal of Clinical Oncology,* 38(14), pp. 1608-1632.

HARE, S.H. and HARVEY, A.J., 2017. mTOR function and therapeutic targeting in breast cancer. *American Journal of Cancer Research,* 7(3), pp. 383-404.

HARRINGTON, L.S., FINDLAY, G.M., GRAY, A., TOLKACHEVA, T., WIGFIELD, S., REBHOLZ, H., BARNETT, J., LESLIE, N.R., CHENG, S., SHEPHERD, P.R., GOUT, I., DOWNES, C.P. and LAMB, R.F., 2004. The TSC1-2 tumor suppressor controls insulin-PI3K signaling via regulation of IRS proteins. *The Journal of Cell Biology,* 166(2), pp. 213-223.

HAY, N. and SONENBERG, N., 2004. Upstream and downstream of mTOR. *Genes & Development,* 18(16), pp. 1926-1945.

HEIKKINEN, T., KORPELA, T., FAGERHOLM, R., KHAN, S., AITTOMÄKI, K., HEIKKILÄ, P., BLOMQVIST, C., CARPÉN, O. and NEVANLINNA, H., 2013. Eukaryotic translation initiation factor 4E (eIF4E) expression is associated with breast cancer tumor phenotype and predicts survival after anthracycline chemotherapy treatment. *Breast Cancer Research and Treatment,* 141(1), pp. 79-88.

HENDRIKS, L.E., KERR, K.M., MENIS, J., MOK, T.S., NESTLE, U., PASSARO, A., PETERS, S., PLANCHARD, D., SMIT, E.F., SOLOMON, B.J., VERONESI, G. and RECK, M., 2023. Non-oncogene-addicted metastatic non-small-cell lung cancer: ESMO Clinical Practice Guideline for diagnosis, treatment and follow-up. *Annals of Oncology,* 34(4), pp. 358-376.

HEUDEL, P., FABBRO, M., ROEMER-BECUWE, C., KAMINSKY, M.C., ARNAUD, A., JOLY, F., ROCHE-FORESTIER, S., MEUNIER, J., FOA, C., YOU, B., PRIOU, F., TAZI, Y., FLOQUET, A., SELLE, F., BERTON-RIGAUD, D., LESOIN, A., KALBACHER, E., LORTHOLARY, A., FAVIER, L., TREILLEUX, I. and RAY-COQUARD, I., 2017. Phase II study of the PI3K inhibitor BKM120 in patients with advanced or recurrent endometrial carcinoma: A

stratified type I-type II study from the GINECO group. *British Journal of Cancer,* 116(3), pp. 303-309.

HOLOHAN, C., VAN SCHAEYBROECK, S., LONGLEY, D.B. and JOHNSTON, P.G., 2013. Cancer drug resistance: An evolving paradigm. *Nature Reviews. Cancer,* 13(10), pp. 714-726.

HORTON, L.E., BUSHELL, M., BARTH-BAUS, D., TILLERAY, V.J., CLEMENS, M.J. and HENSOLD, J.O., 2002. p53 activation results in rapid dephosphorylation of the eIF4E-binding protein 4E-BP1, inhibition of ribosomal protein S6 kinase and inhibition of translation initiation. *Oncogene,* 21(34), pp. 5325-5334.

HU, Q., SUN, W., WANG, C. and GU, Z., 2016. Recent advances of cocktail chemotherapy by combination drug delivery systems. *Advanced Drug Delivery Reviews,* 98, pp. 19-34.

HUA, H., ZHANG, H., CHEN, J., WANG, J., LIU, J. and JIANG, Y., 2021. Targeting Akt in cancer for precision therapy. *Journal of Hematology and Oncology,* 14(1), pp. 1-128.

HUDES, G., CARDUCCI, M., TOMCZAK, P., DUTCHER, J., FIGLIN, R., KAPOOR, A., STAROSLAWSKA, E., SOSMAN, J., MCDERMOTT, D., BODROGI, I., KOVACEVIC, Z., LESOVOY, V., SCHMIDT-WOLF, I., BARBARASH, O., GOKMEN, E., O'TOOLE, T., LUSTGARTEN, S., MOORE, L. and MOTZER, R.J., 2007. Temsirolimus, interferon alfa, or both for advanced renal-cell carcinoma. *The New England Journal of Medicine,* 356(22), pp. 2271-2281.

HYMAN, D.M., SMYTH, L.M., DONOGHUE, M.T.A., CHANG, M.T., REICHEL, J.B., BOUVIER, N., SELCUKLU, S.D., SOUMERAI, T.E., TORRISI, J., ERINJERI, J.P., BERGER, M.F., CHANDARLAPATY, S., SOLIT, D.B., BASELGA, J., TAYLOR, B.S., BARRETT, J.C., DOUGHERTY, B., AMBROSE, H., FOXLEY, A., LINDEMANN, J.P.O., MCEWEN, R., PASS, M., SCHIAVON, G., DEAN, E.J., BANERJI, U., WESTIN, S.N., BEDARD, P.L., BANDO, H., EL-KHOUEIRY, A., MITA, A., PEREZ-FIDALGO, J. and SCHELLENS, J.H.M., 2017. AKT inhibition in solid tumors with AKT1 mutations. *Journal of Clinical Oncology,* 35(20), pp. 2251-2259.

IARC WHO, 2022. *List of classifications by cancer sites with sufficient or limited evidence in humans.* Lyon (France): World Health Organization.

IARC WHO, 2021a-last update, Population Fact Sheets, [Online]. Available: https://gco.iarc.fr/today/data/factsheets/populations/470-malta-fact-sheets.pdf [26 July, 2023].

IARC WHO, 2021b. *Thoracic Tumours: WHO Classification of Tumours.* 5th ed. Lyon (France): International Agency for Research on Cancer.

IARC WHO, 2020. *World Cancer Report: Cancer Research for Cancer Prevention.* Lyon (France): International Agency for Research on Cancer.

IBIDI, 2021-last update, Application note 21: Wound healing assay using the ibidi culture-insert 2 well in a µ-dish, [Online]. Available:

https://ibidi.com/img/cms/support/AN/AN21_Wound_Healing_Assay.pdf [28 April, 2023].

INAMURA, K., 2017. Lung cancer: Understanding its molecular pathology and the 2015 WHO classification. *Frontiers in Oncology,* 7, pp. 193.

INFANTE, J.R., TABERNERO, J., CERVANTES, A., JALAL, S., BURRIS, H.A., MACARULLA, T., PEREZ-FIDALGO, J., NEUWIRTH, R., PATEL, C., GANGOLLI, E., BRAKE, R., STURM, J., WESTIN, E.H. and GORDON, M., 2013. Abstract C252: A phase 1, dose-escalation study of MLN0128, an investigational oral mammalian target of rapamycin complex 1/2 (mTORC1/2) catalytic inhibitor, in patients (pts) with advanced non-hematologic malignancies. *Molecular Cancer Therapeutics,* 12(11), pp. C252.

IWATA, H., BASELGA, J., CAMPONE, M., ARTEAGA, C.L., CORTES, J., JONAT, W., DE LAURENTIIS, M., CIRUELOS, E., JANNI, W., BACHELOT, T., LONNING, P.E., MA, C., O'REGAN, R., DI TOMASO, E., BHARANI-DHARAN, B., DUVAL, V., LAU, H., GERMA, C., URBAN, P. and DI LEO, A., 2013. Ph III randomized studies of the oral pan-PI3K inhibitor buparlisib (BKM120) with fulvestrant in postmenopausal women with HR+/HER2– locally advanced or metastatic breast cancer (BC) after aromatase inhibitor (AI; BELLE-2) or AI and mTOR inhibitor (BELLE-3) treatment. *Journal of Clinical Oncology,* 31(15), pp. TPS650.

JACOBSEN, K., BERTRAN-ALAMILLO, J., MOLINA, M.A., TEIXIDÓ, C., KARACHALIOU, N., PEDERSEN, M.H., CASTELLVÍ, J., GARZÓN, M., CODONY-SERVAT, C., CODONY-SERVAT, J., GIMÉNEZ-CAPITÁN, A., DROZDOWSKYJ, A., VITERI, S., LARSEN, M.R., LASSEN, U., FELIP, E., BIVONA, T.G., DITZEL, H.J. and ROSELL, R., 2017. Convergent Akt activation drives acquired EGFR inhibitor resistance in lung cancer. *Nature Communications,* 8(1), pp. 410-14.

JAIN, S., SHAH, A.N., SANTA-MARIA, C., SIZIOPIKOU, K., RADEMAKER, A., HELENOWSKI, I., CRISTOFANILLI, M. and GRADISHAR, W.J., 2018. Phase I study of alpelisib (BYL-719) and trastuzumab emtansine (T-DM1) in HER2-positive metastatic breast cancer (MBC) after trastuzumab and taxane therapy. *Breast Cancer Research and Treatment,* 171(2), pp. 371-381.

JANKU, F., YAP, T.A. and MERIC-BERNSTAM, F., 2018. Targeting the PI3K pathway in cancer: Are we making headway? *Nature Reviews. Clinical Oncology,* 15(5), pp. 273-291.

JELEŃ, A., ŻEBROWSKA-NAWROCKA, M., SAŁAGACKA-KUBIAK, A., ZAWADZKA, I., ŁOCHOWSKI, M. and BALCERCZAK, E., 2023. The interaction between four polymorphisms and haplotype of ABCB1, the risk of non-small cell lung cancer, and the disease phenotype. *Journal of Oncology,* 2023, pp. 7925378-8.

JIAO, Y., SHI, C., EDIL, B.H., DE WILDE, R.F., KLIMSTRA, D.S., MAITRA, A., SCHULICK, R.D., TANG, L.H., WOLFGANG, C.L., CHOTI, M.A., VELCULESCU, V.E., DIAZ, L.A. Jr, VOGELSTEIN, B., KINZLER, K.W., HRUBAN, R.H. and PAPADOPOULOS, N., 2011. DAXX/ATRX, MEN1, and mTOR pathway genes are frequently altered in pancreatic

neuroendocrine tumors. *Science (American Association for the Advancement of Science),* 331(6021), pp. 1199-1203.

JOLY, M.M., HICKS, D.J., JONES, B., SANCHEZ, V., ESTRADA, M.V., YOUNG, C., WILLIAMS, M., REXER, B.N., SARBASSOV, D.D., MULLER, W.J., BRANTLEY-SIEDERS, D. and COOK, R.S., 2016. Rictor/mTORC2 drives progression and therapeutic resistance of HER2-amplified breast cancers. *Cancer Research (Chicago, Ill.),* 76(16), pp. 4752-4764.

JONES, R.H., CASBARD, A., CARUCCI, M., COX, C., BUTLER, R., ALCHAMI, F., MADDEN, T., BALE, C., BEZECNY, P., JOFFE, J., MOON, S., TWELVES, C., VENKITARAMAN, R., WATERS, S., FOXLEY, A. and HOWELL, S.J., 2020. Fulvestrant plus capivasertib versus placebo after relapse or progression on an aromatase inhibitor in metastatic, oestrogen receptor-positive breast cancer (FAKTION): A multicentre, randomised, controlled, phase 2 trial. *The Lancet Oncology,* 21(3), pp. 345-357.

JURIC, D., RODON, J., TABERNERO, J., JANKU, F., BURRIS, H.A., SCHELLENS, J.H.M., MIDDLETON, M.R., BERLIN, J., SCHULER, M., GIL-MARTIN, M., RUGO, H.S., SEGGEWISS-BERNHARDT, R., HUANG, A., BOOTLE, D., DEMANSE, D., BLUMENSTEIN, L., COUGHLIN, C., QUADT, C. and BASELGA, J., 2018. Phosphatidylinositol 3-kinase α-selective inhibition with alpelisib (BYL719) in PIK3CA-altered solid tumors: Results from the first-in-human study. *Journal of Clinical Oncology,* 36(13), pp. 1291-1299.

KADOMOTO, S., IZUMI, K., HIRATSUKA, K., NAKANO, T., NAITO, R., MAKINO, T., IWAMOTO, H., YAEGASHI, H., SHIGEHARA, K., KADONO, Y., NAKATA, H., SAITO, Y., NAKAGAWA-GOTO, K. and MIZOKAMI, A., 2019. Tumor-associated macrophages induce migration of renal cell carcinoma cells via activation of the CCL20-CCR6 axis. *Cancers (Basel),* 12(1), pp. 89.

KALINSKY, K., HONG, F., MCCOURT, C.K., SACHDEV, J.C., MITCHELL, E.P., ZWIEBEL, J.A., DOYLE, L.A., MCSHANE, L.M., LI, S., GRAY, R.J., RUBINSTEIN, L.V., PATTON, D., WILLIAMS, P.M., HAMILTON, S.R., CONLEY, B.A., O'DWYER, P.J., HARRIS, L.N., ARTEAGA, C.L., CHEN, A.P. and FLAHERTY, K.T., 2021. Effect of capivasertib in patients with an AKT1 E17K-mutated tumor: NCI-MATCH subprotocol EAY131-Y nonrandomized trial. *JAMA Oncology,* 7(2), pp. 271-278.

KANO, H., IZUMI, K., HIRATSUKA, K., TORIUMI, R., NAKAGAWA, R., AOYAMA, S., KAMIJIMA, T., SHIMADA, T., NAITO, R., KADOMOTO, S., IWAMOTO, H., YAEGASHI, H., KAWAGUCHI, S., NOHARA, T., SHIGEHARA, K., KADONO, Y., SAITO, Y., NAKAGAWA-GOTO, K., YOSHIOKA, K., NAKATA, H., LIN, W. and MIZOKAMI, A., 2023. Suppression of androgen receptor signaling induces prostate cancer migration via activation of the CCL20–CCR6 axis. *Cancer Science,* 114(4), pp. 1479-1490.

KAPAŁCZYŃSKA, M., KOLENDA, T., PRZYBYŁA, W., ZAJĄCZKOWSKA, M., TERESIAK, A., FILAS, V., IBBS, M., BLIŹNIAK, R., ŁUCZEWSKI, Ł and LAMPERSKA, K., 2018. 2D and 3D cell cultures – a comparison of different types of cancer cell cultures. *Archives of Medical Science,* 14(4), pp. 910-919.

KOLINSKY, M.P., RESCIGNO, P., BIANCHINI, D., ZAFEIRIOU, Z., MEHRA, N., MATEO, J., MICHALAREA, V., RIISNAES, R., CRESPO, M., FIGUEIREDO, I., MIRANDA, S., NAVA RODRIGUES, D., FLOHR, P., TUNARIU, N., BANERJI, U., RUDDLE, R., SHARP, A., WELTI, J., LAMBROS, M., CARREIRA, S., RAYNAUD, F.I., SWALES, K.E., PLYMATE, S., LUO, J., TOVEY, H., PORTA, N., SLADE, R., LEONARD, L., HALL, E. and DE BONO, J.S., 2020. A phase I dose-escalation study of enzalutamide in combination with the AKT inhibitor AZD5363 (capivasertib) in patients with metastatic castration-resistant prostate cancer. *Annals of Oncology,* 31(5), pp. 619-625.

KREBS, M., SPICER, J., STEELE, N., TALBOT, D., BRADA, M., WILSON, R., JONES, R., BASU, B., DAWES, J., PARMAR, M., PURCHASE, B., TURNER, A., HALL, E., TOVEY, H., BANERJI, U. and YAP, T., 2017. P3.02c-003 TAX-TORC: The novel combination of weekly paclitaxel and the dual mTORC1/2 inhibitor AZD2014 for the treatment of squamous NSCLC. *Journal of Thoracic Oncology,* 12(1), pp. S1272-S1273.

KRENCZ, I., SEBESTYÉN, A., FÁBIÁN, K., MÁRK, Á, MOLDVAY, J., KHOOR, A., KOPPER, L. and PÁPAY, J., 2016. Expression of mTORC1/2-related proteins in primary and brain metastatic lung adenocarcinoma. *Human Pathology,* 62, pp. 66-73.

KRENCZ, I., SEBESTYEN, A. and KHOOR, A., 2020. mTOR in lung neoplasms. *Pathology Oncology Research,* 26(1), pp. 35-48.

LAPLANTE, M. and SABATINI, D.M., 2012. mTOR signaling in growth control and disease. *Cell,* 149(2), pp. 274-293.

LAWRENCE, M.S., SIVACHENKO, A., MCKENNA, A., GABRIEL, S., IMIELINSKI, M., MEYERSON, M., HYE-CHUN, J., STOLL, D., BALASUNDARAM, M., COOPE, R.J.N., DHALLA, N., HE, A., MAYO, M., MOORE, R.A., NIP, K.M., JONES, S.J.M., TABAK, B., CARTER, S.L., ONOFRIO, R.C., CRENSHAW, A., ARDLIE, K., BEROUKHIM, R., LEE, S., YANG, L., LASH, A.E., VIALE, A., LADANYI, M., HOADLEY, K.A., MENG, S., WARING, S., BUDA, E., SIMONS, J.V., STUART, J., JEFFERYS, S.R., O'CONNOR, B.D., PEROU, C.M., MAGLINTE, D.T., LAIRD, P.W., GEHLENBORG, N., GROSS, B., JACOBSEN, A., GAO, J., TAYLOR, B.S., ANTIPIN, Y., REVA, B., MO, Q., SESHAN, V., PAIK, P.K., CASON, R.C., ZHU, J., SZETO, C., SOKOLOV, A., COLLISSON, E., ELLROTT, K., MA, S., CRAFT, B., MARRON, J.S., LIU, Y., ZHANG, Y., REKHTMAN, N., YI, J., CHENEY, R., FUNKHOUSER, W., MYERS, J., BYERS, L.A., DING, L., JOHNSON, B., KOSARI, F., MAHER, C.A., SIEGFRIED, J., SOUGNEZ, C., THOMAS, R.K., VASKE, C., WILKS, C., KAHN, A.B., PIHL, T.D., BACKUS, M., GIRSHIK, S., BARLETTA, S.P., WEAVER, J., BROCK, M.V., ROGERS, K., LEE, B., DHIR, R., TODARO, N., HUANG, M., MORRISON, C., GAUDIOSO, C., ZANKE, B., SEKHON, H., LE, X.V., TIEN, N.V., BANG, N.V., SUSSMAN, H., YANG, L., DAVIDSEN, T., ELEY, G., GUYER, M.S., PETERSON, J. and SHEN, R., 2012. Comprehensive genomic characterization of squamous cell lung cancers. *Nature (London),* 489(7417), pp. 519-525.

LEMJABBAR-ALAOUI, H., HASSAN, O.U.I., YANG, Y. and BUCHANAN, P., 2015. Lung cancer: Biology and treatment options. *Biochimica et Biophysica Acta. Reviews on Cancer,* 1856(2), pp. 189-210.

LEONG, S., MOSS, R.A., BOWLES, D.W., WARE, J.A., ZHOU, J., SPOERKE, J.M., LACKNER, M.R., SHANKAR, G., SCHUTZMAN, J.L., VAN DER NOLL, R., VOEST, E.E. and SCHELLENS, J.H.M., 2017. A phase I dose-escalation study of the safety and pharmacokinetics of pictilisib in combination with erlotinib in patients with advanced solid tumors. *The Oncologist (Dayton, Ohio),* 22(12), pp. 1491-1499.

LEVY, B., SPIRA, A., BECKER, D., EVANS, T., SCHNADIG, I., CAMIDGE, D.R., BAUMAN, J.E., HAUSMAN, D., WALKER, L., NEMUNAITIS, J., RUDIN, C.M., HALMOS, B. and BOWLES, D.W., 2014. A randomized, phase 2 trial of docetaxel with or without PX-866, an irreversible oral phosphatidylinositol 3-kinase inhibitor, in patients with relapsed or metastatic non–small-cell lung cancer. *Journal of Thoracic Oncology,* 9(7), pp. 1031-1035.

LI, J., DAVIES, B.R., HAN, S., ZHOU, M., BAI, Y., ZHANG, J., XU, Y., TANG, L., WANG, H., LIU, Y.J., YIN, X., JI, Q. and YU, D., 2013. The AKT inhibitor AZD5363 is selectively active in PI3KCA mutant gastric cancer, and sensitizes a patient-derived gastric cancer xenograft model with PTEN loss to Taxotere. *Journal of Translational Medicine,* 11(1), pp. 241.

LI, Y., FAN, S., KOO, J., YUE, P., CHEN, Z., OWONIKOKO, T.K., RAMALINGAM, S.S., KHURI, F.R. and SUN, S., 2012. Elevated expression of eukaryotic translation initiation factor 4E is associated with proliferation, invasion and acquired resistance to erlotinib in lung cancer. *Cancer Biology & Therapy,* 13(5), pp. 272-280.

LIANG, S., GUO, R., ZHANG, Z., LIU, D., XU, H., XU, Z., WANG, X. and YANG, L., 2013. Upregulation of the eIF4E signaling pathway contributes to the progression of gastric cancer, and targeting eIF4E by perifosine inhibits cell growth. *Oncology Reports,* 29(6), pp. 2422-2430.

LIN, C., YU, C., HO, C., CHEN, K., SHIH, J., LIN, Z., LIN, Y., LIAO, W., TSAI, S., YAN, L. and YANG, J.C., 2015. P1.12A Phase I dose defining study for MK-2206 combined with gefitinib in NSCLC population enriched with EGFR mutation. *Annals of Oncology,* 26(suppl_2), pp. ii16.

LORTET-TIEULENT, J., RENTERIA, E., SHARP, L., WEIDERPASS, E., COMBER, H., BAAS, P., BRAY, F., COEBERGH, J.W. and SOERJOMATARAM, I., 2013. Convergence of decreasing male and increasing female incidence rates in major tobacco-related cancers in Europe in 1988–2010. *European Journal of Cancer (1990),* 51(9), pp. 1144-1163.

LU, J., ZANG, H., ZHENG, H., ZHAN, Y., YANG, Y., ZHANG, Y., LIU, S., FENG, J., WEN, Q., LONG, M. and FAN, S., 2020. Overexpression of p-Akt, p-mTOR and p-eIF4E proteins associates with metastasis and unfavorable prognosis in non-small cell lung cancer. *PLoS One,* 15(2), pp. e0227768.

LU, S., LIU, H., LU, L., WAN, H., LIN, Z., QIAN, K., YAO, X., CHEN, Q., LIU, W., YAN, J. and LIU, Z., 2016. WISP1 overexpression promotes proliferation and migration of human

vascular smooth muscle cells via AKT signaling pathway. *European Journal of Pharmacology,* 788, pp. 90-97.

MA, C.X., SANCHEZ, C., GAO, F., CROWDER, R., NAUGHTON, M., PLUARD, T., CREEKMORE, A., GUO, Z., HOOG, J., LOCKHART, A.C., DOYLE, A., ERLICHMAN, C. and ELLIS, M.J., 2016. A phase I study of the AKT inhibitor MK-2206 in combination with hormonal therapy in postmenopausal women with estrogen receptor-positive metastatic breast cancer. *Clinical Cancer Research,* 22(11), pp. 2650-2658.

MAIRA, S., PECCHI, S., HUANG, A., BURGER, M., KNAPP, M., STERKER, D., SCHNELL, C., GUTHY, D., NAGEL, T., WIESMANN, M., BRACHMANN, S., FRITSCH, C., DORSCH, M., CHÈNE, P., SHOEMAKER, K., DE POVER, A., MENEZES, D., MARTINY-BARON, G., FABBRO, D., WILSON, C.J., SCHLEGEL, R., HOFMANN, F., GARCÍA-ECHEVERRÍA, C., SELLERS, W.R. and VOLIVA, C.F., 2012. Identification and characterization of NVP-BKM120, an orally available pan-class I PI3-kinase inhibitor. *Molecular Cancer Therapeutics,* 11(2), pp. 317-328.

MALANGA, D., BELMONTE, S., COLELLI, F., SCARFÒ, M., DE MARCO, C., OLIVEIRA, D.M., MIRANTE, T., CAMASTRA, C., GAGLIARDI, M., RIZZUTO, A., MIGNOGNA, C., PACIELLO, O., PAPPARELLA, S., FAGMAN, H. and VIGLIETTO, G., 2016. $AKT1^{E17K}$ is oncogenic in mouse lung and cooperates with chemical carcinogens in inducing lung cancer. *PLoS One,* 11(2), pp. e0147334.

MANCINI, M.L., LIEN, E.C. and TOKER, A., 2016. Oncogenic AKT1(E17K) mutation induces mammary hyperplasia but prevents HER2-driven tumorigenesis. *Oncotarget,* 7(14), pp. 17301-17313.

MARSIGLIANTE, S., VETRUGNO, C. and MUSCELLA, A., 2016. Paracrine CCL20 loop induces epithelial-mesenchymal transition in breast epithelial cells. *Molecular Carcinogenesis,* 55(7), pp. 1175-1186.

MASRI, J., BERNATH, A., MARTIN, J., JO, O.D., VARTANIAN, R., FUNK, A. and GERA, J., 2007. mTORC2 activity is elevated in gliomas and promotes growth and cell motility via overexpression of rictor. *Cancer Research (Chicago, Ill.),* 67(24), pp. 11712-11720.

MATSUMOTO, S., IWAKAWA, R., TAKAHASHI, K., KOHNO, T., NAKANISHI, Y., MATSUNO, Y., SUZUKI, K., NAKAMOTO, M., SHIMIZU, E., MINNA, J.D. and YOKOTA, J., 2007. Prevalence and specificity of LKB1 genetic alterations in lung cancers. *Oncogene,* 26(40), pp. 5911-5918.

MATULONIS, U., VERGOTE, I., BACKES, F., MARTIN, L.P., MCMEEKIN, S., BIRRER, M., CAMPANA, F., XU, Y., EGILE, C. and GHAMANDE, S., 2015. Phase II study of the PI3K inhibitor pilaralisib (SAR245408; XL147) in patients with advanced or recurrent endometrial carcinoma. *Gynecologic Oncology,* 136(2), pp. 246-253.

MAYER, I.A., ABRAMSON, V.G., FORMISANO, L., BALKO, J.M., ESTRADA, M.V., SANDERS, M.E., JURIC, D., SOLIT, D., BERGER, M.F., WON, H.H., LI, Y., CANTLEY, L.C., WINER, E. and ARTEAGA, C.L., 2017. A phase Ib study of alpelisib (BYL719), a PI3Kα-specific

inhibitor, with letrozole in ER+/HER2- metastatic breast cancer. *Clinical Cancer Research,* 23(1), pp. 26-34.

MAYER, I.A. and ARTEAGA, C.L., 2016. The PI3K AKT pathway as a target for cancer treatment. *Annual Review of Medicine,* 67(1), pp. 11-28.

MEENAKSHI, A., 2023-last update, Cell culture media: A review [Online]. Available: https://www.labome.com/method/Cell-Culture-Media-A-Review.html [24 August, 2023].

MENDOZA, M.C., ER, E.E. and BLENIS, J., 2011. The Ras-ERK and PI3K-mTOR pathways: Cross-talk and compensation. *Trends in Biochemical Sciences (Amsterdam. Regular ed.),* 36(6), pp. 320-328.

MESTER, J.L., MOORE, R.A. and ENG, C., 2013. PTEN germline mutations in patients initially tested for other hereditary cancer syndromes: Would use of risk assessment tools reduce genetic testing? *The Oncologist (Dayton, Ohio),* 18(10), pp. 1083-1090.

MIDDLETON, G., FLETCHER, P., POPAT, S., SAVAGE, J., SUMMERS, Y., GREYSTOKE, A., GILLIGAN, D., CAVE, J., O'ROURKE, N., BREWSTER, A., TOY, E., SPICER, J., JAIN, P., DANGOOR, A., MACKEAN, M., FORSTER, M., FARLEY, A., WHERTON, D., MEHMI, M., SHARPE, R., MILLS, T.C., CERONE, M.A., YAP, T.A., WATKINS, T.B.K., LIM, E., SWANTON, C. and BILLINGHAM, L., 2020. The National Lung Matrix Trial of personalized therapy in lung cancer. *Nature (London),* 583(7818), pp. 807-812.

MILELLA, M., FALCONE, I., CONCIATORI, F., INCANI, U.C., DEL CURATOLO, A., INZERILLI, N., NUZZO, C.M.A., VACCARO, V., VARI, S., COGNETTI, F. and CIUFFREDA, L., 2015. PTEN: Multiple functions in human malignant tumors. *Frontiers in Oncology,* 5, pp. 24.

MILLS, G.B., HENNESSY, B.T., SMITH, D.L., RAM, P.T. and LU, Y., 2005. Exploiting the PI3K/AKT pathway for cancer drug discovery. *Nature Reviews. Drug Discovery,* 4(12), pp. 988-1004.

MOSSMANN, D., PARK, S. and HALL, M.N., 2018. mTOR signalling and cellular metabolism are mutual determinants in cancer. *Nature Reviews. Cancer,* 18(12), pp. 744-757.

MOTZER, R.J., ESCUDIER, B., OUDARD, S., HUTSON, T.E., PORTA, C., BRACARDA, S., GRÜNWALD, V., THOMPSON, J.A., FIGLIN, R.A., HOLLAENDER, N., URBANOWITZ, G., BERG, W.J., KAY, A., LEBWOHL, D. and RAVAUD, A., 2008. Efficacy of everolimus in advanced renal cell carcinoma: A double-blind, randomised, placebo-controlled phase III trial. *The Lancet (British edition),* 372(9637), pp. 449-456.

NAING, A., AGHAJANIAN, C., RAYMOND, E., OLMOS, D., SCHWARTZ, G., OELMANN, E., GRINSTED, L., BURKE, W., TAYLOR, R., KAYE, S., KURZROCK, R. and BANERJI, U., 2012. Safety, tolerability, pharmacokinetics and pharmacodynamics of AZD8055 in advanced solid tumours and lymphoma. *British Journal of Cancer,* 107(7), pp. 1093-1099.

NATIONAL CENTER FOR BIOTECHNOLOGY INFORMATION, 2023-last update, PubChem compound summary for CID 25227436, capivasertib [Online]. Available: https://pubchem.ncbi.nlm.nih.gov/compound/Capivasertib#section=Structures [27 July, 2023].

O'BYRNE, K.J., GATZEMEIER, U., BONDARENKO, I., BARRIOS, C., ESCHBACH, C., MARTENS, U.M., HOTKO, Y., KORTSIK, C., PAZ-ARES, L., PEREIRA, J.R., VON PAWEL, J., RAMLAU, R., ROH, J., YU, C., STROH, C., CELIK, I., SCHUELER, A. and PIRKER, R., 2011. Molecular biomarkers in non-small-cell lung cancer: A retrospective analysis of data from the phase 3 FLEX study. *The Lancet Oncology,* 12(8), pp. 795-805.

O'REILLY, K.E., ROJO, F., SHE, Q., SOLIT, D., MILLS, G.B., SMITH, D., LANE, H., HOFMANN, F., HICKLIN, D.J., LUDWIG, D.L., BASELGA, J. and ROSEN, N., 2006. mTOR inhibition induces upstream receptor tyrosine kinase signaling and activates Akt. *Cancer Research (Chicago, Ill.),* 66(3), pp. 1500-1508.

PALM, W., PARK, Y., WRIGHT, K., PAVLOVA, N.N., TUVESON, D.A. and THOMPSON, C.B., 2015. The utilization of extracellular proteins as nutrients Is suppressed by mTORC1. *Cell,* 162(2), pp. 259-270.

PAPADIMITRAKOPOULOU, V., 2012. Development of PI3K/AKT/mTOR pathway inhibitors and their application in personalized therapy for non–small-cell lung cancer. *Journal of Thoracic Oncology,* 7(8), pp. 1315-1326.

PETERS, S., BEXELIUS, C., MUNK, V. and LEIGHL, N., 2016. The impact of brain metastasis on quality of life, resource utilization and survival in patients with non-small-cell lung cancer. *Cancer Treatment Reviews,* 45, pp. 139-162.

PETERSON, T.R., SENGUPTA, S.S., HARRIS, T.E., CARMACK, A.E., KANG, S.A., BALDERAS, E., GUERTIN, D.A., MADDEN, K.L., CARPENTER, A.E., FINCK, B.N. and SABATINI, D.M., 2011. mTOR Complex 1 regulates Lipin 1 localization to control the SREBP pathway. *Cell,* 146(3), pp. 408-420.

PLANCHARD, D., POPAT, S., KERR, K., NOVELLO, S., SMIT, E.F., FAIVRE-FINN, C., MOK, T.S., RECK, M., VAN SCHIL, P.E., HELLMANN, M.D. and PETERS, S., 2018. Metastatic non-small cell lung cancer: ESMO Clinical Practice Guidelines for diagnosis, treatment and follow-up. *Annals of Oncology,* 29 Suppl 4, pp. iv192-iv237.

PLATT, F.M., HURST, C.D., TAYLOR, C.F., GREGORY, W.M., HARNDEN, P. and KNOWLES, M.A., 2009. Spectrum of phosphatidylinositol 3-kinase pathway gene alterations in bladder cancer. *Clinical Cancer Research,* 15(19), pp. 6008-6017.

PORTA, C., PAGLINO, C. and MOSCA, A., 2014. Targeting PI3K/Akt/mTOR signaling in cancer. *Frontiers in Oncology,* 4, pp. 64.

POSTMUS, P.E., KERR, K.M., OUDKERK, M., SENAN, S., WALLER, D.A., VANSTEENKISTE, J., ESCRIU, C. and PETERS, S., 2017. Early and locally advanced non-small-cell lung cancer

(NSCLC): ESMO Clinical Practice Guidelines for diagnosis, treatment and follow-up. *Annals of oncology,* 28(4), pp. iv1-iv21.

PRICE, K.A., AZZOLI, C.G., KRUG, L.M., PIETANZA, M.C., RIZVI, N.A., PAO, W., KRIS, M.G., RIELY, G.J., HEELAN, R.T., ARCILA, M.E. and MILLER, V.A., 2010. Phase II trial of gefitinib and everolimus in advanced non-small cell lung cancer. *Journal of Thoracic Oncology,* 5(10), pp. 1623-1629.

PUGLISI, M., THAVASU, P., STEWART, A., DE BONO, J.S., O'BRIEN, M.E.R., POPAT, S., BHOSLE, J. and BANERJI, U., 2014. AKT inhibition synergistically enhances growth-inhibitory effects of gefitinib and increases apoptosis in non-small cell lung cancer cell lines. *Lung Cancer (Amsterdam, Netherlands),* 85(2), pp. 141-146.

QUOIX, E., ZALCMAN, G., OSTER, J., WESTEEL, V., PICHON, E., LAVOLÉ, A., DAUBA, J., DEBIEUVRE, D., SOUQUET, P., BIGAY-GAME, L., DANSIN, E., POUDENX, M., MOLINIER, O., VAYLET, F., MORO-SIBILOT, D., HERMAN, D., BENNOUNA, J., TREDANIEL, J., DUCOLONÉ, A., LEBITASY, M., BAUDRIN, L., LAPORTE, S. and MILLERON, B., 2011. Carboplatin and weekly paclitaxel doublet chemotherapy compared with monotherapy in elderly patients with advanced non-small-cell lung cancer: IFCT-0501 randomised, phase 3 trial. *The Lancet (British edition),* 378(9796), pp. 1079-1088.

RIBAS, R., PANCHOLI, S., GUEST, S.K., MARANGONI, E., GAO, Q., THULEAU, A., SIMIGDALA, N., POLANSKA, U.M., CAMPBELL, H., RANI, A., LICCARDI, G., JOHNSTON, S., DAVIES, B.R., DOWSETT, M. and MARTIN, L., 2015. AKT antagonist AZD5363 influences estrogen receptor function in endocrine-resistant breast cancer and synergizes with fulvestrant (ICI182780) *in vivo*. *Molecular Cancer Therapeutics,* 14(9), pp. 2035-2048.

RICHARDSON, P.G., ENG, C., KOLESAR, J., HIDESHIMA, T. and ANDERSON, K.C., 2012. Perifosine, an oral, anti-cancer agent and inhibitor of the Akt pathway: Mechanistic actions, pharmacodynamics, pharmacokinetics, and clinical activity. *Expert Opinion on Drug Metabolism & Toxicology,* 8(5), pp. 623-633.

RICOULT, S.J.H., YECIES, J.L., BEN-SAHRA, I. and MANNING, B.D., 2016. Oncogenic PI3K and K-Ras stimulate *de novo* lipid synthesis through mTORC1 and SREBP. *Oncogene,* 35(10), pp. 1250-1260.

RIELY, G.J., BRAHMER, J.R., PLANCHARD, D., CRINÒ, L., DOEBELE, R.C., MAS LOPEZ, L.A., GETTINGER, S.N., SCHUMANN, C., LI, X., ATKINS, B.M., EBBINGHAUS, S. and ROSELL, R., 2012. A randomized discontinuation phase II trial of ridaforolimus in non-small cell lung cancer (NSCLC) patients with KRAS mutations. *Journal of Clinical Oncology,* 30(15_suppl), pp. 7531.

ROBICHAUD, N., HSU, B.E., ISTOMINE, R., ALVAREZ, F., BLAGIH, J., MA, E.H., MORALES, S.V., DAI, D.L., LI, G., SOULEIMANOVA, M., GUO, Q., DEL RINCON, S.V., MILLER, W.H., CAJAL, S.R.Y., PARK, M., JONES, R.G., PICCIRILLO, C.A., SIEGEL, P.M. and SONENBERG, N., 2018. Translational control in the tumor microenvironment promotes lung metastasis: Phosphorylation of eIF4E in neutrophils. *Proceedings of the National Academy of Sciences – PNAS USA,* 115(10), pp. E2202-E2209.

ROSENBERG, L., YOON, C.H., SHARMA, G., BERTAGNOLLI, M.M. and CHO, N.L., 2018. Sorafenib inhibits proliferation and invasion in desmoid-derived cells by targeting Ras/MEK/ERK and PI3K/Akt/mTOR pathways. *Carcinogenesis (New York),* 39(5), pp. 681-688.

RYAN, C. and BURKE, L., 2017. Pathology of lung tumours. *Surgery (Oxford),* 35(5), pp. 234-242.

SAMUELS, Y., WANG, Z., BARDELLI, A., SILLIMAN, N., PTAK, J., SZABO, S., YAN, H., GAZDAR, A., POWELL, S.M., RIGGINS, G.J., WILLSON, J.K.V., MARKOWITZ, S., KINZLER, K.W., VOGELSTEIN, B. and VELCULESCU, V.E., 2004. High frequency of mutations of the PIK3CA gene in human cancers. *Science (American Association for the Advancement of Science),* 304(5670), pp. 554.

SANCAK, Y., BAR-PELED, L., ZONCU, R., MARKHARD, A.L., NADA, S. and SABATINI, D.M., 2010. Ragulator-Rag complex targets mTORC1 to the lysosomal surface and is necessary for its activation by amino acids. *Cell,* 141(2), pp. 290-303.

SANDERS, M.J., GRONDIN, P.O., HEGARTY, B.D., SNOWDEN, M.A. and CARLING, D., 2007. Investigating the mechanism for AMP activation of the AMP-activated protein kinase cascade. *Biochemical Journal,* 403(1), pp. 139-148.

ŞANLI, F., BARLAK, N., KILINÇ, A., ÇAPIK, Ö, AYTATLI, A. and KARATAS, O.F., 2020. The AKT antagonist AZD5363 suppresses features associated with cancer progression in human larynx cancer cells. *The European Research Journal,* 6(5), pp. 380-387.

SARBASSOV, D.D., ALI, S.M., SENGUPTA, S., SHEEN, J., HSU, P.P., BAGLEY, A.F., MARKHARD, A.L. and SABATINI, D.M., 2006. Prolonged rapamycin treatment inhibits mTORC2 assembly and Akt/PKB. *Molecular Cell,* 22(2), pp. 159-168.

SARKER, D., ANG, J.E., BAIRD, R., KRISTELEIT, R., SHAH, K., MORENO, V., CLARKE, P.A., RAYNAUD, F.I., LEVY, G., WARE, J.A., MAZINA, K., LIN, R., WU, J., FREDRICKSON, J., SPOERKE, J.M., LACKNER, M.R., YAN, Y., FRIEDMAN, L.S., KAYE, S.B., DERYNCK, M.K., WORKMAN, P. and DE BONO, J.S., 2015. First-in-human phase I study of pictilisib (GDC-0941), a potent pan-class I phosphatidylinositol-3-kinase (PI3K) Inhibitor, in patients with advanced solid tumors. *Clinical Cancer Research,* 21(1), pp. 77-86.

SAURA, C., BENDELL, J., JERUSALEM, G., SU, S., RU, Q., DE BUCK, S., MILLS, D., RUQUET, S., BOSCH, A., URRUTICOECHEA, A., BECK, J.T., DI TOMASO, E., STERNBERG, D.W., MASSACESI, C., HIRAWAT, S., DIRIX, L. and BASELGA, J., 2014. Phase Ib study of buparlisib plus trastuzumab in patients with HER2-positive advanced or metastatic breast cancer that has progressed on trastuzumab-based therapy. *Clinical Cancer Research,* 20(7), pp. 1935-1945.

SAVILL, K.M.Z., LEE, B.B., OEH, J., LIN, J., LIN, E., CHUNG, W., YOUNG, A., CHEN, W., MIŚ, M., MESH, K., EASTHAM, J., GNAD, F., JIANG, Z., STAWISKI, E.W., HALEY, B., DAEMEN, A., WANG, X., KOEPPEN, H., MODRUSAN, Z., MARTIN, S.E., SAMPATH, D. and LIN, K.,

2022. Distinct resistance mechanisms arise to allosteric vs. ATP-competitive AKT inhibitors. *Nature Communications,* 13(1), pp. 2057.

SAXTON, R.A. and SABATINI, D.M., 2017. mTOR signaling in growth, metabolism, and disease. *Cell,* 168(6), pp. 960-976.

SCHEFFLER, M., BOS, M., GARDIZI, M., KÖNIG, K., MICHELS, S., FASSUNKE, J., HEYDT, C., KÜNSTLINGER, H., IHLE, M., UECKEROTH, F., ALBUS, K., SERKE, M., GERIGK, U., SCHULTE, W., TÖPELT, K., NOGOVA, L., ZANDER, T., ENGEL-RIEDEL, W., STOELBEN, E., KO, Y., RANDERATH, W., KAMINSKY, B., PANSE, J., BECKER, C., HELLMICH, M., MERKELBACH-BRUSE, S., HEUKAMP, L.C., BÜTTNER, R. and WOLF, J., 2015. PIK3CA mutations in non-small cell lung cancer (NSCLC): Genetic heterogeneity, prognostic impact and incidence of prior malignancies. *Oncotarget,* 6(2), pp. 1315-1326.

SCHMID, P., ABRAHAM, J., CHAN, S., WHEATLEY, D., BRUNT, A.M., NEMSADZE, G., BAIRD, R.D., PARK, Y.H., HALL, P.S., PERREN, T., STEIN, R.C., MANGEL, L., FERRERO, J., PHILLIPS, M., CONIBEAR, J., CORTES, J., FOXLEY, A., DE BRUIN, E.C., MCEWEN, R., STETSON, D., DOUGHERTY, B., SARKER, S., PRENDERGAST, A., MCLAUGHLIN-CALLAN, M., BURGESS, M., LAWRENCE, C., CARTWRIGHT, H., MOUSA, K. and TURNER, N.C., 2020. Capivasertib plus paclitaxel versus placebo plus paclitaxel as first-line therapy for metastatic triple-negative breast cancer: The PAKT trial. *Journal of Clinical Oncology,* 38(5), pp. 423-433.

SCRIMA, M., DE MARCO, C., FABIANI, F., FRANCO, R., PIROZZI, G., ROCCO, G., RAVO, M., WEISZ, A., ZOPPOLI, P., CECCARELLI, M., BOTTI, G., MALANGA, D. and VIGLIETTO, G., 2012. Signaling networks associated with AKT activation in non-small cell lung cancer (NSCLC): New insights on the role of phosphatydil-inositol-3 kinase. *PLoS One,* 7(2), pp. e30427.

SENGUPTA, S., PETERSON, T.R. and SABATINI, D.M., 2010. Regulation of the mTOR Complex 1 pathway by nutrients, growth factors, and stress. *Molecular Cell,* 40(2), pp. 310-322.

SHAPIRO, G.I., RODON, J., BEDELL, C., KWAK, E.L., BASELGA, J., BRANA, I., PANDYA, S.S., SCHEFFOLD, C., LAIRD, A.D., NGUYEN, L.T., XU, Y., EGILE, C. and EDELMAN, G., 2014. Phase I safety, pharmacokinetic, and pharmacodynamic study of SAR245408 (XL147), an oral pan-class I PI3K inhibitor, in patients with advanced solid tumors. *Clinical Cancer Research,* 20(1), pp. 233-245.

SHAPIRO, G.I., BELL-MCGUINN, K.M., MOLINA, J.R., BENDELL, J., SPICER, J., KWAK, E.L., PANDYA, S.S., MILLHAM, R., BORZILLO, G., PIERCE, K.J., HAN, L., HOUK, B.E., GALLO, J.D., ALSINA, M., BRAÑA, I. and TABERNERO, J., 2015. First-in-human study of PF-05212384 (PKI-587), a small-molecule, intravenous, dual inhibitor of PI3K and mTOR in patients with advanced cancer. *Clinical Cancer Research,* 21(8), pp. 1888-1895.

SHAW, R.J., 2009. LKB1 and AMP-activated protein kinase control of mTOR signalling and growth. *Acta Physiologica (Oxf),* 196(1), pp. 65-80.

SHRESTHA BHATTARAI, T., SHAMU, T., GORELICK, A.N., CHANG, M.T., CHAKRAVARTY, D., GAVRILA, E.I., DONOGHUE, M.T.A., GAO, J., PATEL, S., GAO, S.P., REYNOLDS, M.H., PHILLIPS, S.M., SOUMERAI, T., ABIDA, W., HYMAN, D.M., SCHRAM, A.M., SOLIT, D.B., SMYTH, L.M. and TAYLOR, B.S., 2022. AKT mutant allele-specific activation dictates pharmacologic sensitivities. *Nature Communications,* 13(1), pp. 2111.

SINUÉS, B., FANLO, A., BERNAL, M.L., MAYAYO, E., BELLO, S., RUBIO, E. and ISLA, D., 2003. MDR-1 C3435T genetic polymorphism and tobacco-related lung cancer. *Oncology,* 64(2), pp. 183-185.

SJÖDAHL, G., LAUSS, M., GUDJONSSON, S., LIEDBERG, F., HALLDÉN, C., CHEBIL, G., MÅNSSON, W., HÖGLUND, M. and LINDGREN, D., 2011. A systematic study of gene mutations in urothelial carcinoma; inactivating mutations in tsc2 and pik3r1. *PLoS One,* 6(4), pp. e18583.

SMYTH, L.M., BATIST, G., MERIC-BERNSTAM, F., KABOS, P., SPANGGAARD, I., LLUCH, A., JHAVERI, K., VARGA, A., WONG, A., SCHRAM, A.M., AMBROSE, H., CARR, T.H., DE BRUIN, E.C., SALINAS-SOUZA, C., FOXLEY, A., HAUSER, J., LINDEMANN, J.P.O., MAUDSLEY, R., MCEWEN, R., MOSCHETTA, M., NIKOLAOU, M., SCHIAVON, G., RAZAVI, P., BANERJI, U., BASELGA, J., HYMAN, D.M. and CHANDARLAPATY, S., 2021. Selective AKT kinase inhibitor capivasertib in combination with fulvestrant in PTEN-mutant ER-positive metastatic breast cancer. *NPJ Breast Cancer,* 7(1), pp. 44.

SMYTH, L.M., TAMURA, K., OLIVEIRA, M., CIRUELOS, E.M., MAYER, I.A., SABLIN, M., BIGANZOLI, L., AMBROSE, H.J., ASHTON, J., BARNICLE, A., CASHELL, D.D., CORCORAN, C., DE BRUIN, E.C., FOXLEY, A., HAUSER, J., LINDEMANN, J.P.O., MAUDSLEY, R., MCEWEN, R., MOSCHETTA, M., PASS, M., ROWLANDS, V., SCHIAVON, G., BANERJI, U., SCALTRITI, M., TAYLOR, B.S., CHANDARLAPATY, S., BASELGA, J. and HYMAN, D.M., 2020. Capivasertib, an AKT kinase inhibitor, as monotherapy or in combination with fulvestrant in patients with AKT1 E17K-mutant, ER-positive metastatic breast cancer. *Clinical Cancer Research,* 26(15), pp. 3947-3957.

SOLOMON, B. and PEARSON, R.B., 2009. Class IA Phosphatidylinositol 3-Kinase Signaling in non-small cell lung cancer. *Journal of Thoracic Oncology,* 4(7), pp. 787-791.

SOMMER, E.M., DRY, H., CROSS, D., GUICHARD, S., DAVIES, B.R. and ALESSI, D.R., 2013. Elevated SGK1 predicts resistance of breast cancer cells to Akt inhibitors. *Biochemical Journal,* 452(3), pp. 499-508.

SONENBERG, N. and HINNEBUSCH, A.G., 2009. Regulation of translation initiation in eukaryotes: Mechanisms and biological targets. *Cell,* 136(4), pp. 731-745.

SORIA, J., ADJEI, A.A., BAHLEDA, R., BESSE, B., FERTE, C., PLANCHARD, D., ZHOU, J., WARE, J., MORRISSEY, K., SHANKAR, G., LIN, W., SCHUTZMAN, J.L., DY, G.K. and GROEN, H.J.M., 2017. A phase IB dose-escalation study of the safety and pharmacokinetics of pictilisib in combination with either paclitaxel and carboplatin (with or without bevacizumab) or pemetrexed and cisplatin (with or without bevacizumab) in patients

with advanced non–small cell lung cancer. *European Journal of Cancer (1990),* 86, pp. 186-196.

SPOERKE, J.M., O'BRIEN, C., HUW, L., KOEPPEN, H., FRIDLYAND, J., BRACHMANN, R.K., HAVERTY, P.M., PANDITA, A., MOHAN, S., SAMPATH, D., FRIEDMAN, L.S., ROSS, L., HAMPTON, G.M., AMLER, L.C., SHAMES, D.S. and LACKNER, M.R., 2012. Phosphoinositide 3-kinase (PI3K) pathway alterations are associated with histologic subtypes and are predictive of sensitivity to PI3K inhibitors in lung cancer preclinical models. *Clinical Cancer Research,* 18(24), pp. 6771-6783.

STEEG, P.S., 2016. Targeting metastasis. *Nature reviews. Cancer,* 16(4), pp. 201-218.

SUBHANI, S., JAMIL, K. and NIRNI, S.S., 2015. Association of MDR1 gene (C3435T) polymorphism and gene expression profiling in lung cancer patients treated with platinum-based chemotherapy. *Molecular Diagnosis & Therapy,* 19(5), pp. 289-297.

SUNG, H., FERLAY, J., SIEGEL, R.L., LAVERSANNE, M., SOERJOMATARAM, I., JEMAL, A. and BRAY, F., 2021. Global cancer statistics 2020: GLOBOCAN estimates of incidence and mortality worldwide for 36 cancers in 185 countries. *CA: A Cancer Journal for Clinicians,* 71(3), pp. 209-249.

TAN, A.C., 2020. Targeting the PI3K/Akt/mTOR pathway in non-small cell lung cancer (NSCLC). *Thoracic Cancer,* 11(3), pp. 511-518.

TAN, C.Y. and HAGEN, T., 2013. Post-translational regulation of mTOR complex 1 in hypoxia and reoxygenation. *Cellular Signalling,* 25(5), pp. 1235-1244.

TANG, Y., LUO, J., YANG, Y., LIU, S., ZHENG, H., ZHAN, Y., FAN, S. and WEN, Q., 2022. Overexpression of p-4EBP1 associates with p-eIF4E and predicts poor prognosis for non-small cell lung cancer patients with resection. *PloS One,* 17(6), pp. e0265465.

TANIGUCHI, C.M., WINNAY, J., KONDO, T., BRONSON, R.T., GUIMARAES, A.R., ALEMÁN, J.O., LUO, J., STEPHANOPOULOS, G., WEISSLEDER, R., CANTLEY, L.C. and KAHN, C.R., 2010. The phosphoinositide 3-kinase regulatory subunit p85α can exert tumor suppressor properties through negative regulation of growth factor signaling. *Cancer Research (Chicago, Ill.),* 70(13), pp. 5305-5315.

TARANTELLI, C., LUPIA, A., STATHIS, A. and BERTONI, F., 2020. Is there a role for dual PI3K/mTOR inhibitors for patients affected with lymphoma? *International Journal of Molecular Sciences,* 21(3), pp. 1060.

TEWARI, D., PATNI, P., BISHAYEE, A., SAH, A.N. and BISHAYEE, A., 2022. Natural products targeting the PI3K-Akt-mTOR signaling pathway in cancer: A novel therapeutic strategy. *Seminars in Cancer Biology,* 80, pp. 1-17.

THORPE, L.M., YUZUGULLU, H. and ZHAO, J.J., 2015. PI3K in cancer: Divergent roles of isoforms, modes of activation and therapeutic targeting. *Nature Reviews. Cancer,* 15(1), pp. 7-24.

THUN, M.J., HANNAN, L.M., ADAMS-CAMPBELL, L., BOFFETTA, P., BURING, J.E., FESKANICH, D., FLANDERS, W.D., SUN, H.J., KATANODA, K., KOLONEL, L.N., LEE, I.-., MARUGAME, T., PALMER, J.R., RIBOLI, E., SOBUE, T., AVILA-TANG, E., WILKENS, L.R. and SAMET, J.M., 2008. Lung cancer occurrence in never-smokers: An analysis of 13 cohorts and 22 cancer registry studies. *PLoS Medicine,* 5(9), pp. 1357-1371.

TIAN, T., LI, X. and ZHANG, J., 2019. mTOR signaling in cancer and mTOR inhibitors in solid tumor targeting therapy. *International Journal of Molecular Sciences,* 20(3), pp. 755.

TOLCHER, A., HONG, D., SULLIVAN, R., MIER, J., SHAPIRO, G., CHMIELOWSKI, B., RIBAS, A., POSTOW, M., PEARLBERG, J., BRAIL, L., LEE, L., ULLMANN, C.A.D. and WOLCHOK, J.D., 2017. Abstract CT089: IPI-549-01 - A phase 1/1b, first-in-human study of IPI-549, a PI3K-γ inhibitor, as monotherapy and in combination with nivolumab in patients with advanced solid tumors. *Cancer Research (Chicago, Ill.),* 77(13), pp. CT089.

TOREN, P., KIM, S., CORDONNIER, T., CRAFTER, C., DAVIES, B.R., FAZLI, L., GLEAVE, M.E. and ZOUBEIDI, A., 2015. Combination AZD5363 with enzalutamide significantly delays enzalutamide-resistant prostate cancer in preclinical models. *European Urology,* 67(6), pp. 986-990.

TURNER, N.C., ALARCÓN, E., ARMSTRONG, A.C., PHILCO, M., LÓPEZ CHUKEN, Y.A., SABLIN, M., TAMURA, K., GÓMEZ VILLANUEVA, A., PÉREZ-FIDALGO, J.A., CHEUNG, S.Y.A., CORCORAN, C., CULLBERG, M., DAVIES, B.R., DE BRUIN, E.C., FOXLEY, A., LINDEMANN, J.P.O., MAUDSLEY, R., MOSCHETTA, M., OUTHWAITE, E., PASS, M., RUGMAN, P., SCHIAVON, G. and OLIVEIRA, M., 2019. BEECH: A dose-finding run-in followed by a randomised phase II study assessing the efficacy of AKT inhibitor capivasertib (AZD5363) combined with paclitaxel in patients with estrogen receptor-positive advanced or metastatic breast cancer, and in a PIK3CA mutant sub-population. *Annals of Oncology,* 30(5), pp. 774.

TURNER, N.C., OLIVEIRA, M., HOWELL, S.J., DALENC, F., CORTES, J., GOMEZ MORENO, H.L., HU, X., JHAVERI, K., KRIVOROTKO, P., LOIBL, S., MORALES MURILLO, S., OKERA, M., PARK, Y.H., SOHN, J., TOI, M., TOKUNAGA, E., YOUSEF, S., ZHUKOVA, L., DE BRUIN, E.C., GRINSTED, L., SCHIAVON, G., FOXLEY, A. and RUGO, H.S., 2023. Capivasertib in hormone receptor–positive advanced breast cancer. *The New England Journal of Medicine,* 388(22), pp. 2058-2070.

TZATSOS, A., 2009. Raptor binds the SAIN (Shc and IRS-1 NPXY Binding) domain of insulin receptor substrate-1 (IRS-1) and regulates the phosphorylation of IRS-1 at Ser-636/639 by mTOR. *The Journal of Biological Chemistry,* 284(34), pp. 22525-22534.

VAN GEEL, R., TABERNERO, J., ELEZ, E., BENDELL, J.C., SPREAFICO, A., SCHULER, M., YOSHINO, T., DELORD, J.P., YAMADA, Y., LOLKEMA, M., FARIS, J.E., ESKENS, F., SHARMA, S., YAEGER, R., LENZ, H.J., WAINBERG, Z.A., AVSAR, E., CHATTERJEE, A., JAEGER, S., TAN, E., MAHARRY, K., DEMUTH, T. and SCHELLENS, J., 2017. A Phase Ib dose-escalation study of encorafenib and cetuximab with or without alpelisib in metastatic BRAF-mutant colorectal cancer. *Cancer Discovery,* 7(6), pp. 610-619.

VEERMAN, G.D.M., BOOSMAN, R.J., JEBBINK, M., OOMEN-DE HOOP, E., VAN DER WEKKEN, A.J., BAHCE, I., HENDRIKS, L.E.L., CROES, S., STEENDAM, C.M.J., DE JONGE, E., KOOLEN, S.L.W., STEEGHS, N., VAN SCHAIK, R.H.N., SMIT, E.F., DINGEMANS, A.C., HUITEMA, A.D.R. and MATHIJSSEN, R.H.J., 2023. Influence of germline variations in drug transporters ABCB1 and ABCG2 on intracerebral osimertinib efficacy in patients with non-small cell lung cancer. *EClinicalMedicine,* 59, pp. 101955.

WAINBERG, Z.A., SHAPIRO, G., CURIGLIANO, G., KRISTELEIT, R.S., LEONG, S., ALSINA, M., MILELLA, M., BRITTEN, C.D., GELMON, K.A., OLSZANSKI, A.J., VAISHAMPAYAN, U.N., LOPEZ-MARTIN, J., KERN, K.A., PIERCE, K.J., PEREA, R., HOUK, B., PATHAN, N. and RAZAK, A.R., 2016. Phase I study of the PI3K/mTOR inhibitor gedatolisib (PF-05212384) in combination with docetaxel, cisplatin, and dacomitinib. *Journal of Clinical Oncology,* 34(15), pp. 2566.

WANG, B., SHI, L., SUN, X., WANG, L., WANG, X. and CHEN, C., 2016. Production of CCL20 from lung cancer cells induces the cell migration and proliferation through PI3K pathway. *Journal of Cellular and Molecular Medicine,* 20(5), pp. 920-929.

WANG, J., XU, X., WANG, T., GUO, Q., DAI, X., GUO, H., ZHANG, W., CHENG, S., CHEN, X. and DING, L., 2021. Ceritinib increases sensitivity of AKT inhibitors to gastric cancer. *European Journal of Pharmacology,* 896, pp. 173879.

WANG, L., HARRIS, T.E. and LAWRENCE, J.C., 2008. Regulation of proline-rich Akt substrate of 40 kDa (PRAS40) function by mammalian target of rapamycin complex 1 (mTORC1)-mediated phosphorylation. *The Journal of Biological Chemistry,* 283(23), pp. 15619-15627.

WONG, D.W., LEUNG, E.L., SO, K.K., TAM, I.Y., SIHOE, A.D., CHENG, L., HO, K., AU, J.S., CHUNG, L. and PIK WONG, M., 2009. The EML4-ALK fusion gene is involved in various histologic types of lung cancers from nonsmokers with wild-type EGFR and KRAS. *Cancer,* 115(8), pp. 1723-1733.

XU, T., ZONG, Y., PENG, L., KONG, S., ZHOU, M., ZOU, J., LIU, J., MIAO, R., SUN, X. and LI, L., 2016. Overexpression of eIF4E in colorectal cancer patients is associated with liver metastasis. *OncoTargets and Therapy,* 9, pp. 815-822.

YAMAMOTO, N., FUJIWARA, Y., TAMURA, K., KONDO, S., IWASA, S., TANABE, Y., HORIIKE, A., YANAGITANI, N., KITAZONO, S., INATANI, M., TANAKA, J. and NISHIO, M., 2016. Phase Ia/Ib study of the pan-class I PI3K inhibitor pictilisib (GDC-0941) administered as a single agent in Japanese patients with solid tumors and in combination in Japanese patients with non-squamous non-small cell lung cancer. *Investigational New Drugs,* 35(1), pp. 37-46.

YANG, J., NIE, J., MA, X., WEI, Y., PENG, Y. and WEI, X., 2019. Targeting PI3K in cancer: Mechanisms and advances in clinical trials. *Molecular Cancer,* 18(1), pp. 26.

YAO, J.C., SHAH, M.H., ITO, T., BOHAS, C.L., WOLIN, E.M., VAN CUTSEM, E., HOBDAY, T.J., OKUSAKA, T., CAPDEVILA, J., DE VRIES, E.G.E., TOMASSETTI, P., PAVEL, M.E., HOOSEN,

S., HAAS, T., LINCY, J., LEBWOHL, D. and ÖBERG, K., 2011. Everolimus for advanced pancreatic neuroendocrine tumors. *The New England Journal of Medicine,* 364(6), pp. 514-523.

YAP, T.A., PATNAIK, A., FEAREN, I., OLMOS, D., PAPADOPOULOS, K., TUNARIU, N., SULLIVAN, D., YAN, L., DE BONO, J.S. and TOLCHER, A.W., 2010. First-in-class phase I trial of a selective Akt inhibitor, MK2206 (MK), evaluating alternate day (QOD) and once weekly (QW) doses in advanced cancer patients (pts) with evidence of target modulation and antitumor activity. *Journal of Clinical Oncology,* 28(15), pp. 3009.

YAP, T.A., YAN, L., PATNAIK, A., FEAREN, I., OLMOS, D., PAPADOPOULOS, K., BAIRD, R.D., DELGADO, L., TAYLOR, A., LUPINACCI, L., RIISNAES, R., POPE, L.L., HEATON, S.P., THOMAS, G., GARRETT, M.D., SULLIVAN, D.M., DE BONO, J.S. and TOLCHER, A.W., 2011. First-in-man clinical trial of the oral pan-AKT inhibitor MK-206 in patients with advanced solid tumors. *Journal of Clinical Oncology,* 29(35), pp. 4688-4695.

YIP, P.Y., 2015. Phosphatidylinositol 3-kinase-AKT-mammalian target of rapamycin (PI3K-Akt-mTOR) signaling pathway in non-small cell lung cancer. *Translational Lung Cancer Research,* 4(2), pp. 165-176.

YODER, L.H., 2006. An overview of lung cancer symptoms, pathophysiology, and treatment. *Medsurg Nursing,* 15(4), pp. 231-234.

YU, F., ZHAO, J., HU, Y., ZHOU, Y., GUO, R., BAI, J., ZHANG, S., ZHANG, H. and ZHANG, J., 2016. The combination of NVP-BKM120 with trastuzumab or RAD001 synergistically inhibits the growth of breast cancer stem cells *in vivo*. *Oncology Reports,* 36(1), pp. 356-364.

YU, J.S.L. and CUI, W., 2016. Proliferation, survival and metabolism: The role of PI3K/AKT/mTOR signalling in pluripotency and cell fate determination. *Development (Cambridge),* 143(17), pp. 3050-3060.

ZAPPA, C. and MOUSA, S.A., 2016. Non-small cell lung cancer: Current treatment and future advances. *Translational Lung Cancer Research,* 5(3), pp. 288-300.

ZAWADZKA, I., JELEŃ, A., PIETRZAK, J., ŻEBROWSKA-NAWROCKA, M., MICHALSKA, K., SZMAJDA-KRYGIER, D., MIROWSKI, M., ŁOCHOWSKI, M., KOZAK, J. and BALCERCZAK, E., 2020. The impact of ABCB1 gene polymorphism and its expression on non-small-cell lung cancer development, progression and therapy – preliminary report. *Scientific Reports,* 10(1), pp. 6188.

ZHANG, Y., ZHENG, Y., FAHEEM, A., SUN, T., LI, C., LI, Z., ZHAO, D., WU, C. and LIU, J., 2016. A novel AKT inhibitor, AZD5363, inhibits phosphorylation of AKT downstream molecules, and activates phosphorylation of mTOR and SMG-1 dependent on the liver cancer cell type. *Oncology Letters,* 11(3), pp. 1685-1692.

ZHAO, J.J., LIU, P., CHENG, H. and ROBERTS, T.M., 2009. Targeting the phosphoinositide 3-kinase pathway in cancer. *Nature Reviews. Drug Discovery,* 8(8), pp. 627-644.

ZHENG, M., 2016. Classification and pathology of lung cancer. *Surgical Oncology Clinics of North America,* 25(3), pp. 447-468.

ZHONG, J., GUO, Z., FAN, L., ZHAO, X., ZHAO, B., CAO, Z., CHENG, L., SHI, Y., LI, X., ZHANG, Y., AN, T., WU, M., WANG, Y., ZHUO, M., LI, J., YANG, X., CHEN, H., JIA, B. and ZHAO, J., 2019. ABCB1 polymorphism predicts the toxicity and clinical outcome of lung cancer patients with taxane-based chemotherapy. *Thoracic Cancer,* 10(11), pp. 2088-2095.

ZHU, C., DA CUNHA SANTOS, G., DING, K., SAKURADA, A., CUTZ, J., LIU, N., ZHANG, T., MARRANO, P., WHITEHEAD, M., SQUIRE, J.A., KAMEL-REID, S., SEYMOUR, L., SHEPHERD, F.A. and TSAO, M., 2008. Role of KRAS and EGFR as biomarkers of response to erlotinib in National Cancer Institute of Canada Clinical Trials Group Study BR.21. *Journal of Clinical Oncology,* 26(26), pp. 4268-4275.

ZUKIN, M., BARRIOS, C.H., PEREIRA, J.R., DE ALBUQUERQUE RIBEIRO, R., DE MENDONÇA BEATO, C.A., DO NASCIMENTO, Y.N., MURAD, A., FRANKE, F.A., PRECIVALE, M., DE LIMA ARAUJO, L.H., DA ROCHA BALDOTTO, C.S., METON VIEIRA, F., SMALL, I.A., FERREIRA, C.G. and LILENBAUM, R.C., 2013. Randomized phase III trial of single-agent pemetrexed versus carboplatin and pemetrexed in patients with advanced non–small-cell lung cancer and Eastern Cooperative Oncology Group Performance Status of 2. *Journal of Clinical Oncology,* 31(23), pp. 2849-2853.